The Enantioselective-Controlled Delivery of Propranolol by Cellulose Membrane Grafted with Molecularly Imprinted Polymer

Chatchada Bodhibukkana

A Thesis Submitted in Partial Fulfillment of the Requirements for the

Degree of Doctor of Philosophy in Pharmaceutical Sciences

Prince of Songkla University

2008

i

Thesis Title   The Enantioselective-Controlled Delivery of Propranolol by

                       Cellulose Membrane Grafted with Molecularly Imprinted

                       Polymer

Author   Miss Chatchada Bodhibukkana

Major program   Pharmaceutical Sciences

Major Advisor   **Examining Committee**

…………………………………………   ………………………………Chairperson

(Assoc. Prof. Dr. Roongnapa Srichana)   (Assoc. Prof. Dr. Ruedeekorn Wiwattanapatapee)

                                           ………………………………Committee

Co-advisor   (Assoc. Prof. Dr. Varaporn Junyaprasert)

…………………………………………   ………………………………Committee

(Assoc. Prof. Dr. Teerapol Srichana)   (Assoc. Prof. Dr. Roongnapa Srichana)

…………………………………………   ………………………………Committee

(Prof. Gary P. Martin)   (Assoc. Prof. Dr. Teerapol Srichana)

        The Graduate School, Prince of Songkla University, has approved this

thesis as partial fulfillment of the requirements for the Doctor of Philosophy Degree

in Pharmaceutical Sciences

                            …………………………………………

                            (Assoc. Prof. Dr. Krerkchai Thongnoo)

                            Dean of Graduate School

ชื่อวิทยานิพนธ์	ระบบเลือกนำส่งอิแนนทิโอเมอร์ของ propranolol โดยใช้เซลลูโลสเมมเบรนที่กราฟต์ด้วยพอลิเมอร์ที่มีรอยพิมพ์ประทับโมเลกุล
ผู้เขียน	นางสาวชัชฎา โพธิพุกกณะ
สาขาวิชา	เภสัชศาสตร์
ปีการศึกษา	2550

บทคัดย่อ

ในการศึกษานี้มีวัตถุประสงค์ที่จะพัฒนาเมมเบรนประกอบ (composite membrane) ของเซลลูโลสเมมเบรนจากแบคทีเรียและพอลิเมอร์ที่มีรอยพิมพ์ประทับ (Molecularly imprinted polymer, MIP) เพื่อใช้ในการเลือกนำเฉพาะส่งอิแนนทิโอเมอร์ที่เฉพาะเจาะจงของ *S*-enantiomer จาก racemic propranolol เมมเบรนประกอบสังเคราะห์ขึ้นโดยการ เปลี่ยนแปลงหมู่ฟังก์ชั่นที่รูพรุนของเซลลูโลสเมมเบรนด้วยการสังเคราะห์ชั้นของพอลิเมอร์ที่มีรอยพิมพ์ประทับโมเลกุล การทำปฏิกิริยา silanisation ที่รูพรุนแบบอสมมาตรของเซลลูโลสเมมเบรนก่อนที่จะสังเคราะห์ชั้นของพอลิเมอร์มีความจำเป็นต่อการเตรียมเมมเบรนเพื่อให้สามารถทำปฏิริยาพอลิเมอร์ไรเซชั่นได้ ซึ่งชั้นของ MIP ที่มีความจำเพาะต่อ *S*-propranolol จะถูกสังเคราะห์ขึ้นโดยการ โคพอลิเมอร์ไรเซชั่นระหว่าง methacrylic acid และ ethylene glycol dimethacrylate ซึ่งเป็น cross-linker และมี *S*- propranolol เป็นตัวพิมพ์ โดยในขั้นตอนสุดท้ายโมเลกุลตัวพิมพ์จะถูกสกัดออกไปเหลือไว้เพียงรอยพิมพ์ประทับที่เฉพาะเจาะจงเท่านั้น ซึ่งจากการศึกษาสามารถพบการนำส่งที่เฉพาะของ *S*-propranolol ในเมมเบรนประกอบ แม้ว่าการเลือกนำส่งที่เฉพาะเจาะจงของ S-MIP membrane นั้นส่วนใหญ่เป็นผลมาจากเซลลูโลสเมมเบรนก็ตามโดยที่ชั้นของพอลิเมอร์ที่มีรอยพิมพ์ประทับจะเป็นตัวช่วยส่งเสริมให้เมมเบรนประ-กอบมีประสิทธิภาพมากยิ่งขึ้น และนอกเหนือจากนี้การนำส่งเฉพาะอิแนนทิโอเมอร์สามารถพบได้เช่นเดียวกันเมื่อทำศึกษาด้วย propranolol prodrug ซึ่งแสดงให้เห็นว่า

รูปร่างและการจัดเรียงตัวของหมู่ฟังก์ชั่นของ prodrugs มีความสำคัญต่อการเลือกจดจำ
อิแนนทิโอเมอร์ของ S-MIP membrane โดยที่เมมเบรนจะแสดงการจดจำต่อโมเลกุลได้
ดีที่สุดเมื่อโมเลกุลนั้นมีความคล้ายคลึงตัวพิมพ์ต้นแบบมากที่สุด

นอกจากนี้ในการศึกษาแบบ *in vitro* study นั้น S-MIP membrane สามารถเลือก
ปลดปล่อยเฉพาะ *S*-propranolol จาก racemic propranolol ในการศึกษาการเลือกนำ
ส่งผ่านผิวหนังหนูทดลอง ซึ่งผลการทดลองแสดงให้เห็นถึงศักยภาพของเมมเบรนประ-
กอบของเซลลูโลสเมมเบรนจากแบคทีเรียและพอลิเมอร์ที่มีรอยพิมพ์ประทับโมเลกุล
สำหรับใช้เป็นระบบเลือกนำส่งทางผิวหนังเฉพาะอิแนนทิโอเมอร์สำหรับ racemic
propranolol และนอกจากนี้ผลการทดลองยังชี้ให้เห็นว่าการเลือกปลดปล่อยของ S-MIP
membrane เป็นการเลือกปลดปล่อยแบบ facilitate transport โดยผ่านกลไก 'fixed
carrier' เมื่อทำการศึกษาในสารละลายบัฟเฟอร์ ซึ่งปัจจัยต่างๆ (เช่น pH ของสารละลาย)
ที่มีผลต่อการเกิดปฏิกิริยาระหว่าง *S*-propranolol และ 'fixed carrier' จะสามารถส่งผล
ต่อการเลือกปลดปล่อยเฉพาะอิแนนทิโอเมอร์ของเมมเบรนและความสามารถของ S-
MIP composite membrane ได้ ซึ่งการจดจำโมเลกุลของตัวพิมพ์นั้นจะสูงสุดใน
สารละลายบัฟเฟอร์ pH 7.4 และการเลือกนำส่งที่เฉพาะของ *S*-enantiomer จาก racemic
propranolol จะสูงกว่ากรณีของการเลือกนำส่ง racemic propranolol prodrugs โดยที่
propranolol prodrug ไม่สามารถเพิ่มการแพร่ผ่านของยาเข้าสู่ผิวหนังหนูทดลองได้ และ
เมื่อทำการศึกษาผลของ poloxamer และ chitosan gel ต่อการเลือกนำส่งเฉพาะอิแนนทิ
โอเมอร์ พบว่า chitosan gel แสดงความสามารถที่ดีในการเป็นตัวกลางในการนำส่งที่
เฉพาะเจาะจงของ *S*-propranolol ในขณะที่ poloxamer gel ซึ่งมีความหนืดมากกว่าไม่
แสดงความแตกต่างของอิแนนทิโอเมอร์ โดย chitosan gel ให้การนำผ่านที่สูง (high
flux) พร้อมทั้งมีความสามารถในการนำส่งเฉพาะอิแนนทิโอเมอร์ของ *S*-propranolol
ผ่านผิวหนังหนูทดลอง ดังนั้น chitosan gel จึงถูกเลือกเพื่อนำไปใช้เป็น reservoir
สำหรับระบบนำส่งยาสู่ผิวหนังต่อไป enantiomer-controlled delivery patch ชนิด
reservoir เตรียมขึ้นโดยการนำ chitosan gel ที่มี racemic propranolol HCl ใส่เข้าไป
ระหว่าง S-MIP composite membrane และ laminated backing ซึ่ง transdermal patch ที่
เตรียมขึ้นมานั้นสามารถแสดงความสามารถในการนำส่ง *S*-propranolol อย่างมีนัยสำคัญ

เมื่อแปะที่ผิวหนังหนูทดลองในการศึกษาแบบในกาย (*in vivo*) ซึ่งค่าเภสัชจลนศาสตร์ (C_{max}, T_{max} และ AUC_{0-24}) ที่ได้จากแผ่นแปะนั้นสามารถเทียบเคียงได้กับการให้ *S*-propranolol gel แบบ topical application จากผลการทดลองชี้ให้เห็นว่า S-MIP composite membrane มีศักยภาพสำหรับการนำไปใช้เป็นระบบนำส่งอิแนนทิโอเมอร์ที่ เฉพาะเจาะจงทางผิวหนังของ racemic propranolol

Thesis Title   The Enantioselective-Controlled Delivery of Propranolol by
Cellulose Membrane Grafted with Molecularly Imprinted
Polymer

Author   Miss Chatchada Bodhibukkana

Major program   Pharmaceutical Sciences

Academic year   2007

ABSTRACT

The aim of this thesis was to develop a composite membrane of bacterially-derived cellulose and molecularly imprinted polymer (MIP) for use as a transdermal enantioselective controlled-release system of racemic propranolol. The composite membranes were produced by the controlled pore functionalization of bacterial cellulose membranes using a molecularly imprinted polymer layer synthesis. The reactive pore-filling of an asymmetric porous cellulose membrane with a MIP thin-layer was modified using a silanised coupler as an additional anchor for the MIP. MIP thin-layers with specific binding sites for S-propranolol were synthesized by copolymerization of methacrylic acid with a cross-linker, ethylene glycol dimethacrylate in the presence of S-propranolol the template molecule and the latter was subsequently extracted. Selective transport of S-propranolol through the MIP composite membrane was obtained, although this was determined mostly by the parent cellulose membrane with some ancillary contributory effect from the MIP layer.

In addition, an enantioselectivity in the transport of propranolol prodrug enantiomers was found, suggesting that the shape and functional groups orientation, which are similar to that of the print molecule were essential for enantiomeric recognition of the MIP composite membrane.

The enantioselectivity of S-MIP membranes was also shown when the release of propranolol enantiomers was studied *in vitro* using rat skin, with racemic propranolol contained in the donor compartment. The results obtained, demonstrated the potential use of the composite membrane of bacterially-derived cellulose and molecularly imprinted polymer as a transdermal enantioselective controlled-release system of racemic propranolol. The result obtained from the *in vitro* release study showed that the selective release characteristic of the S-MIP membrane is the facilitated permeation *via* the 'fixed-carrier' mechanism such that the interaction between 'fixed-carrier' sites and *S*-propranolol can occur in aqueous buffers, and factors such as pH have been shown to have an influence. The template recognition of the S-MIP composite membrane was found to be highest in pH 7.4 buffer and the selective controlled delivery of the active *S*-enantiomer from racemic propranolol was greater than that from racemic propranolol prodrugs. In addition, the propranolol prodrug did not show the ability in increasing the penetration of the drug across the excised rat skin. Subsequently, the MIP thin-layer composited cellulose membrane with selectivity for *S*-propranolol was employed as the enantioselective-controlled release system. The effect of gel reservoir (poloxamer and chitosan) on enantioselective delivery was investigated. The chitosan gel allowed excellent selectivity for delivery of the *S*-propranolol enantiomer, whilst the more rheologically

structured poloxamer gel formulation provided no selective release of *S*-propranolol. The chitosan gel exhibited high flux and had the ability to enantioselective deliver *S*-propranolol across excised rat skin. The reservoir patch for enantiomer-controlled delivery of propranolol was therefore fabricated by incorporating the chitosan gel formulation containing racemic propranolol hydrochloride into the MIP composite membrane laminated backing. These patch devices were shown to exhibit the significant stereoselectivity uptake of propranolol when attached to the skin, using pharmacokinetic studies in Wistar rats. *S*-Propranolol enantiomer plasma concentration profiles for the transdermal patch in the *in vivo* study were comparable to data for the gel formulations that were applied directly to skin, and containing a single *S*-enantiomer of propranolol. The results demonstrate that the transdermal patch based on the MIP composite membrane-controlled release system may have potential in the enantioselective-controlled delivery of the *S*-isomer of racemic propranolol.

ACKNOWLEDGEMENTS

Chatchada Bodhibukkana

CONTENTS

CONTENTS (continued)

CONTENTS (continued)

CONTENTS (continued)

CONTENTS (continued)

CONTENTS (continued)

CONTENTS (continued)

CONTENTS (continued)

CONTENTS (continued)

LIST OF TABLES

LIST OF FIGURES

LIST OF FIGURES (continued)

LIST OF FIGURES (continued)

CHAPTER 1

INTRODUCTION

1.1. Literature reviews

1.1.1 Chirality

1.1.1.1. History of optical isomerism

The first half of the nineteenth century was great age of geometric optics. Optical activity, the ability of a substrate to rotate the plane of polarization of light, was discovered in 1815 at the College de France by the French physicist Jean-Babtiste Biot. In 1845 at the Ecole Normale in Paris, Louise Pasteure made a set of observations that led him a few years latter to make a proposal, which is the foundation of stereochemistry. A logical extension of this idea occurred in 1874 when a theory of organic structure in three dimensions was advanced independently and almost simultaneously by Jacobus Henricus van't Hoff and Joseph Achille Le Bel. By this time it was known from the work of Kekule in 1858 that carbon is tetravalent. Van't Hoff specifically proposed that the spatial arrangement was tetrahedral, a compound containing a carbon substituted with four different groups, or defined as an

asymmetric carbon (Figure 1.1). This asymmetric carbon, they proposed, was the cause of molecular asymmetry and therefore optical activity (Drayer, 1988).
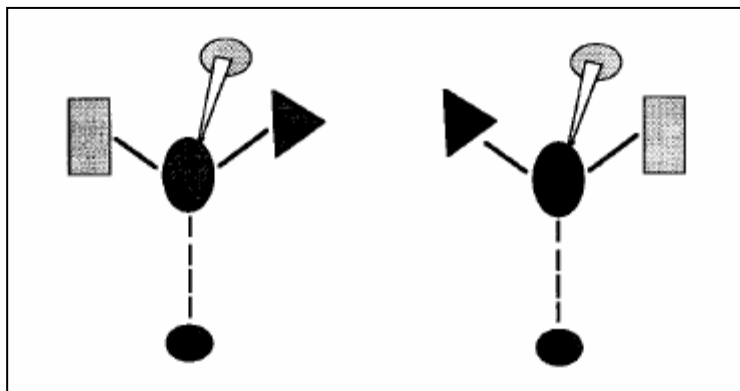
Figure 1.1. Molecular asymmetry arising from the attachment of four different ligands to a tetravalent carbon atom (Landoni et al., 1997).

1.1.1.2. Stereochemistry and biological activities

For an understanding of the effect of stereochemistry on the biological activities of drugs, it is important to refer to the characteristics of the enzymes and cell receptors. All enzymes and most cell receptors are enantiomeric. Therefore, for chiral compounds (such as drugs, vitamins and pesticides) to bind, they must also be appropriate so they can fit properly. The preference of enzymes and cell receptors for one particular enantiomer over the other is called *enantiomeric selectivity*. For an understanding of the stereochemistry and biological activities, there are series of the investigations.

The concept of stereoselective binding of a drug to a receptor evolved through historical development. Pasteur was the first to notice the close juxtaposition of biological catalysis and biological activity. In his studies of the underlying causes of both fermentation and infectious diseases, he became convinced that microbes, although capable of mediating a useful biotransformation, could also bring death and destruction to mankind. Thus, at the molecular level biocatalysis and biological activity are two sides of the same coin; the former involving reaction of a substrate with a biopolymer (enzyme) and the latter a biopolymer (enzyme or receptor site) with a bioactive molecule. The common denominator is *chirality* (Aboul-Enein and Basha, 1997).

In his studies of sugar, Emil Fisher observed that the enzyme emulsion catalyzes the hydrolysis of β-methyl-D-glucoside as a substrate. This observation led Fisher to purpose his famous *lock-and-key* concept of enzyme specificity. In his own words, "to use a picture, I would say that the enzyme and the glucoside must fit each other like a lock and key, in order to affect a chemical reaction on each other." The lock and key concept offered a simple explanation for the enigma of a biological asymmetric synthesis and it has played an important role in the development of our understanding of enzyme mechanisms. It must be mentioned, however, that this led to the popular "one enzyme-one substrate" concept, a misconception that is prevalent among chemists (Sheldon, 1993).

Most drugs are specific and their action is usually explained on the basis of *receptor theory*. The basis idea of receptor sites can be traced back to Paul Ehrlich who proposed the term chemoreceptors to describe these binding sites. Receptor molecules in the body are proteins that exhibit high affinities for binding ligands of a certain molecular structure; this is completely analogous to enzyme substrate binding. The binding of a substrate to a receptor triggers a mechanism (e.g., the modification of enzyme activity, transport of ions, etc.) that manifests itself in a biological response. Whatever their physiological function, receptors have one thing in common. They are themselves chiral molecules and can, therefore, be expected to be enantioselective in their binding to messenger molecules (Aboul-Enein and Basha, 1997).

The idea of enantioselectivity in drug-receptor interactions dates back to 1926 when Cushny proposed that different bioactivities of two enantiomers arise from binding sites of the same chirality. This was further elaborated Easson and Stedman in 1933 to become the widely-accepted *three-point contact model*. They postulated that the more active enantiomer binds more tightly because the sequence of the three groups around the asymmetric carbon atom forms a triangular face of a tetrahedron that matches a complementary triad of the chiral binding site of receptor protein. The less active enantiomer binds ineffectively since it has a mirror-image sequence of the three groups, which leads to a mismatch with the receptor binding sites. Drug-receptor interactions can involve electrostatic effects, hydrophobic interactions, hydrogen bonding, and charge transfer processes, such as π-π interactions. The three-point contact model for pharmacological enantioselectivity

became widely and was later applied to understanding enzyme specificity following its rediscovery by Ogston in 1948. Furthermore, the model has formed a useful basis for understanding chromatographic separations of enantiomers on chiral columns (Sheldon, 1993).

A further consideration of the enantioselectivity of drug-receptor interactions led Pfeiffer in 1956 to postulate that "the lower the effective dose of drug, the greater the difference in the pharmacological effect of the optical isomers". This simple statement became known as *Pfeiffer's rule*. It is a logical corollary of the idea that a receptor-drug interaction involves a 'lock-and-key' fit of the molecule with the right configuration at the receptor site: the better the fit, the better drug. If both enantiomers can fit into the active site, it is unlikely to be a good fit. This can be compared to a hand and a glove; if both a right and a left hand can fit equally well into a glove, it is unlikely to be a well-fitting glove. Although Pfeiffer's rule was developed in the context of pharmacological activity, it is self-evident that it applies equally well to all bioactive substances (Sheldon, 1993).

1.1.1.3. Classification of drug activity (Powell, Ambre and Ruo, 1988)

In the use of drugs to treat patients, the clinician, if aware that drug is an enantiomer or epimer, might assume that the isomer combination will either not detract from the therapeutic goal or will benefit the patient. However, with an

enantiomeric drug, there are four different possibilities with regard to the pharmacologic activity.

1. All the pharmacological activity may reside in one isomer.

The second isomer in this example might be regarded as an isomeric impurity. An example is α-methyldopa, where all the antihypertensive activity is in the *S*-isomer. However, care must be taken in considering the second isomer inactive, since the definition of inactivity is limited to those pharmacologic tests that have been used. Latter studies may find that the inactive isomer dose possess activity that may or may not be desirable.

2. The isomers may have nearly identical qualitative and quantitative pharmacological activity.

The isomers of promethazine have nearly equivalent properties with regard to antihistaminic properties and toxicity. In practical terms, the above two possibilities are the least complicated, in that the isomers act with the same pharmacological characteristics regardless of the situation encountered.

3. The isomers have qualitative similar pharmacological activity but have different quantitative potencies.

Most drugs that exist as stereoisomers are in this category. Examples of drug of this type are propranolol and warfarin. These drugs can present several interesting problems.

4. The isomers have qualitative different pharmacological activities.

Examples include labetalol and ketamine. For this type of agent, the different pharmacologic activity may offer a true therapeutic advantage or may be entirely undesirable. With the α, β sympathetic blocking agent labetalol, the primary α-blocking effect is in the *S*, *R* isomer, while the β-blocking activity is in *R*, *R* isomer of the diastereomer. While clinicians are certain to know that labetalol is unique among β-blocking drugs because of its combined α-blocking characteristics, likely few know that this is a combination drug product of different chemical entities.

The other examples of the stereoisomer drugs with their activities are shown in Table 1.1.

Table 1.1. Activities of some stereoisomers (Ahuja, 1991 and Ahuja, 1997a).

Compound	Activities
Drugs	
Amphetamine	*d*-isomer is a potent central nervous system stimulant, while *l*-isomer has little, if any, effect.
Diethylstilbestrol	*trans*-isomer is much more estrogenic than *cis*-isomer.
Epinephrine	(-)-isomer is more than 10 times more active a vasoconstrictor than (+)-isomer.

Table 1.1. Activities of some stereoisomers (Ahuja, 1991 and Ahuja, 1997a) (continued).

Compound	Activities
Drugs	
Quinine/Quinidine	Quinidine is (+)-enantiomer, with cardiac suppressant effect; quinine is (-)-enantiomer with other medicinal uses.
Propranolol	Racemic compound is used as drug, however only *S*-isomer has the desired adrenergic blocking activity.
Warfarin	Racemic warfarin is administered but *S*-isomer is 5 times more potent as a blood anticoagulant than *R*-isomer.
Vitamin	
Ascorbic acid	(+)-isomer is a good antiascorbic, which (-)-has no such

properties.

Flavoring agents

Asparagine   *D*-aspasagine tastes sweet, while *L*-enantiomer tastes bitter.

Limonene   *S*-limonene smells like lemons, while *R*-limonene smells like oranges.

Carvone   *S*-carvone smells like caraway, while *R*-carvone smells like spearmint.

Insecticide

Bermethrine   *d*-isomer is much more toxic than *l*-isomer.

1.1.1.4. Chiral separations

The distribution of worldwide approved drugs from 1983-2002 and FDA-approved drugs from 1991-2002 indicate that single-enantiomers surpassed achirals whereas racemic drugs represented the minority category. The distributions of the 15 FDA-approved drugs in the period of January-August 2003 are 64% single enantiomers, 14% racemates and 22% achirals (Zhang et al., 2005). As mentioned above, living organisms are based on a plethora of chiral molecules and often display different biological responses to drug enantiomers. These facts moved the Food and Drug Administration in 1992 to issue a *Policy Statement for the Development of New Stereoisomeric Drugs*, starting that for every new racemic drug, the two enantiomers must be treated as separate substances in pharmacokinetic and toxicology profiling.

Currently, there is intense debate between pharmaceutical scientists, pharmaceutical companies, and drug regulatory agencies on the relative merits of clinical use of stereochemically pure enantiomers as opposed to racemates. The decision to market the stereochemically pure enantiomer of some drugs is cleared. For example, the use of D,L dopa leads to granulocytopenia; however, the clinical use of pure enantiomer L-dopa has not shown this adverse effect. The following advantages provide an impetus towards effort's to develop pure drug enantiomer:

1. Separating unwanted pharmacodynamic side effects from toxic effects if these reside exclusively in one enantiomer.

2. Expose the patient to less body load and thus reduce metabolic/renal/hepatic drug load.

3. Easier assessment of physiology, disease, and drug co-administration effects.

4. Reduce drug interactions.

5. Avoid enantiomer-enantiomer drug interactions.

6. Avoid bioconversion.

7. Easier assessment of efficacy and toxicity through pharmacokinetic/pharmacodynamic monitoring of stereochemically pure active enantiomer.

From the perspective of the pharmaceutical industry, commercially pure enantiomers, once developed, may be eligible for patient protection and market exclusivity (Davies and Teng, 2003). To obtain the single enantiomers of chiral compounds, two approaches can basically be envisaged (Figure 1.2).
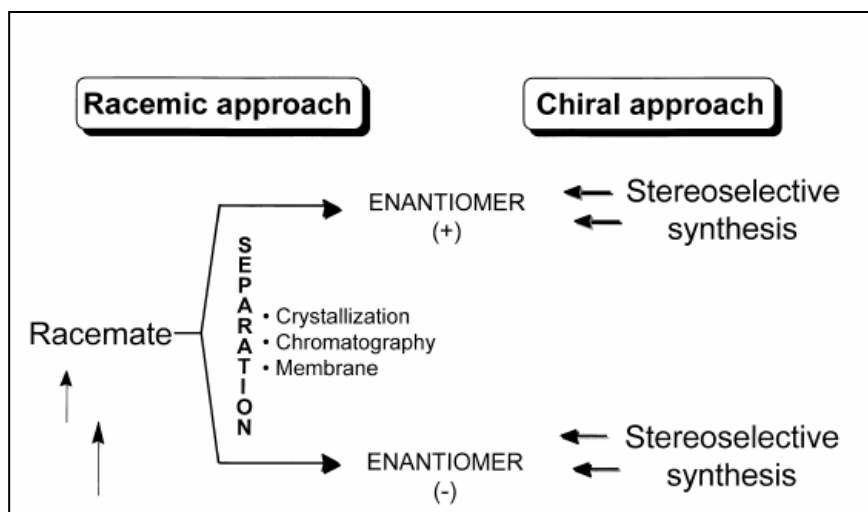
Figure 1.2. Approaches to optically active compounds (Francotte, 2001).

The first one, 'the chiral approach', consists in designing an enantioselective synthesis of desired enantiomer. If both enantiomers are needed, it is necessary to develop two independent syntheses. The chiral approach includes enantioselective synthesis using chiral synthons and auxiliaries, enzymes or stereoselective catalytic processes. In contrast to the chiral approach, 'the racemic approach' implies the preparation of the racemate which is subsequently resolved into the corresponding enantiomers (Francotte, 2001). In the racmic approach, the enantiomer obtained from the chiral separation methods. Some chiral separation techniques are summarized in Figure 1.3.
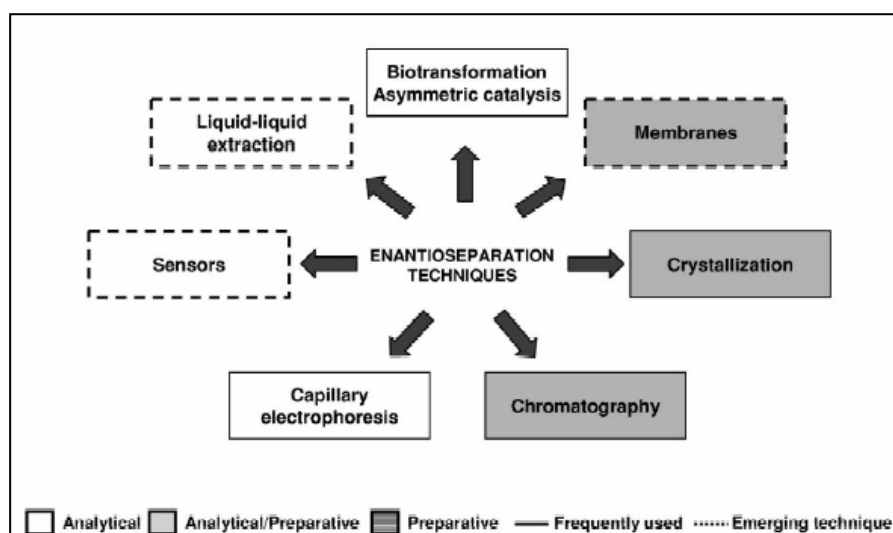
Figure 1.3. Techniques used for the separation of enantiomers (Maier et al., 2001).

The most widely used approach in quality control of pharmaceuticals and pharmacokinetic studies of drugs is chromatrography separation, which has become a powerful and important technology (Figure 1.4).
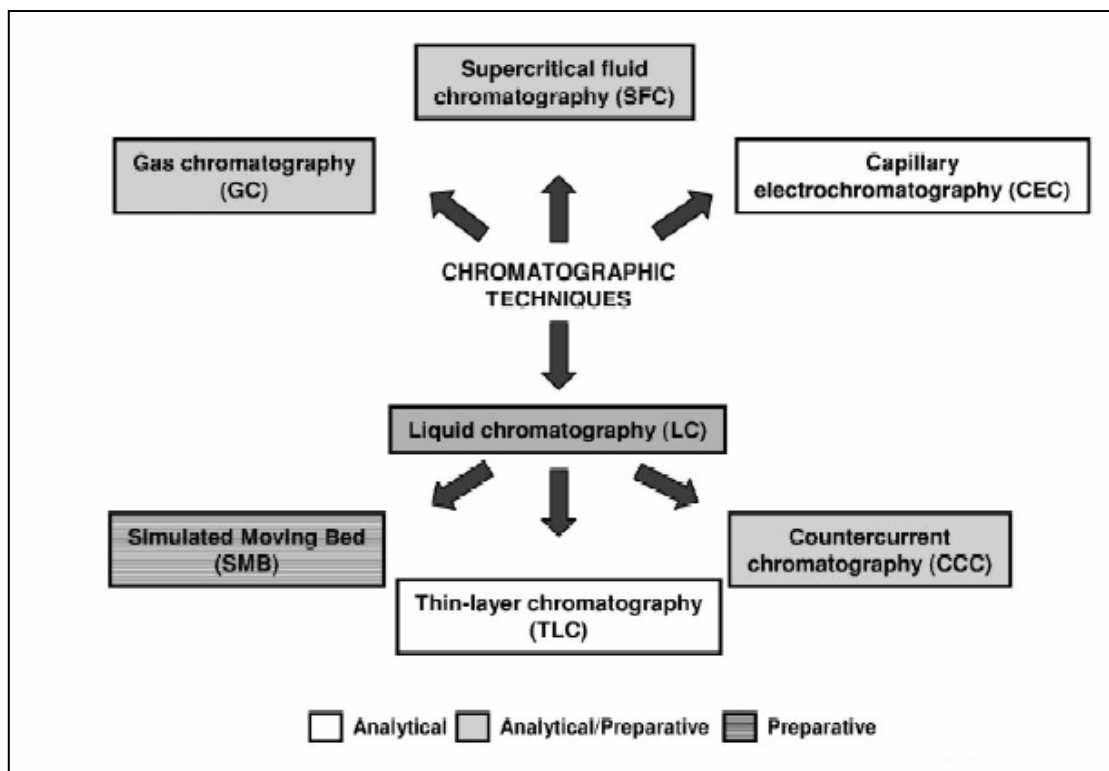
Figure 1.4. Chromatographic techniques used for the separation of enantiomers (Maier et al., 2001).

Typically, the chiral separation methods can be divided into two categories: one is a *direct method*, which is based on a diastereomer formation on a stationary phase or in a mobile phase. The other is an *indirect method*, which is based on a diastereomer formation by reaction with a homochiral reagent (Haginaka, 2002). In the direct approach transient rather than covalent diasteromeric complexation occurs between a chiral selector and the analyte. Discrimination of enantiomers is considered to depend on a three-point interaction between one enantiomer and the chiral selector. At least one of these interactions must be stereochemically dependent such that the other enantiomer can only form a less stable two-point complex. The chiral discriminator may be present in the mobile phase for use with conventional HPLC columns or it may be incorporated into the stationary phase to provide specialized chiral stationary phases (Porter, 1991). The indirect methods were divided into two categories: one is to derivatize the enantiomers using a homochiral derivatizing reagent and to separate the derivative using an achiral stationary phases. The other is to derivatize the enantiomers using an achiral derivatizing reagent and to separate the derivatives using a chiral stationary phase (Haginaka, 2002).

1.1.2. Transdermal drug delivery

1.1.2.1. Basic structure of the skin

The skin is the largest organ of the body, accounting for more than 10% of body mass, and the one that enables the body to interact most intimately

with its environment. The skin consists of four layers: the stratum corneum (noviable epidermis), the remaining layers of the epidermis (viable epidermis), dermis, and subcutaneous tissue. There are also several appendages: hair follicles sweat ducts, apocrine glands, and nails. In general, the functions of the skin may be classified as protective, maintaining homeostasis or sensing. The thickness of the skin is in the range of 0.5 mm (e.g. eyelid) to 4 mm (e.g. palm or sole). Figure 1.5 shows the basic structure of the human skin (Barry, 1983).
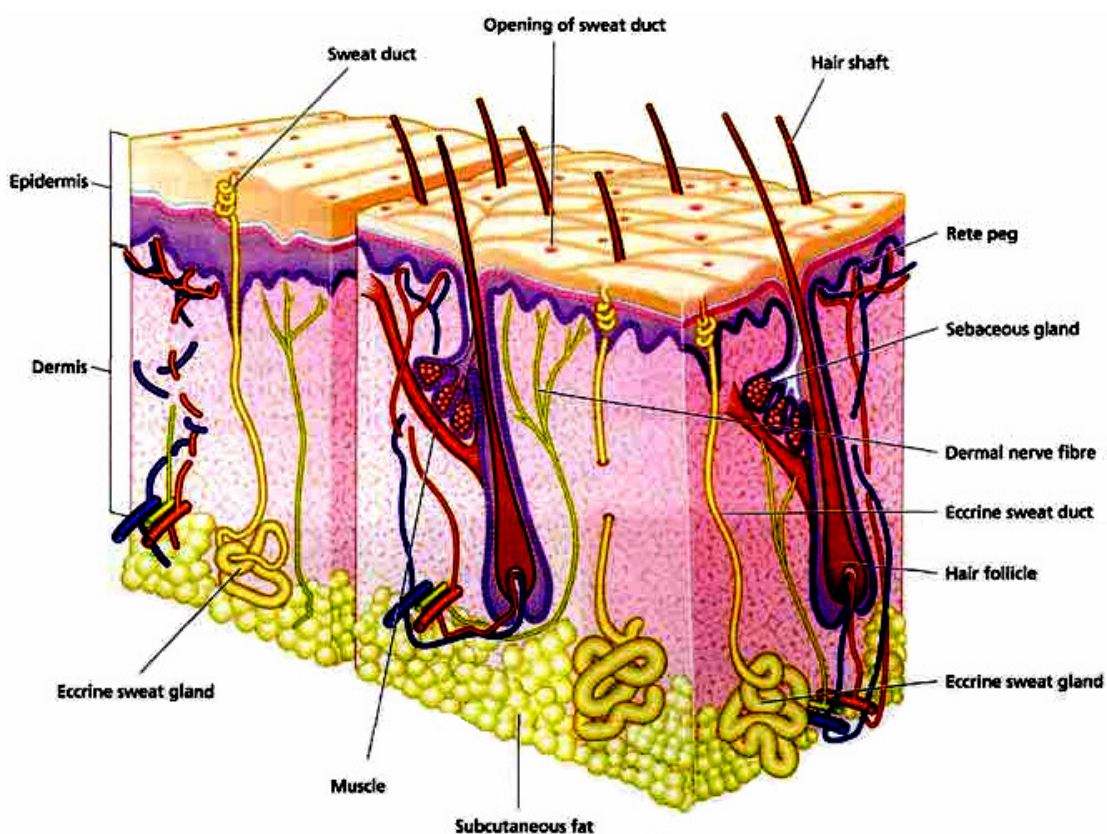
Figure 1.5. The three-dimensional structure of the skin; (left) the thick hairless skin of the palm of the hand, (right) the thin hairy skin of the forearm. (Downloaded from: http://www.pg.com/science/skincare/Skin_tws_9.htm)

Epidermis

The thickness of the epidermis varies, ranging from about 0.8 mm on the palms and the soles down to 0.06 mm on the eyelids. Cells provide epithelial tissue differ from those of all other organs in that as they ascend from the proliferative layer of basal cells they changed in an ordered fashion from metabolivally active and dividing cells to dense, dead, keratinized protein (Figure 1.6).
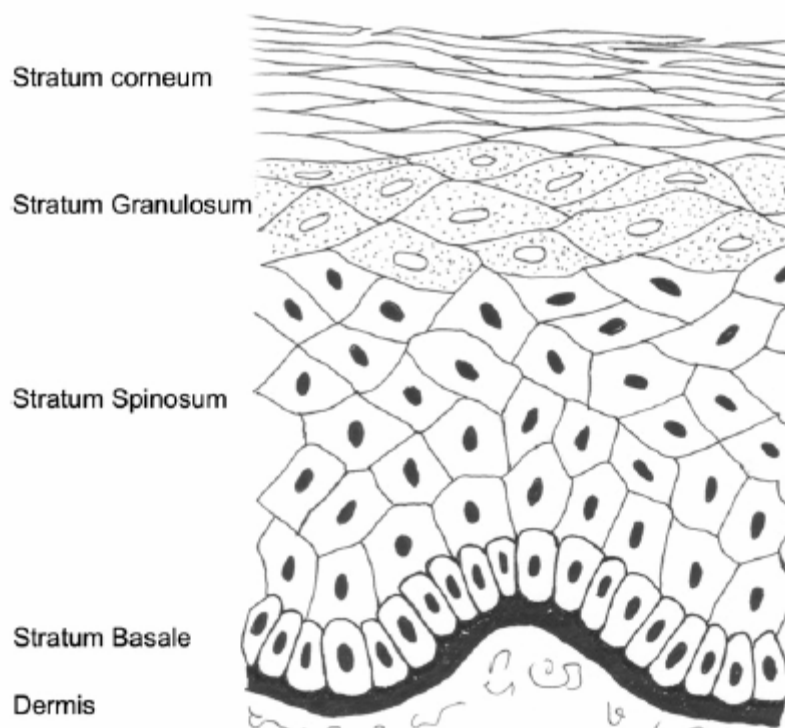
Figure 1.6. The different forms of the cells of the epidermis: as the cells move upwards they gradually change shape. Stratum lucidum (the clear layer) (not shown) is only found in the very thick epidermis of palms or soles. (Wickett and Visscher, 2006)

The epidermis have 5 layers: stratum basale, stratum spinosum, stratum granulosum, stratum lucidum and stratum corneum.

1. Stratum basal or basal layer

The basal cells are nucleated, columnar, and about 6 μm wide, with their long axis at right angles to the dermoepidermal junction; they connect by cytoplasmic intercellular bridges. Mitosis of the basal cells constantly renews the epidermis and this proliferation in healthy skin balances the loss of dead horny cells from the skin surface. The basal cell layer also includes melanocytes, which produce and distribute melanin granules to the keratinocytes in a complex interaction. Below the basal cell layer lays the complex dermoepidermal junction, which constitutes an anatomic function unit. The junction serves the three functions of dermal-epidermal adherence, mechanical support for the epidermis, and control of passage of cells and some large molecules across the junction.

2. Stratum spinosum or spinous layer

As the cells produced by the basal layer move outward, they alter morphologically and histochemically. The cells flatten and their nuclei shrink. These polygonal cells are called prickle cells because they interconnect by fine

prickles. Each prickle encloses an extension of the cytoplasm, and the opposing tips of the prinkles of adjacent cells adhere to form intercellular bridges-the desmosomes.

3. Stratum granulosum or granular layer

As the keratinocytes approach the surface, they manufacture basic-staining particles, the keratohyalin granules. It was suggested that these granules represent an early form of keratin. This keratogenous or transition zone is a region of intense biochemical activity and morphological change. The term "transition zone" defines a region between living cells and dead keratin, even when no granules form.

4. Stratum lucidum or lucid layer

The region is in the palm of the hand and the sole of the foot. This layer is an anatomical distinct, poorly staining hyaline zone forms a thin, translucent layer immediately above the granular layer.

5. Stratum corneum

As the final stage of differentiation, epidermal cells construct the most superficial layer of the epidermis, the stratum corneum. It is the heterogenous outermost layer of the epidermis and is approximately 10-20 μm thick. It is nonviable epidermis and consists of 15-25 flattened, stacked, hexagonal, and cornified cells embedded in a mortar of intercellular lipid. Each stratum corneum cell

is composed mainly of insoluble bundle keratins (~70%) and lipid (~20%) encased in a cell envelope, accounting for about 5% of the stratum corneum weight. The intercellular region consists mainly of lipids and desmosomes for corneocyte cohesion. The composition of the stratum corneum is shown in Table 1.2. A total turnover of the stratum corneum occurs once every 2-3 weeks. The stratum corneum also functions as a barrier to prevent the loss of internal body components, particularly water, to the external environment. In addition, the stratum corneum plays a crucial role in controlling the percutaneous absorption of drug molecules. The selective permeability of its elegant structure provides a central theme in many aspects of the study of the biopharmaceutics of topical products.

Table 1.2. Composition of the stratum corneum (Flynn, 1995).

Tissue Component	Gross composition	Percentage of dry weight
Cell membrane	Lipid, protein	~ 5
Intercellular space	Mostly lipid, some protein and polysaccharide	~20
Intracellular space	Fibrous protein,	~65-70
	Non-fibrous (soluble)	~ 5
Overall protein	protein	~ 10
	Water soluble,	~ 65-70
	Keratin,	~5

Overall lipid	Cell wall	10-20
Other		Up to 10
Water (normal hydration)		15-20
Water (fully hydrated)		Upwards of 300

6. Other cells of the epidermis

Langerhans'cells are dendritic cells with a labular nucleus, a clear cytoplasm containing characteristic Langerhans'cells granules, and well-developed endoplasmic reticulum, Golgi complex, and lysosomes. These cells are also involved in the immune response in the skin. Merkel's cell corpuscles attach to adjacent epidermal cells by numerous desmosomes. They are associated with the sensation of touch.

Dermis

The dermis, 3 to 5 mm thick, is much wider than overlying epidermis which it supports. The main structural component of the dermis is referred to as papillary layer and reticular layer. The dermis consists of collagenous fiber (70%), providing a scaffold of support and cushioning, and elastic connective tissue, providing elasticity, in a semigel matrix of mucopolysaccharides. The main cells present are the fibroblast, which produce the connective tissue components of collagen, laminin, fibronectin, and vitronectin; mast cells, which are involved in the

immune and inflammatory response; and melanocytes involved in the production of melanin.

Contained within the dermis is an extensive vascular network providing for the skin nutrition, repair, and immune responses and, for the rest of the body, heat exchange, immune response, and the thermal regulation. Skin blood vessels derive from those in the subcutaneous tissues, with an arterial network supplying the papillary layer, the hair follicles, the sweat and apocrine glands, the subcutaneous area, as well as the dermis itself. These arteries feed into arterioles, capillaries, venules, and then, into veins. The lymphatic system is an important component of the skin in regulating its interstitial pressure, mobilization of defense mechanisms, and in waste removal. It exists as a dense, flat meshwork in the papillary layers of the dermis and extends into the deeper regions of the dermis. A liberal nerve supply serves the skin, with great variations from region to region. Cutaneous nerves, nerve endings, and capillaries modulate the sensations of pain, pruritus (itching), touch, and temperature.

Subcutaneous tissue

The deepest layer of the skin is the subcutaneous tissue or hypodermis. The hypodermis acts as a heat insulator, a shock absorber, and an energy storage region. This layer is a network of the fat cells arranged in lobules and linked to the dermis by interconnecting collagen and elastin fibers. The sheet of fat lies between the relatively flexible skin and the unyielding, deep fascia, and its thickness varies with the age, sex, endocrine, and nutritional status of the individual.

The subcutaneous tissue provides a thermal barrier and a mechanical cushion; it is a site of synthesis and a depot of readily available high-energy chemicals.

Skin appendages

The highly vascularized dermis and the epidermis support several appendages. There are four skin appendages; the hair follicles with their associated sebaceous glands, eccrine sweat glands, apocrine glands, and the nails. Each appendage has a different function. The hair follicles are distributed across the entire skin surface with the exception of the soles of the feet, the palms of the hand and the lips. Although hair serves no vital purpose in humans, its psychological functions are all important. Eccrine sweat glands develop over the skin surface but not over mucous membranes. Sweat production accounts for about 80% of the water lost through the skin, with the transepidermal flux contributing the remainder. The principal function of the gland is to assist in heat control, as high external temperatures and vigorous exercise stimulate secretion. However, because the autonomic nervous system innervates the glands, emotional stress can also provoke sweating, that is, the clammy palm syndrome. Apocrine sweat glands are epidermal appendages which develop throughout the skin of the embryo as part of the pilosebaceous follicle. Most of the glands subsequently disappear so that the characteristic adult distribution is in the axilla, the perianal region, and the areola of the breast. The apocrine gland secretes a small quantity of a milky or oily fluid. The nail plate consists of "hard" keratin, with relatively high sulfur content, mainly in the form of the amino acid cysteine, which constitutes 9.4% by weight of the nail. Appendages are often faced as channels bypassing the stratum corneum barrier and

generally through to facilitate the dermal absorption of topical agents (Flynn, 1995 and Walters, 2002).

1.1.2.2. Basic skin functions (Barry, 1983, Flynn, 1995 and Walters and Roberts, 2002).

The skin performs many varied functions. The main functions of the skin are described below.

1. to protect from potentially harmful external stimuli: (a) mechanical impact; (b) thermal impact; (c) chemical impact; (d) microorganisms; (e) radiation; or (f) electrical impact.

2. To contain body fluid and tissues.

3. To receive external stimuli or to mediate sensation: (a) tactile; (b) pain; or (c) heat.

4. To regulate body temperature.

5. To synthesize and to metabolize compounds such as vitamin production.

6. To dispose of chemical wastes via grandular secretions.

7. To attract the opposite sex (apocrine secretions are evolutionarily defunct in this role).

8. To regulate blood pressure.

1.1.2.3. Routes of absorption across the skin

When molecules contact the skin, there are two potential pathways of the viable tissue (Figure 1.7) (Mills and Cross, 2006).

1. Appendageal transport

2. Epidermal transport
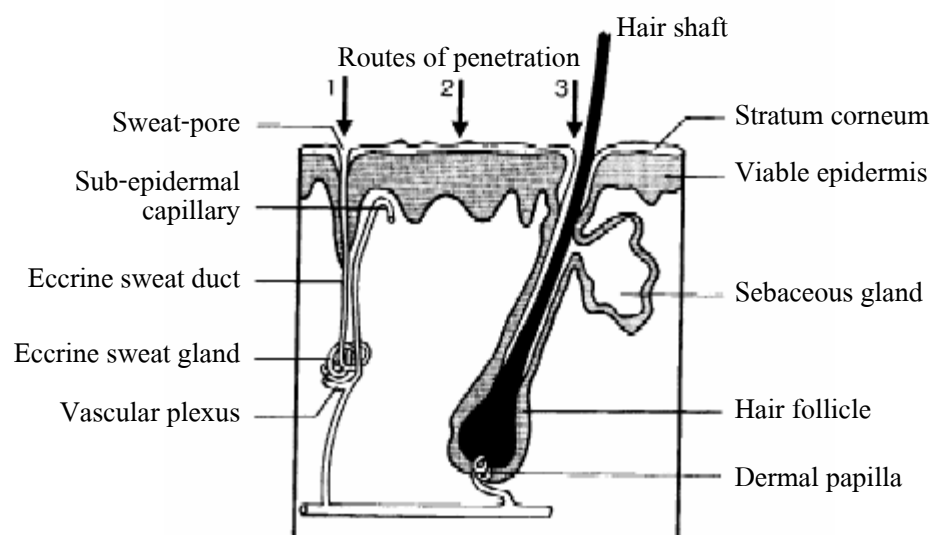
Figure 1.7. The schematic of skin structure and macroroutes of the drug penetration: (1) via the sweat ducts; (2) across the continuous stratum corneum or (3)

through the hair follicles with their associated sebaceous glands (Barry, 2002).

1. *Appendageal transport*

The appendageal pathways include the transport via the sweat ducts and through the hair follicles with their associate sebaceous glands as shown in Figure 1.7. The hair follicles and sweat glands have openings that effective bypass the subcutaneous barrier to the underlying dermal structure (Mills and Cross, 2006). Fraction appendageal area available for transport is only about 0.1%. This route usually contributes negligibly to steady state drug flux. The pathway may be important for ions and large polar molecules that struggle to cross intact stratum corneum. Appendages may also provide shunts, important at short times prior to steady state diffusion. Additionally, polymers and colloidal particles can target the follicle (Barry, 2001a).

2. *Epidermal transport*

The main barrier for transdermal delivery is stratum corneum, which its "brick and mortar" structure is analogous to a wall (Figure 1.8). The corneocytes of hydrated keratin comprise the "bricks", embedded in a "mortar", composed of multiple lipid bilayers of ceramides, fatty acids, cholesterol and cholesterol esters (Barry, 2001b). Drugs can penetrate across stratum corneum *via* two pathways; intercellular and transcellular pathways.
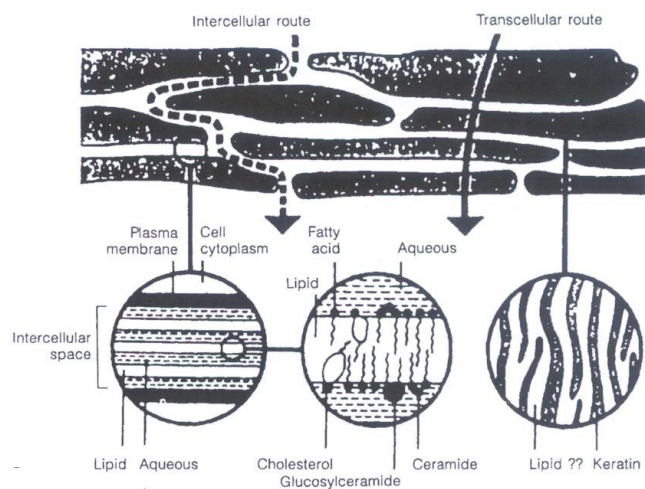
Figure 1.8. Simplified diagram of stratum corneum and the two micro routes of drug penetration across the stratum corneum (Barry, 2001a)**.**

For intercellular pathway, drugs move within intercellular lipids between keratinocyte. The speed of the solute movement through the skin, it is known as the diffusivity of the drug, and is limited by the binding of the drug to the keratinocytes, the viscosity of the intercellular environment and the tortuosity of the pathway. On the other hand, transcellular would require repeated partitioning of the solute between lipophilic and hydrophilic compartments, including the almost impenetrable intracellular matrix of the keratinocytes (Mills and Cross, 2006).

For transcellular pathway, it was originally believe that transcellular diffusion mechanisms dominated over the intercellular and transappendageal routes during the passage of solutes through the subcutaneous. Whereas, the intercellular pathway was initially dismissed as a potentially significant diffusion pathway because of the small volume they occupy. The physical structure of the intercellular lipids was thought to be a significant factor in the barrier properties of the skin. However, most experimental evidence now suggests that transport through the subcutaneous is by the intercellular route (Roberts et al., 2002).

1.1.2.4. Transdermal drug delivery system

Development of a new drug requires investment of 10-20 years and millions of dollars. Therefore, the development of drug delivery system has become increasingly important. Transdermal drug delivery system is one of the most interesting drug delivery system due to many advantages over the classical systems (oral or parenteral system). The application of preparations to the skin for cosmetic and medical purposes is as old as the history of medicine itself and references to the use of ointments, salves and pomades may be found in the early records of Babylonian and Egyptian medicine (Hadgraft and Lane, 2005).

Transdermal delivery is the delivery of drugs through the skin to affect a pharmacological action or actions at a location or locations remote from the site of action. Transdermal therapy can be regional or systemic as opposed to topical therapies wherein and confined to the skin tissues (Ramachandran and Fleisher, 2000).

The advantages of transdermal drug delivery systems

1.   To avoid the problems of stomach emptying, pH effects, and enzyme deactivation associated with gastrointestinal passage (Walters and Roberts, 2002).

2.   To avoid the hepatic first-pass metabolism (Walters and Roberts, 2002).

3.   To enable control of input, as exemplified by termination of delivery through removal of the device (Walters and Roberts, 2002).

4.   To substitute for oral administration of medication when that route is unstable, as in instances of vomiting and/or diarrhea (Ansel et al., 1995).

5.   To avid the risks and inconveniences of parenteral therapy and the variable absorption and metabolism associated with oral therapy (Ansel et al., 1995).

6.   To provide the capacity for multiday therapy with a single application, thereby improving patient compliance over use of other dosage forms requiring more frequent dose administration (Rolland, 1993 and Ansel et al., 1995).

7.   To extend the activity of drugs having short half-lives through the reservoir of drug present in the therapeutic delivery system and its controlled release characteristics (Ansel et al., 1995).

8.   To provide ease of rapid identification of the medication in emergencies (Ansel et al., 1995).

9. Reduction of potential adverse side effects (Rolland, 1993).

10. Good patient compliance (Rolland, 1993).

11. Ease of self-administration (Rolland, 1993).

The disadvantages of transdermal drug delivery systems

1. The variability in percutaneous absorption owing to sites, disease, age, and species differences (Walters and Roberts, 2002).

2. The skin's metabolic effect, thereby reducing the efficacy of the drug (Walters and Roberts, 2002).

3. The reservoir capacity of the skin (Walters and Roberts, 2002).

4. Irritation and other toxicity caused by topical products. Therefore, the transdermal route of administration is unsuitable for drugs that irritate or sensitize the skin (Ansel et al., 1995 and Walters and Roberts, 2002).

5. Technical difficulties are associated with the adhesion of the systems to different skin types and under various environmental conditions, and the development of rate-controlling drug delivery features which are economically feasible and therapeutically advantageous for more than a few drug substances (Ansel et al., 1995).

6. Only relatively potent drugs are suitable candidates for transdermal delivery due to the natural limits of drug entry imposed by the skin's impermeability (Ansel et al., 1995).

The success of the transdermal drug delivery is evidenced by the fact that there are more than 35 transdermal drug delivery products approved in the USA for the treatment of a wide variety of conditions including: hypertension, angina, motion sickness, female menopause, male hypogonadism, severe pain, local pain control, nicotine dependence, contraception and urinary incontinence (Table 1.3) (Thomas and Finnin, 2004).

Table 1.3. Examples of the transdermal drug delivery products (Vasil'ev et al., 2001, Tan and Pfister, 1999 and Scheindlin, 2004).

Drug	Trade name	Action
Scopolamine	Scopoderm Transdermal-Scop	Anti-motion sickness
Nitroglycerine	Nitroderm Nitrodur	Antianginal
Isosorbide dinitrate	Frandol-Tape	Antianginal
Clonidine	Catapres	Antihypertensive
Estradiol	Estraderm	Female hormonal
Nicotinine	Nicotinel	Antinicotinic
Fentanyl	Duragesic	Narcotinic analgesic
Testosterone	Androderm Testoderm	Male hormonal
Lidocaine	Lidoderm	Local pain control

1.1.3. Molecularly imprinted polymer

1.1.3.1. The concept of molecular imprinting

Since the Nobel Prize was awarded to Cram, Lehn, and Pederson in 1987, the term 'molecular recognition' has been recognized all over the world. Since molecular recognition is the origin of biological functions, the preparation and combination of synthetic molecules capable of molecular recognition may regenerate bio-functionalized artificial molecules. Such biomimetic molecules would be extremely useful as substitutes for biomolecules in biotechnological, medical, and bioanalytical fields. Therefore, the design and synthesis of artificial receptors have attracted a great deal of attention and experiments have been conducted in many laboratories. One such biomimetic strategy involving the formation of supramolecules, 'molecular imprinting' is recognized as a tailor-made way of preparing functionalized synthetic polymers capable of molecular recognition of given molecules (Takeuchi and Haginaka, 1999).

The history of molecular imprinting is usually traced back to the experiments of Dickey in the 1940s and 1950s who was inspired to create affinity for dye molecules in silica gel by a theory of Linus Pauling as to how antibodies are formed. Dickey's silicas can be considered to be the first imprinted materials (Mayes and Whitcombe, 2005). The imprinting of organic polymers was first reported by

Wulff in 1972 (Wulff, 1995). Whereas, non-covalent imprinting in the form we know today was introduced about a decade later.

The concept of molecular imprinting is depicted in Figure 1.9. Two principally different approaches to molecular imprinting may be distinguished. The *non-covalent*, or self-assembly, approach where complex formation is the result of non-covalent or metal ion coordination interactions. The *covalent*, or pre-organized, approach which employs reversible covalent bonds, usually involves a prior chemical synthesis step to link the monomers to the template (Andersson, 2000).
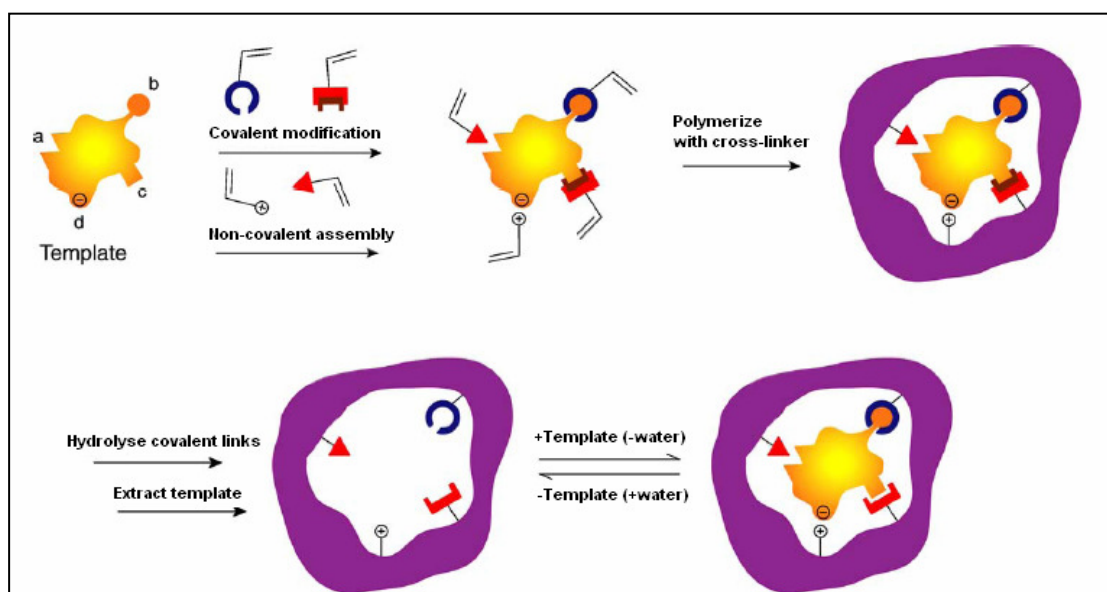
Figure 1.9. Schematic representation of the two most common imprinting strategies: Covalent imprinting and Non-covalent imprinting (Mayes and Whitcombe, 2005).

Molecular imprinting processes are composed of the following three steps (Figure 1.9):

1.   Preparation of covalent conjugate or non-covalent adduct between a functional monomer and a template molecule,

2.   Polymerization of this monomer-template conjugate (or adduct), and

3.   Removal of the template from the polymer.

In step 1, functional monomer and template are connected by a covalent linkage (in 'covalent imprinting') or they are placed nearby through non-covalent interactions (in 'non-covalent imprinting'). In step 2, the structures of these conjugates (or adducts) are frozen in a three-dimensional network of polymers. The functional residues (derived from the functional monomers) are topographically complementary to the template. In step 3, the template molecules are removed from the polymer. Here, the space in the polymer originally occupied by the template molecule is left as a cavity. Under appropriate conditions, these cavities satisfactorily remember the size, shape, and spatial arrangement functional groups of the template, and bind this molecule (or its analog) efficiently and selectively (Komiyama et al., 2003).

For the covalent approach, the most common types of linkages are either esters of carboxylic/boronic acids, ketals or imines (Schiff bases). After the polymer is formed, the template is extracted by cleavage of these covalent bonds. Rebinding of the template to the matrix is then achieved by re-establishing the

covalent bonds between the template and the polymer. The other, non covalent approach exclusively uses non-covalent interactions in the recognition of the templates. Typical interaction types that have been exploited are ionic interactions, hydrogen bonds, π-π interactions, and hydrophobic interactions (Mosbach and Ramström, 1996).

1.1.3.2. Configurations and applications of molecular imprinted polymers

Many particular features have made molecularly imprinted polymers (MIPs) the target of intense investigation including their high affinity and selectivity, which are similar to those of natural receptors, their unique stability which is superior to that demonstrated by natural biomolecules and the simplicity of their preparation and the ease of adaptation to different practical applications. The resulting polymers are robust, inexpensive and, in many cases, possess an affinity and specificity that is suitable for industrial application (Piletsky et al., 2001). MIPs have been used in many fields such as separation processes, drug delivery, analysis (Mayes and Mosbach, 1997 and Andersson, 2000), immunoassay and antibody mimics (Kempe and Mosbach, 1995a), biosensor recognition elements (Hillberg et al., 2005) and catalysis and artificial enzymes (Pasetto et al., 2005 and Kalim et al., 2005). The applications of MIP in separation sciences expand in many fields including liquid chromatrography (Kempe and Mosbach, 1995b, Plunkett and Arnold, 1995, and Ellwanger et al., 2000), solid phase extraction (Walshe et al., 1997a and Masqué et al.,

2001), capillary electrophoresis (Schweitz et al., 1998) and membrane separation (Ulbricht, 2004).

MIPs synthesized from various polymerization methods can give the different formats of the polymers. The configurations of MIP are bulk polymer, monodisperse, microbeads and membrane. Figure 1.10 shows the relation between the configurations of MIP and its applications. Before generating the molecularly imprinted material, the user has considered the later purpose, in order to predetermine the adequate format of the polymer.
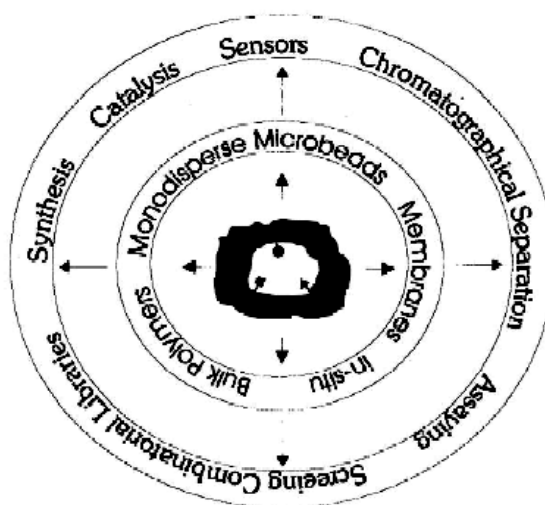
Figure 1.10. Configurations and applications of molecularly imprinted polymers (Brüggemann et al., 2000).

1.1.3.3. Molecularly imprinted membrane

Interest in membrane technology has been increasing in various fields of science and technology and advanced synthetic membranes with the recognition are explored widely. The development of synthetic membranes always inspire by the fact that the selective transport through biological membranes is enabled by highly specialized macromolecular and supramolecular assemblies based on and involved in molecular recognition.

Molecularly imprinted membrane (MIM) is one of the advanced membranes. It has been developed based on the hypothesis that combination of imprinting and membrane technologies has been proposed to develop stable permselective or affinity membranes for separation of special target molecules from a mixture of structurally similar compound (Sergeyeva et al., 2001). MIM is a membrane either composed of a MIP or containing a MIP. Therefore, MIM can be classified in two categories; monolith membrane and composite membrane.

Three main strategies can be envisioned for the preparation of MIM:

1. *sequential approach from presynthesized MIPs towards MIM*

The membranes are prepared from previously synthesized 'conventional' MIP. For example, the MIP nanoparticles were arranged as a filter cake between two microfiltration membranes.

2.   *simultaneous formation of MIP sites in and morphology of self-supported MIM*

The synchronization of imprinting and solidification are critical importance for MIM shape, structure and function. Two main routes towards MIM had been used, the "traditional" *in situ* crosslinking polymerization and the "alternative" polymer solution phase inversion, both in the presence of templates. The main problem of this approach is high levels of cross-linking traditionally used in molecular imprinting for achieving a desirable selectivity. Therefore, MIMs from this approach are poor mechanical stability and low fluxs. For improving the properties for the membrane, the phase inversion approach was developed. Although the stability of the membranes improved, the flux of the MIM synthesized via phase inversion still low.

3.   *preparation of the composite membrane*

For this approach, MIPs are prepared on or in support membranes with suited morphology. The preparation of MIP composite membranes should allow to adjust membrane pore structure and MIP recognition sequentially and by two different materials. The MIMs have been studied widely and synthesized *via* different methods. Figure 1.11 shows the different types of composite imprinting membrane. In conclusion, the sequential approach will allow to use the base membrane pore structure (barrier pore size) and layer topology (symmetric versus asymmetric) as well as the location of the MIP—on top of ("asymmetric") or inside ("symmetric") the support membrane to prepare different MIM types, with the MIP either as selective barrier or transport phase or as an affinity adsorber layer (Ulbricht, 2004).
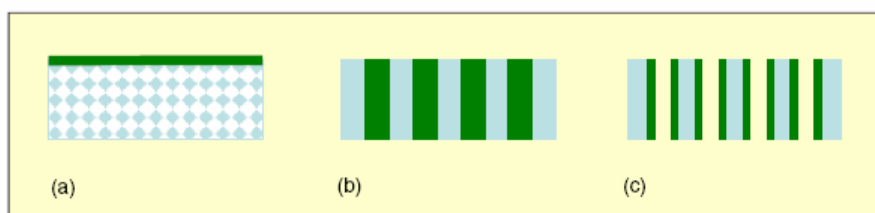
Figure 1.11. Schematic depiction of three main composite membrane types: (a) thin-film, (b) pore-filling, (c) pore surface-functionalized (relative dimensions not to scale) (Ulbricht, 2006).

Molecularly imprinted membrane has been used in many applications such as sensor (Sergeyeva et al., 1999, Pogorelova et al., 2004 and Suedee et al., 2004), catalytic (Kalim et al., 2005), selective transport (Mathew-Krotz and Shea, 1996 and Chen et al., 2006) and separations. Especially in separation, the applications of molecularly imprinted polymers to membrane separation have been investigated extensively after the first report of Piletsky et al. (Yoshikawa, 2002), for examples in solid phase extraction (Sergeyeva et al., 2001 and Malaisamy and Ulbricht, 2004), separations (Hilal et al., 2003 and Kietczyński and Bryjak, 2005), microfiltration membranes (Kochkodan et al., 2001 and Hilal and Kochkodan, 2003) and chiral separations.

1). MIM for chiral separations

The separations of carbohydrate enantiomers and diastereomers on covalently imprinted polymers, made using sugar-boronate complexes as templates, were studied by Wulff et al. in 1977. Significant improvements were made with the covalent imprinting strategy, but the greatest advances in chiral separations with MIPs have been achieved with non-covalent imprinting of organic polymers as introduced by Mosbach et al. (Kempe and Mosbach, 1995a and Ansell, 2005). Early works of the use of MIPs in chiral separation were based on MIP-based chiral stationary phases in chromatrography (Owens et al., 1999 and Sellergren, 2001). Many racemic substances can be separated by imprinting materials *via* liquid chromatrography and capillary electrophoresis such as amino acid derivatives (O'shannessy et al., 1989 and Andersson et al., 1990) , cinchonine (Huang et al., 2004), nateglinide (Yin et al., 2005) and antihistamine drugs (Haginaka and Kagawa, 2004).

After the increasing of the knowledge of the imprinting membrane and the development of the composite MIM, the studies of MIMs in chiral separations of various substances have been extensively explored for examples, glutamic acid derivative (Kondo et al., 2000), naproxen (Donato et al., 2005) and phenylanaline (Jiang et al., 2006 and Sekine et al., 2007).

2). MIM for drug delivery

There are huge interesting and potential of MIP in drug delivery that can bring intelligent drug release or can target a therapeutic to a particular site of action (Figure 1.12) (Bures et al., 2001 and Sellergren and Allender et al., 2000) or can enhance the drug loading capacity of the polymer or can modify the release of the drug (Nostrum, 2005). For example, the release of the drug can be governed by the chemical stimuli (Alvarez-Lorenzo and Concheiro, 2004 and Bures et al., 2001) or external environment such as temperature (Watanabe et al., 1998), pH and surface antigen, therefore the drug would be released in an appropriate amount or at the desired target organ which is the aims of controlled release system (Figure 1.13).
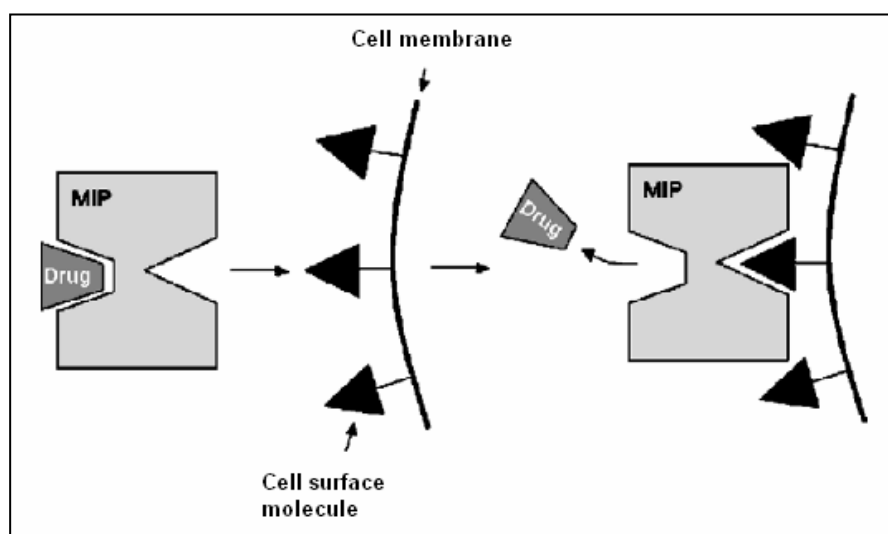
Figure 1.12. Targeted drug delivery using a molecularly imprinted carrier (Sellergren and Allender, 2005).
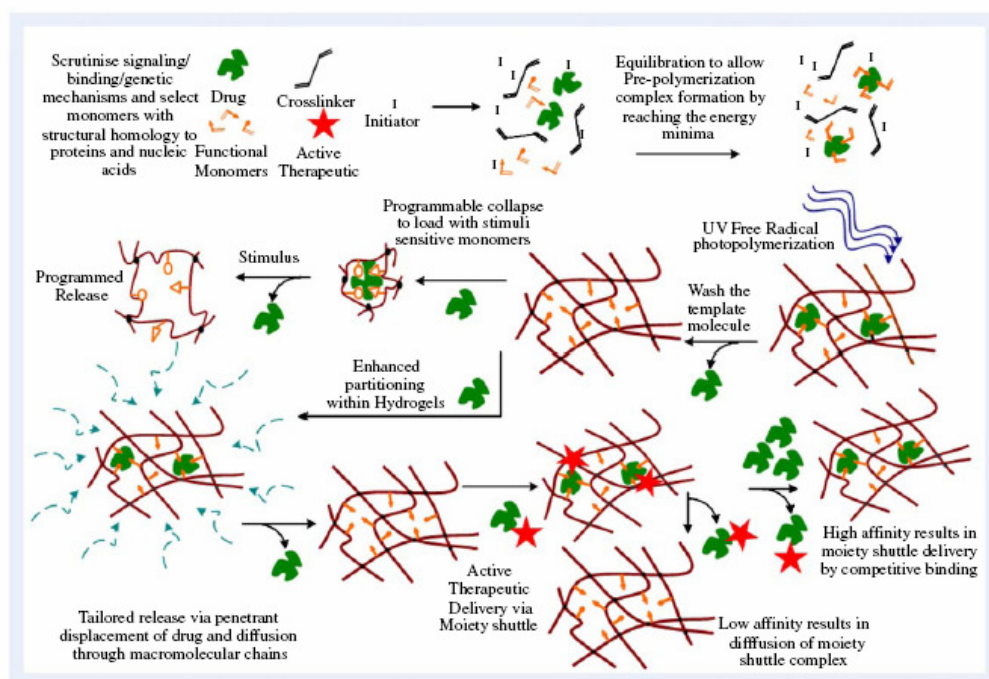
Figure 1.13. Imprinting technique for synthesized the imprinted hydrogel (Venkatesh et al., 2007).

Figure 1.13 is the illustration of a mixture of functional monomers and drug are mixed together to form a pre-polymerization complex. Upon rebinding the molecule of interest and depending on the macromolecular structure, one could have programmable collapse and release from a stimulus, or enhanced loading and affinity within hydrogels. The technique can be generalized, considering the drug could be a moiety, which could act as a moiety shuttle to deliver an active therapeutic, such as with a prodrug mechanism (Venkatesh et al., 2007).

To approach the high outcome, MIP was synthesized in varies method to make the suitable forms for each propose. Although, the studies of MIP for drug delivery purposes mainly focus on developing the microparticle or nanoparticle imprinted polymer but the advantages of MIM have been shown in many studies especially in ocular drug delivery. The benefits of MIM for ocular therapy are improving the loading capacity and sustaining of the drug level. The imprinted soft contact lens containing various drug were synthesized for example timolol (Hiratani and Alvarez-Lorenzo, 2002 and Hiratani et al., 2005), norfloxacin (Alvarez-Lorenzo et al., 2006) and H_1-antihistamine (Venkatesh et al., 2007).

1.2. Objectives of the thesis

The objectives of this thesis are 1) to prepare the composite MIP cellulose membrane, 2) to determine the enantioselective properties of the synthesized membranes, 3) to prepare the transdermal patch containing the MIP membrane and 4) to evaluate the efficacy of the patch comprising of the composite MIP cellulose membrane, either *in vitro* and *in vivo* using Wistar rat.

In this study, the bacterially-derived cellulose membrane was chosen as a membrane base for the composite MIP membrane because of the enantioselective property itself (see section 2.1). The bacterial cellulose membranes were prepared from the cultivation of *Acetobacter xylinum* TISTR 975. Three types of the different bacterial cellulose membranes were obtained from various cultivation conditions. The bacterial cellulose membranes were characterized and determined the enantioselective

binding and transport parameters for *S*-propranolol. The binding characteristic of the membranes were examined by batch binding assay and the transport studies were investigated by using Franz diffusion cells. The amounts of propranolol enantiomers were determined by HPLC assay with a chiral column.

The enantioselective transport mechanism of the composite membrane was investigated from the release studies. The different composite membranes were synthesized by using different template polymers (*R*- or *S*-propranolol). The selectivity of the composite MIP membranes and all the reference membranes (non-imprinted membrane and cellulose membrane) were examined.

The *in vitro* - release of the composite membranes were studied with the excised rat skin. The different concentrations of the propranolol were filled into the donor compartment and then the enantioseletivity release of *S*-propranolol was determined in order to search the appropriate concentration of the drug giving the best result. In addition, different propranolol ester prodrugs were synthesized. Subsequently, enantioselective releases of the propranolol prodrugs for the composite MIP membranes were evaluated. The enantiomer release data of the composite MIP membrane obtained with racemic propranolol in donor phase of Franz diffusion cells were compared with these of racemic propranolol prodrugs, prior to evaluate.

The effects of the two different gel formulations on the enantioselective transport of the composite MIP membrane were studied by using Franz diffusion cells. The suitable gel formulation was chosen as a drug reservoir for the transdermal patch.

Furthermore, the reservoir type-enantioselective transdermal patch of racemic propranolol was fabricated with the composite MIP membrane and a gel reservoir. *In vivo* study of the MIP patches were examined and the enantioselective transport of the MIP patches containing racemic propranolol were evaluated upon comparison with the gel formulation containing of either racemic propranolol or pure *S*-propanolol.

1.2.1. Propranolol: the drug of interest

Propranolol, a non-selective β-adrenergic blocker, was synthesized in 1963, described first in 1964, shown to be effective in treatment of hypertension that same year, and marketed in England in 1965. After that a large series of similar drugs have been synthesized (Kaplan and Lieberman, 1998). The purposed mechanisms of β-blockers in hypertensive actions are reduction in cardiac output, effect on central nervous system, inhibition of rennin, reduction in venous return and plasma volume, reduction in peripheral vascular resistance, improvement in vascular compliance, resetting of baroreceptor levels, effects on prejunctional β-receptors, reduction in norepinephrine release and attenuation of pressure response to catecholamines with exercise and stress (Frishman and Jorde, 2000).

Propranolol exists as a white or almost white crystalline powder with a melting point of 163 to 166 °C (The United States Pharmacopeia, 2007 and O'Neil et al., 2001). The molecular weight of propranolol and propranolol HCl are 259.3 and 295.8 g mol^{-1}. Propranolol is soluble in water and ethanol and practically insoluble in ether, benzene and ethyl acetate (O'Neil et al., 2001).

Propranolol is used for management of many various cardiovascular diseases such as hypertension, angina pectoris, phenochromocytoma, essential tremor, tetralogy of Fallot cyanotic spells and cardiac arrhythmias and for prevention of myocardial infraction and migraine headache (Lacy et al, 2007). Its bioavailability, following oral administration, is low (15-23%) and variable because of an extensive and highly variable first pass metabolism in the liver. The metabolism pathway of propranolol is shown in Figure 1.14. In addition, due to its short plasma half-life (3-6 hours), patients are routinely asked to take propranolol in divided daily doses every 6 to 8 h. Such frequent drug administration may reduce patient compliance and thus therapeutic efficacy (Taylan et al., 1996). Among β-blocker drugs, interpatient variation of propranolol seems to be highest (20-fold) because of its low oral bioavailability (Frishman and Jorde, 2000). Propranolol is available in solution and tablet for oral administration, solution for injection administration and capsule for oral-sustained release form (Lacy et al, 2007). Although commercially sustained-release propranolol can prolong the duration of action, the oral bioavailability is still low (20%) (Frishman and Jorde, 2000)**.**
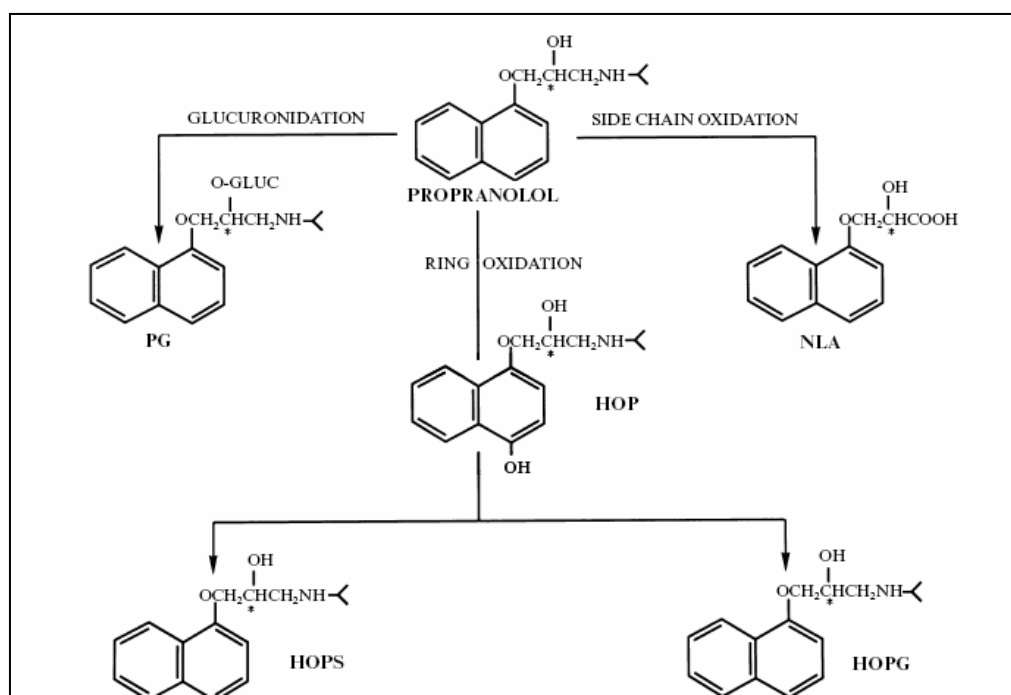
Figure 1.14. Schematic of propranolol's metabolism through three primary metabolic pathways. Chiral centres are depicted by the asterisk (*). Abbreviations: PG, propranolol glucuronide; HOP, 4-OH propranolol; HOPS, 4-OH propranolol sulphate; HOPG, 4-OH propranolol glucuronide; NLA, naphthoxylactic acid (Sowinski et al., 1996).

Different ways of enhancing its bioavailability have been explored. Developing the sustained release system method is expected that hepatic first-pass metabolism can be exacerbated. These included microcapsules (Pongpaibul and Whitworth, 1986), tablet coated with a macroporous membrane (Shivanand and Sprockel, 1993) and biphasic HALO^{TM} capsules (Barnwell et al., 1996). Changing the route of administration is the other method that can avoid the first-pass metabolism. Some studies were focused on the buccal administration (Brun et al., 1989, Chen and Hwang, 1992 and Taylan et al., 1996) and rare was studied in rectal administration (Morimoto et al., 1989). The most interesting method to improve the drug efficacy is transdermal administration. Additionally, the commercial available form of the drug, propranolol HCl, is hydrophilic in nature and hence its absorption through the skin is poor. For this reason, different ways of enhancing its skin penetration have been explored both passive transdermal and active transdermal delivery. For active delivery, iontophoresis with the chemical enhancers was studied to increase the permeation of propranolol (Chesnoy, 1999). Many types of chemical enhancers were studied for passive method such as n-nonanol and n-nonane (Hori et al., 1989), n-nonane (Melendres, 1993), fatty acids (Scott et al., 2001), terpenes (Kunta rt al., 1997) and terpenes/ethanol (Zhao and Singh, 1999). Few studies were developed the drug

system for transdermal purpose including disperse system (Ktistis and Niopas, 1998) and organogel-based system (Bhatnagar and Vyas, 1994). Due to the approval of transdermal drug delivery patches and the developing of the materials for transdermal patch production, the transdermal patches have been explored (Thacharodi and Rao, 1995, Krishna and Pandit, 1996, Guyot and Fawaz, 2000, Amnuaikit et al., 2005). In addition, lipophilic prodrugs have been studied as potential methods for increasing the skin permeability of propranolol (Ahmed et al., 1995 and Ahmed et al., 1997).

Propranolol is safe and can be used in children, adverse reactions and overdosage/toxicology of the drug can be found. The overdosage/toxicology reactions of propranolol are summarized in Table 1.4.

Table 1.4. The overdosage/toxicology reactions of propranolol (Lacy et al, 2000).

Organ systems	Overdosage/Toxicology
Cardiovascular system	Hypotension, bradycardia, atrioventricular block, intraventricular conduction disturbances, and cardiogenic shock
Central nervous system	Convulsions, coma, seizures
Respiratory system	Respiratory arrest
Endocrine system	Hyperkalemia and hypoglycemia

Stereoselective property of propranolol

It is known that, propranolol shows stereoselective activity, which the *S*-isomer is 130 times more potent than the *R*-isomer (Sheldon,1993). The side chain with an isopropyl or bulkier substituent on the amine appears to favor interaction with β-receptors (Figure 1.15). The nature of the substituent on the aromatic ring determines whether the effect will be predominantly activation or blockade. These substituents also affect cardio-selectivity. The alphatic hydroxyl group appears to be essential for activity, and the *S*-enantiomers of the β-adenergic antagonist are much more potent than the *R*-enantiomers. (Aboul-Enein and Basha, 1997).

Propranolol

R-propranolol   *S*-propranolol
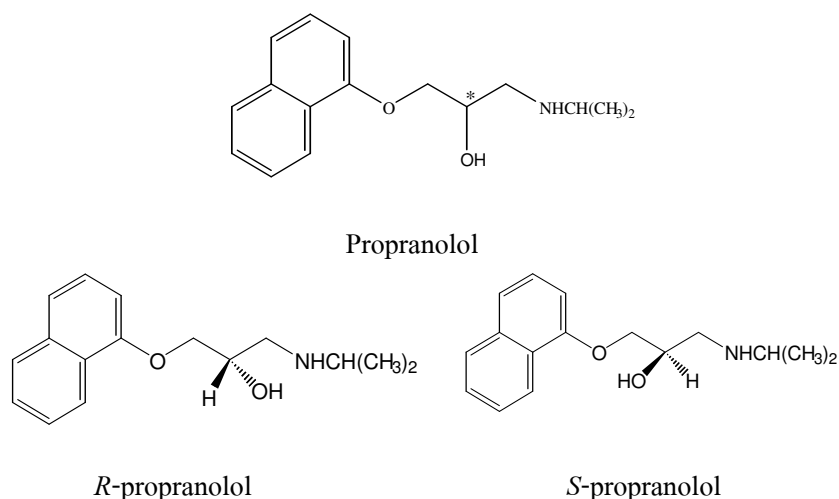
Figure 1.15. Chemical structure of propranolol, *R*-propranolol and *S*-propranolol and Chiral centres are depicted by the asterisk (*).

However, propranolol is available in a racemic mixture. As mentioned in previous section, propranolol enantiomers can interact with protein and receptor differently, resulting in the different in pharmacokinetic activities as well as pharmacological action of its enantiomers (Mehvar and Brocks, 2001). Therefore, there are many studies involved the stereoselective pharmacokinetic of propranolol in animal models and humans. Although such studies are widely, the pharmacokinetic parameters from different studies are varied therefore it remains difficult to identify the exact parameters.

a. Pharmacological actions

With propranolol *in vivo* the antianginal and antihypertensive effects are caused by the *S*-enantiomer, the *R*-enantiomer being ineffective. Propranolol is also a class II antiarrhythmic agent and again it is the *S*-enantiomer which has the greater effect on ventricular fibrillation, whereas both enantiomers have similar effects on the refractory period (Crossley, 1995).

In animals, *S*-propranolol is about 100 times more potent than *R*-propranolol in blocking ionotropic and chronotropic response to isoproterenol (β_1 and β_2). Both isomers posses a similar potency for the membrane-stabilizing action that is characteristic of class I antiarrhythmic drugs and is also referred to as the quinidine-like effect. Similar differences in isomer potency have been demonstrated in human. In hypertensive patients, the same daily dose of racemic propranolol and the non-β blocking *R*-isomer inhibited thrombin and arachidonic acid induced platelet

aggregation and thromboxane synthesis. Only the β blocking *S*-isomer is effective against angina (Aboul-Enein and Basha, 1997).

b. Absorption

Generally there is little enantiomeric differentiation in passive transport across membranes such as the gut wall, because these processes are dominated by the lipid and aqueous solubilities and are the same for both enantiomers. Racemates, however, can have significantly altered solubility and other physical properties. So, for example, *S*-propranolol demonstrates a threefold greater ability to penetrate skin than the racemate and would be the candidate of choice for transdermal delivery (Crossley, 1995).

c. Distribution

The influence of aging on the pharmacokinetics and tissue distribution of *R*- and *S*-propranolol was studied in 3-, 12-, and 24- month-old-rats. After both i.v. and oral administration of racemic propranolol, the plasma concentrations were higher for the *R*- than *S*-enantiomer. For the tissue concentrations, the reverse was true. The free fraction of *S*-propranolol in plasma was about four times larger than that of *R*-propranolol, and this is the main factor responsible for the differences in kinetics between the two enantiomers. There was a suggestion for a difference in tissue binding between the two enantiomers. With aging, the plasma and tissue concentrations of both enantiomers increase, probably due to a decrease in

blood clearance. Tissue binding did not change much with aging. Notwithstanding the marked differences between the kinetics of the propranolol enantiomers, the changes that occur with aging affect both enantiomers to the same degree (Ahuja, 1997b).

Propranolol binds to α_1-acid glycoprotein (AGP) favoring the S-enantiomer, whereas for binding to human serum albumin (HSA) the R-enantiomer is favoured (Drayer, 1988).

Mehvar and Brocks (2001) reviewed the stereospecific pharmacokinetics of β-blockers in humans. From the studies of tissue distribution of propranolol enantiomers, they suggested that while the concentrations of the enantiomers of propranolol in different tissues may be stereoselective, the actual tissue uptake and binding of these drugs in most cases is non-steroselective.

d. Metabolism

Metabolic processes involve the interaction with enzyme systems which have two functions in the body. One is to aid in the creation of new materials for cellular construction and the production of chemicals to aid in its function. The other main function is to break down and elimination the substances from the body. As with all receptor-like interactions, these enzyme systems display great substituent and stereo-chemical sensitivity. The rate of metabolism of two enantiomers would be expected to differ where they form diastereomeric complexes with the metabolizing enzyme (Crossley, 1995).

Propranolol has a wide range of metabolic routes at its disposal, sometimes producing biologically active metabolites. The processes are varied and stereoselective, with $R > S$ selectivity being observed for N-dealkylation and para-hydroxylation but $S > R$ selectivity being observed for deamination and glucoronidation. This combination leads to an overall predominance of the S-enantiomer in the plasma in man. In the dog, however, $R > S$ is observed for N-dealkylation and deamination but $S > R$ selectivity for para-hydroxylation and glucuronidation leading to overall predominance of the R-enantiomer (Crossley, 1995).

The metabolism of S-propranolol occurs principally by glucoronidation in dogs and humans and this enantiomer noncompetitively inhibits the glucoronidation of the R-propranolol in microsomal preparations from dog liver, with corresponding effect on its half-life in humans (Crossley, 1995).

e. Excretion

In rabbits, high intravenous doses of propranolol induce small stereoselective differences in the elimination of the enantiomers of propranolol. In this case, S-propranolol is eliminated more rapidly than R-propranolol (Marier et al., 1998).

Propranolol was chosen as a model drug in this thesis because of the more attractive properties of propranolol. Propranolol is a chiral drug. In case of propranolol, it is administered as racemates since the distomer displays no undesirable side effects. *S*-propranolol (eutomer) is 130 times as active as its *R*-propranolol (distomer) which effectively means that the latter is totally inactive. Propanolol is marketed as the racemate, the decision to make this drug as racemate was probably influenced by the fact that it is difficult to separate by classical method (Sheldon, 1993).

1.2.2. Cellulose membrane: the membrane of interest

Polysaccharides, such as cellulose and amylase, are the most readily available polymers with optical activity and known to exhibit resolution as a chiral stationary phase. The first utilization of the chirality of cellulose for resolution was demonstrated by Kotake et al. They separated racemic amino acid derivatives into two spots of enantiomers by paper chromatography. The enantioselectivity of the cellulose derivatives was shown from the studies of Okamota and co-workers (Okamoto et al., 1986a and Okamoto et al., 1986b). Hence, the studies of cellulose derivatives-based chiral stationary phases in liquid chromatrography have been extensively investigated (Aboul-Enein, 2001, Franco et al., 2001, Yashima, 2001 and Bonato et al., 2002). The structure of the cellulose derivatives used as chiral stationary phases are shown in Figure 1.16.
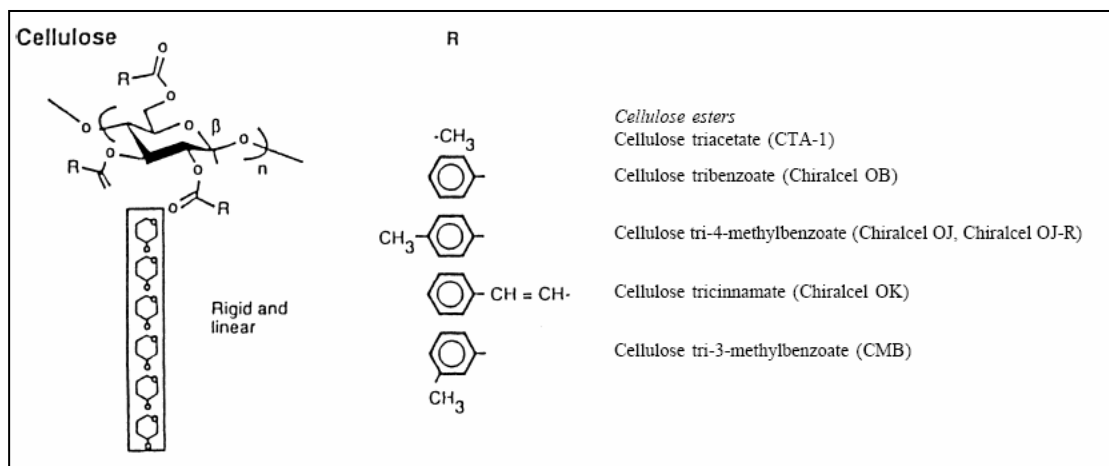
Figure 1.16. Structure of the cellulose chiral stationary phases (Aboul-Enien, 2001).

There are two mechanisms involved the stereoselective properties of the cellulose and cellulose derivatives. The first mechanism is inclusion; the solute molecules can enter the chiral cavities or channels and form inclusion complexes. The two enantiomers of a chiral solute will fit differently into these cavities, forming diastereomeric complexes and leading to the separation of the two isomers. The other is the formation of the solute-chiral stationary phase complex through hydrogen bonding. However, the inclusion complexes play an important role for enantioselective properties (Wainer, 1988). The more information of bacterial cellulose is detailed in Chapter 3.

CHAPTER 2

THE STUDY OF PROPRANOLOL PROPERTIES AND

METHOD VALIDATION

2.1. Propranolol

2.1.1. Separation of propranolol enantiomers

Many researches have been explored the method to separate the propranolol enantiomers. The reported methods included liquid chromatrography with chiral stationary phase or chiral selectors (Dyas, 1992, Facklam and Modler, 1994, Welch and Perrin, 1995, Götmar et al., 2001 and Kafková et al., 2005), capillary electrophoresis with molecularly imprinted polymer (Walshe et al., 1997b), capillary electrophoresis with chiral selector (Na et al., 2004), membrane strategy (Gumí et al., 2005a and Gumí et al., 2005b) and biphasic system (Viegas et al., 2007).

Many chiral selectors have been widely used for enantioselectvie separation of racemic propranolol in chromatrographic or capillary electrophoresis methods. These chiral selectors included β-cyclodextrin derivatives (Ching et al., 2000

and Wang et al., 2006) and amino acid derivatives (Campo et al., 1996 and Walshe et al., 1997). The other chiral selectors are cellulose derivatives (Heard and Suedee, 1996 and Suedee et al., 1998) which afford the good ability for separation of racemic propranolol.

2.2. The objective of the study

The purposes of this study are to determine the physical properties of propranolol HCl and to validate the chiral-HPLC analysis methods for separation of propranolol enantiomer from racemic propranolol with the different chiral columns.

2.3. Experimental

2.3.1. Chemicals and reagents

(R)-(+)-propranolol HCl, (S)-(-)-propranolol HCl and ($\pm$)-Propranolol HCl were obtained from Sigma- Aldrich Chemical Company (Milwaukee, WI, USA). Citric acid (Laboratory reagent grade) was obtained from Fisher Scientific, Leicestershire, UK. Disodium hydrogen phosphate ($Na_2HPO_4 \cdot 12H_2O$) was obtained from Analar analytical reagent; BDH Chemical Ltd., London, United Kingdom. Sodium perchlorate was purchased from BOH laboratory Supplies, Poole, England.

2.3.2. Apparatus

The propranolol enantiomers concentrations were analyzed by using HPLC method with chiral column (chiral-HPLC method). The chiral columns employed were Chiralcel OD-R column and Chiral-AGP column. Chiralcel OD-R column was a 250×4.6 mm I.D. and particle size 10 μm (Daicel, Chemical Industries Ltd., Japan). Chiral-AGP column was a 150×4 mm I.D. and particle size 5 μm (CHIRAL-AGP^{TM}, ChromTech Ltd., UK).

High-performance liquid chromatography was carried out using a Shimadzu HPLC system comprised a Shimadzu LC-10AD pump, FCL-10AL gradient valve, DGU-14A in-line solvent degasser, SCL-10A system controller, SIL-10AD auto injector (20 μl injection loop), equipped with a Shimadzu SPD-10A UV–Vis detector. Data were collected and analyzed on a personal computer using Class VP software (version 4.2, Shimadzu) (Shimadzu Corporation, Kyoto, Japan).

2.3.3. Analysis

The samples were analyzed directly by reverse phase chiral HPLC. Two chiral columns were used: (1) Diacel OD-R column (mobile phase 60:40, 1 N sodium perchlorate:acetonitrile and a flow rate of 1.0 ml/min; typical retention time were 10 min for *R*-propranolol and 12 min for *S*-propranolol) and (2) Chiral-AGP column (mobile phase 0.5% v/v 2-propanol in 20 mM ammonium acetate buffer (pH 4.1) and a

flow rate of 1.0 ml/min; typical retention time were 6 min for *R*-propranolol and 8 min for *S*-propranolol).

2.3.4. Method validation

2.3.4.1. Reproducibility on racemic propranolol HCl

A stock solution (100 μg ml^{-1}) was prepared by dissolving 10 mg of ($\pm$)-propranolol HCl in 100 ml of phosphate buffer solution pH 7.4 (μ=0.55). To determine the reproducibility of the chiral-HPLC system of racemic propranolol, standard solution of racemic propranolol hydrochloride (concentration 1 μg ml^{-1}) was injected 20 times and the injection volume was 20 μl (see section 2.3.2). The reproducibility on racemic propranolol was evaluated from %CV of peak area for each enantiomer.

2.3.4.2. Linearity and range

A series of standard solutions of racemic propranolol HCl in phosphate buffer solution pH 7.4 was prepared to make the different concentrations. The standard solutions of racemic propranolol HCl were ranged in 1-25 μg ml^{-1}. The solutions were injected and a calibration curve was plotted from the relationship between peak area and concentration of the standards.

2.3.4.3. Limit of detection and quantification

Calibration curves were constructed from the chiral-HPLC assay of the standard solutions (section 2.3.4.2.), from which the limit of quantification (LOQ) and limit of detection (LOD) were calculated using equation 2.1 and 2.2

$$LOD = y_B + 3s_B \qquad\qquad (2.1)$$

$$LOQ = y_B + 10s_B \qquad\qquad (2.2)$$

where s_B is the standard error of the y estimate and y_B the intercept from the regression equation.

2.3.4.4. Accuracy and precision (intra-day and inter-day precision)

The accuracy of the method was determined by comparing the measured concentration with the actual concentration (Equation 2.3):

$$Accuracy = \frac{A}{T} \; x \; 100 \qquad\qquad (2.3)$$

where A is the actual drug concentration and T is the theoretical drug concentration.

Three calibration curves from the same preparation were analyzed on the day of preparation to evaluate the intra-day precision. For inter-day

precision evaluation, three calibration curves made from three stock solutions were analyzed on three different days.

2.3.5. Solubility study of racemic propranolol HCl

The solubility of racemic propranolol HCl was studied in phosphate buffer solution pH 7.4 (37 °C). This study was useful for determination of the sink condition during the diffusion study.

An equilibrium solubility determination was undertaken in phosphate buffer solution pH 7.4 (37 °C). The excess propranolol HCl was added to 1 ml of buffer. The samples were shaken mechanically in a temperature-controlled water bath at 37°C for 24 h. The resulting saturated solutions were filtered and the filtrate solutions were diluted. The solubility of each drug was determined by chiral-HPLC assay (section 2.3.3.).

2.3.6. Stability studies

2.3.6.1. Stability of racemic propranolol HCl in pH 5.5 citrate and pH 7.4 phosphate buffer solution

The stability studies of racemic propranolol HCl were studied under the studied conditions to ensure the stability of the drug during the experiments. The racemic propranolol HCl (50 mg) was incubated separately with pH 5.5 citrate or

pH 7.4 phosphate buffer solution (1 ml) at both room temperature (30°C) and 37°C for 3 days. The *R*- and *S*-propranolol HCl (50 mg) were incubated separately with pH 7.4 phosphate buffer solution (1 ml) at 32°C. All of the experiments were run in triplicate. At the end of the incubation times, the drug solution concentrations were analyzed by chiral-HPLC method. The % stability of the propranolol and propranolol enantiomers were calculated from the equation:

$$\% \ Stability \quad = \quad \frac{C_d}{C_0} \ * \ 100 \qquad\qquad (2.4)$$

where C_d is the concentration of the propranolol or propranolol enantiomers at the day of the study, and C_0 the concentration of the propranolol or propranolol enantiomers at the initial of the study.

2.3.6.2. Stability of R- and S-propranolol HCl during polymerization process

To ensure the stability of templates during the polymerization, *R*- and *S*-propranolol HCl (50 mg) were incubated separately at 60°C in 1 ml of DMF (or chloroform) for 24 h. Samples were removed at the end of the incubation times and assayed for enantiomer content according to the method described in Section 2.3.3.

2.3.6.3. Stability studies of propranolol HCl in spent receiving fluid

For *in vi*tro penetration study across the rat skin, the stability of propranolol in spent receiving fluid was studied. The spent fluid was prepared by incubating rat skin in phosphate buffer solution pH 7.4 at 32°C for 24 h before study. *R*- and *S*-propranolol HCl were incubated in the spent fluid for 3 days. The experiment was also run in triplicate. After incubation, the solution was filtered and analyzed by chiral-HPLC assay (see section 2.3.3.).

2.3. Results and discussion

2.3.1. Method validation

The retention time of *R*-propranolol and *S*-propranolol, for method 1 (Chiralcel OD-R column) were 10 and 12 min, respectively and for method 2 (Chiral-AGP^{TM} column) were 6 and 8 min, respectively. The HPLC chromatogram of the method 1 and 2 are shown in Figure 2.1 and 2.2, respectively.
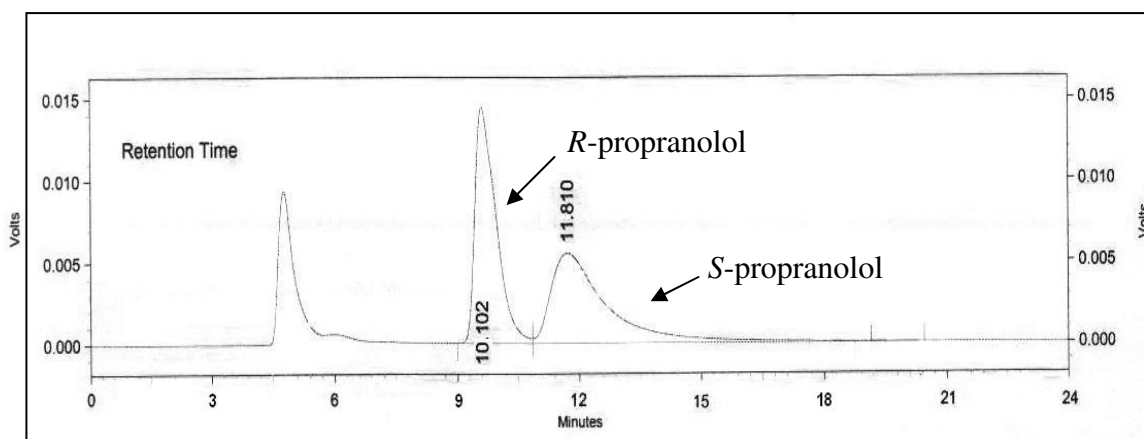
Figure 2.1. Chromatogram of *R*-and *S*-propranolol analyzed from Chiralcel OD-R column.
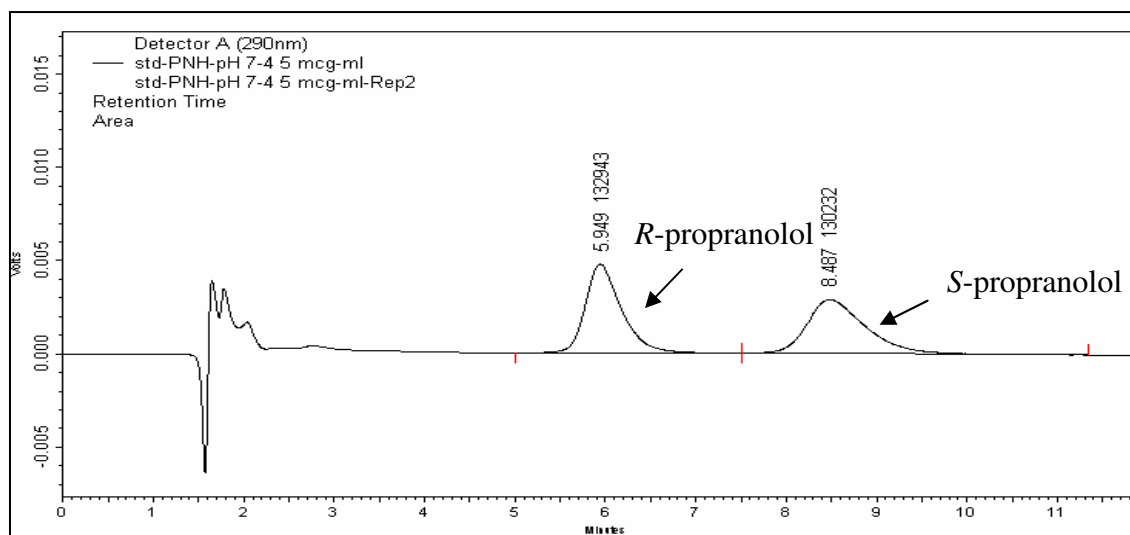
Figure 2.2. Chromatogram of *R*-and *S*-propranolol analyzed from Chiral-AGP™ column.

The % CV for reproducibility study of the two methods were less than 2% and both methods also showed the good linearity in the propranolol concentration range of 1-25 μg ml^{-1}. In addition, intra-day and inter-day variation coefficient (%CV) of both methods were less than 2%. The linearity, sensitivity and accuracy of the two methods were summarized in Table 2.1.

From these results, the selectivity and accuracy of the methods were high enough for the further experiments, hence it can be said that both chiral-analysis methods are suitable for determination of racemic propranolol HCl and its enantiomers.

Table 2.1. The linearity, sensitivity and the accuracy of the propranolol enantiomers analysed by chiral-HPLC methods.

Methods	Substance	Linearity	LOD* ($\mu g\ ml^{-1}$)	LOQ** ($\mu g\ ml^{-1}$)	% Accuracy
1 (Chiralcel OD-R)	*R*-propranolol	0.9998	0.34	0.86	98.56±1.21
	S-propranolol	0.9999	0.23	0.57	99.06±0.54
2 (Chiral-AGPTM)	*R*-propranolol	0.9996	0.14	0.42	98.20±1.64
	S-propranolol	0.9997	0.08	0.23	98.76±0.86

* LOD is the lower limit of detection

**LOQ is the lower limit of quantification

2.3.2. Solubility study of racemic propranolol HCl

The solubility of racemic propranolol HCl was studied in phosphate buffer solution pH 7.4. This study was useful for preparation of the saturated solution in the diffusion study. The solubility of racemic propranolol HCl in PBS pH 7.4 was 148 mg ml^{-1}. The physical properties of racemic propranolol and propranolol enantiomers studied by Totuitou et al. (1994) were summarized in Table 2.2 and the DSC curve of propranolol enantiomers are shown in Figure 2.3. The physical properties of the propranolol enantiomers are generally the same but for the solubility study and DSC curves of both propranolol enantomers seem to be slightly different.

Table 2.2. The physical properties of racemic propranolol and propranolol enantiomers

from literature (Totuitou et al., 1994).

Substance	M.W.	pKa	m.p. (°C)	Solubility (mg ml^{-1})	
				Normal saline	pH 7.4
R-propranolol	259.3	9.2	71.5	0.55	0.70
S-propranolol	259.3	9.2	71.5	0.44	0.73
rac-propranolol	259.3	9.2	92.3	0.22	0.47

M.W.: molecular weight (g moL^{-1}); pK_a: partition coefficient; m.p.: melting point temperature; solubility at 37°C.
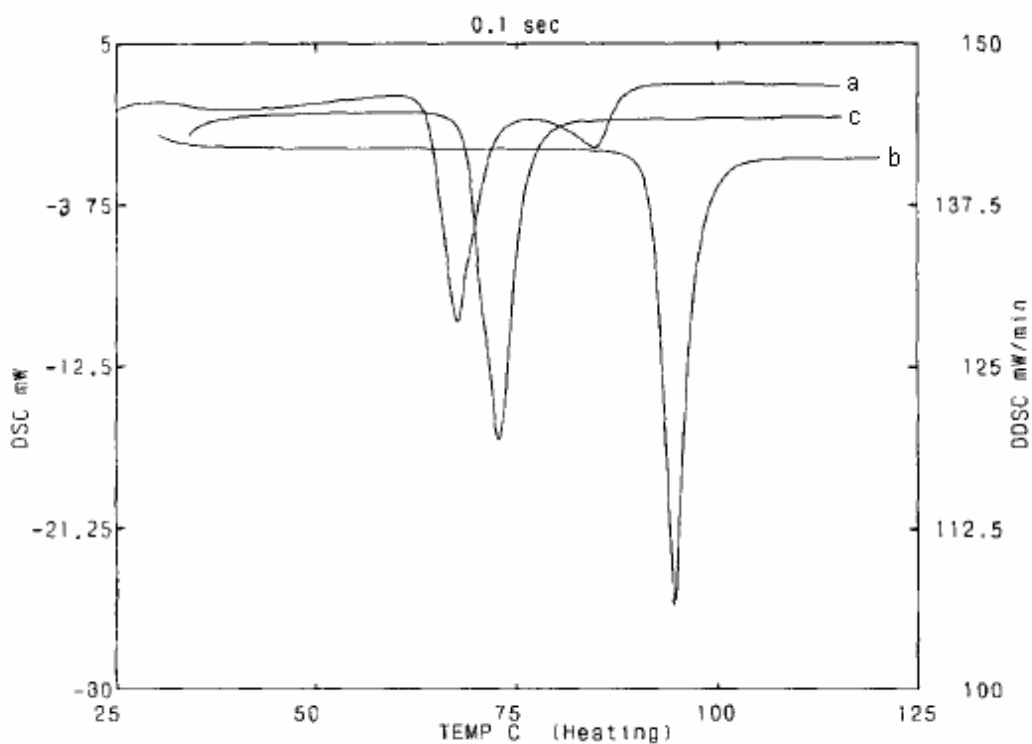
Figure 2.3. DSC curves for: (a) *S*-propranolol : *R*-propranolol (0.172 : 0.828); (b) *R*-propranolol and (c) *S*-propranolol (Totuitou et al., 1994).

2.3.3. Stability of propranolol HCl and its enantiomers

The aim of the stability studies was to ensure the stability of each enantiomer during the experiments of this project. The stability studies of racemic propranolol HCl and its enantiomers were studied under various conditions. The first involved dissolving the racemic propranolol HCl in citrate buffer pH 5.5 and phosphate buffer pH 7.4 at room temperature and 37°C for 3 days (Table 2.3). The stability of both enantiomers were higher than 98% and the enantiomers were more stable in acidic condition. The second examined the stability of the pure enantiomers in phosphate buffer pH 7.4 and spent receiving fluid for 3 days (Table 2.4). The stabilities of each enantiomers were good under both sets of conditions (% stability > 98%). The last stability experiment was to study the stability of the template (*R*-propranolol and *S*-propranolol) during polymerization condition. At 60°C, where the polymerization procedure of the imprinting was effected, it was found that 14.7±3.0% (n=3) racemised when the pure *R*-enantiomer was incubated alone in DMF for 24 h. In contrast, under the same conditions only 1.5±0.3% (n=3) of the pure *S*-isomer was found to racemise. However when the individual *R*- and *S*-propranolol enantiomer was incubated in chloroform at temperature 60°C, both remained stable with no racemisation of enantiomer after 24 h. This indicates that the type of solvent in which the enantiomers are dissolved affects the stability of the propranolol enantiomers. However the total recovery of enantiomer from the template was found to be 98% and less than 1% racemisation had been found to occur in either individual enantiomer.

Table 2.3. % Stability of racemic propranolol HCl in PBS pH 7.4, room temperature (~30°C) and 37°C.

Medium	Substance	% Stability (RT)		% Stability (37°C)	
		Day 1	Day 3	Day 1	Day 3
Buffer pH 5.5	*R*-propranolol	98.32±0.27	98.68±0.57	98.01±1.13	102.48±1.59
	S-propranolol	98.97±0.53	100.05±0.66	98.09±0.59	101.03±1.04
Buffer pH 7.4	*R*-propranolol	98.89±0.72	99.19±1.21	98.70±0.82	98.65±0.51
	S-propranolol	98.47±0.37	98.44±0.27	98.21±0.23	98.12±0.23

Table 2.4. % Stability of propranolol enantiomers in PBS pH 7.4 and spent receiving fluid at 32 °C.

Medium	Substance	% Stability (32°C)	
		Day 1	Day 3
Buffer pH 7.4	*R*-propranolol	99.65±1.48	106.43±0.97
	S-propranolol	99.68±1.12	105.40±1.75
Spent receiving fluid	*R*-propranolol	100.07±1.24	100.85±1.53
	S-propranolol	100.86±1.30	101.51±1.79

CHAPTER 3

SYNTHESIS AND CHARACTERIZATION OF THE

COMPOSITE MOLECULARLY IMPRINTED POLYMER

MEMBRANE

3.1. Bacterial cellulose membrane

Cellulose is the most abundant biopolymer on earth. Cellulose is an unbranched polymer of β-1,4-linked glucopyranose residues (Figure 3.1). Cellulose is practically insoluble in water or other usual solvents, but is dissolved by concentrate solution of zinc chloride, by ammoniacal copper hydroxide solution, and also by caustic alkali with carbon disulfide (O' Neil et al., 2001). Although individual strand of cellulose are intrinsically no less hydrophilic, or no more hydrophobic, than some other soluble polysaccharides (such as amylose) this tendency to form crystals utilizing extensive intra- and intermolecular hydrogen bonding makes it completely insoluble in normal aqueous solutions (although it is soluble in more exotic solvents such as aqueous *N*-methylmorpholine-*N*-oxide, CdO/ethylenediamine (cadoxen), LiCl/*N,N'*-dimethylacetamide or near-supercritical water). It is thought that water molecules catalyze the formation of the natural cellulose crystals by helping to align

the chains through hydrogen-bonded bridging (http://www.lsbu.ac.uk/water/ hycel.html).
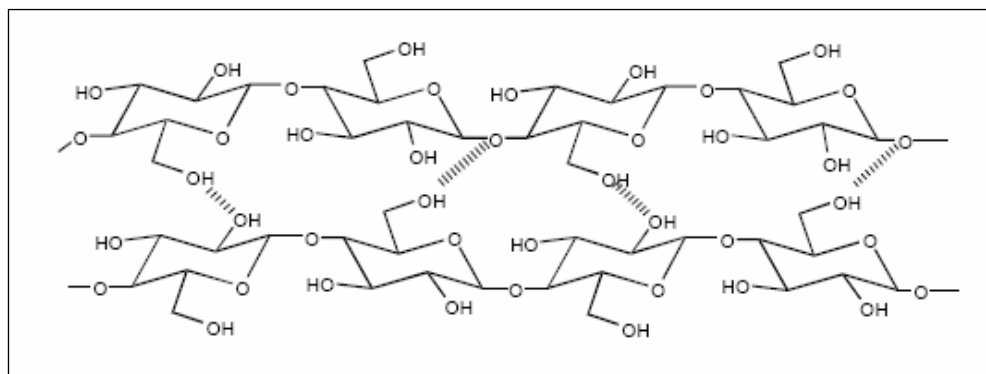
Figure 3.1. Structure formula of cellulose.

Cellulose is synthesized by a variety of living organisms, including plants, most algae, bacteria, and some animals (Browm et al., 1996). Bacteial cellulose belongs to specific products of primary metabolism and is mainly a protective coating, whereas plant cellulose plays a structure role (Rezaee et al., 2005). Plant and bacterial cellulose are chemically the same but the degree of polymerization differs from about 13000 to 14000 for plant and 2000-60000 for bacterial cellulose (Jonas and Farah et al., 1998). Plant cellulose is extensively used in the paper and textile industries. Cellulose is the major constituent of cotton and wood leading to a significant demand on wood biomass, hence the production of cellulose by bacteria could be an interestingly alternative way (Vandamme et al., 1998). Bacterial cellulose demonstrates unique properties including high mechanical strength, high crystallinity, high water holding capacity and high porosity (Czaja et al., 2004) and the flat pellicle of bacterial cellulose can be easily processed into a porous membrane possessing

good mechanical strength, unlike the cellulose from plant biomass. Plant cellulose is often interspersed with lignin, hemicellulose and pectin leading to nonuniformity in porosity and unpredictable permeability. In contrast the porosity of membranes from bacterial cellulose can be suitably tailored by varying the physiological conditions of bacterial growth such as composition of the culture media, its pH, temperature, oxygen tension as well as by chemical modifications (Dubey et al., 2002 and Pandey et al., 2005). In addition, the thickness and permeability flux of the bacterial cellulose membrane can be controlled by time and cell density used during membrane forming (Wanichapichart et al., 2003). So far, the bacterial cellulose in many fields such as an acoustic transducer diaphragm (Nishi et al., 1990), fuel cells (Evans et al., 2003), electronic paper (Shah and Brown, 2004) and wound healing (Czaja et al., 2006). In comparison with other polymer material, bacterial cellulose can be economically produced and processed, also has high resistance to corrosive chemicals and is biocompatible and biodegradable too, and hence ecofriendly. The difference of the microfibril of bacterial cellulose and plant cellulose is shown in Figure 3.2.
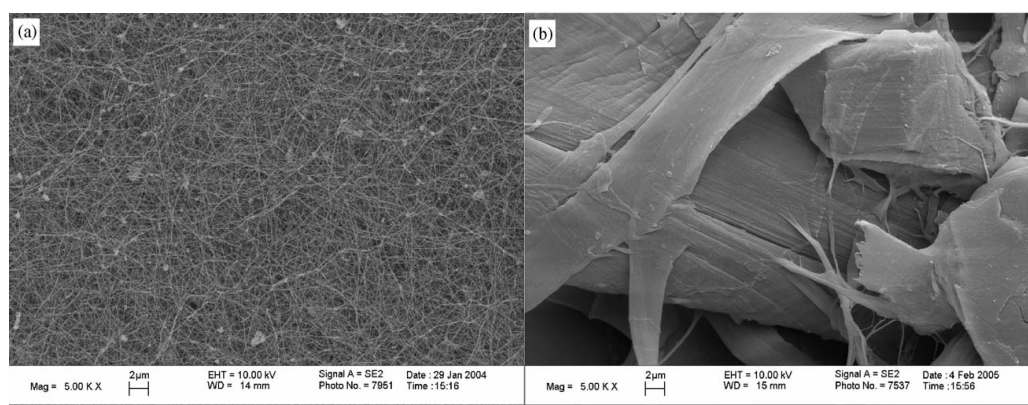
Figure 3.2. A comparison of microfibril of cellulose between bacterially derived cellulose (from *Acetob*acter *xylinum*) (a) and wood pulp (b). Both pictures are the same magnitude (at 5000x) (Czaja et al., 2006).

Cellulose consists of amorphous and crystalline regions existing together. The degree of crystallinity is known to vary depending on the origin and mode of chemical treatment of the material. Two common crystalline forms of cellulose, designated as I and II. Cellulose I is metastable which is synthesized by the majority of plants and also by *A. xylinum* and can be irreversibly into another crystalline state, cellulose II, the most stable allomorph known. Cellulose I has parallel glucan chains and strong intramolecular hydrogen bonds. The native cellulose I exists as two crystalline suballomorphs, cellulose 1_α and 1_β. Cellulose II is arranged in a random manner. It is mostly antiparallel and linked with a large number of hydrogen bonds that results in higher thermodynamic stability of the cellulose II (Brown et al., 1996).

Biosynthesis of cellulose in Acetobacter xylinum.

The most well known bacteria with cellulose producing abilities are found in the genus *Acetobacter*. and of this is *Acetobacter xylinum* (reclassified as *Gluconacetobacter xylinus*). *A. xylinum* is claimed to be an effective cellulose-producing bacterium (Wanichapichart et al., 2002). Table 3.1. shows the list of bacterial cellulose producer. Advantages of using a bacterium system for production of cellulose is that the bacterium grows rapidly under controlled conditions and produces cellulose from a variety of carbon sources.

Table 3.1. Lists of bacterial cellulose producers and their biological roles (Jonas and Farah, 1998).

Organisms (genus)	Biological role
Acetobacter	To keep in aerobic environment
Achromobacter	Flocculation in wastewater
Aerobacter	Flocculation in wastewater
Agrobacterium	Attach to plant tissues
Alcaligenes	Flocculation in wastewater
Pseudomonas	Flocculation in wastewater
Rhizobium	Attached to most plants
Sarcina	Unknown
Zoogloez	Flocculation in wastewater

There are two methods to produce bacterial cellulose: (a) stationary culture, which results in the accumulation of a gelatinous membrane of cellulose on the surface of the medium; (b) agitated culture, where cellulose is synthesized in deep media in the form of fibrous suspensions, pellets, or irregular masses (Chao et al., 2000 and Czaja et al., 2004). Therefore, the static condition is more suitable for cellulose membrane production.

Acetobactor xylinum, a rod shaped, aerobic gram negative bacterium which occurs as a contaminant in vinegar production produces a white gelatinous material (pellicle). The synthesis of cellulose in *A. xylinum* occurs between the outer

membrane and cytoplasma membrane by a cellulose-synthesizing complex, which is in association with pores at the surface of the bacterium (Figure 3.3).
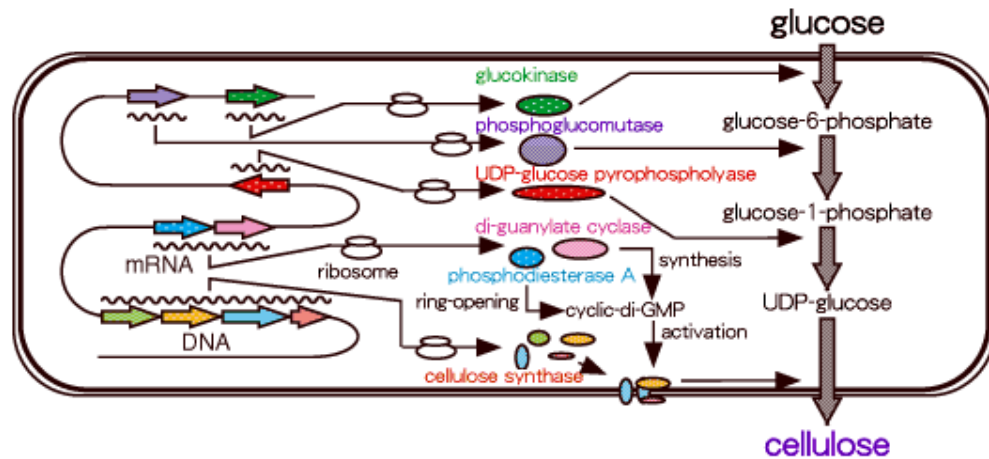
Figure 3.3. The predicted pathway of cellulose synthesis and secretion when glucose is taken into *Acetobactor xylinum* from the outside of the cell. (downloaded from: http://www.res.titech.ac.jp/~junkan/english/ cellulose/)

The biosynthetic pathway for cellulose from substrate glucose to cellulose involves a number of reactions. Firstly, glucose is converted to glucose-6-phosphate by the enzyme glucokinase. In the second step, glucose-6-phosphate is converted to glucose-1-phosphate by the enzyme phophoglucomutase. Subsequently, glucose-1-phosphate is converted to UDP-glucose in the presence of UTP and the enzyme UDPG pyrophosphorylase. UDP-glucose is used as a substrate for cellulose by enzyme cellulosesynthase (Jonas and Farah, 1998, Vandamme et al., 1998 and Czaja et al., 2006).

3.2. The objective of the study

The aim of this study is to prepare the bacterial cellulose membrane for use as the membrane base of the production of the MIP composite membranes. For the preparation of the cellulose membranes, the effect of cultured conditions of the bacterial cellulose on the enantioselective property of cellulose membrane was studied. The bacterial cellulose membranes produced from the various cultured conditions were characterized *via* scanning electron microscope, electrical resistance, atomic force microscopy, tensile strength and chromatographic methods. In addition, the composite MIP membranes were prepared using the cellulose membranes having different thickness and the enantioselective property of the prepared composite MIP membranes were evaluated in parallel experiment with the reference membranes.

3.3. Experimental

3.3.1. Chemicals and reagents

Yeast extract and peptone was obtained from Difco Laboratories (MO, USA). Methacrylic acid (MAA), ethylene glycol dimethacrylate (EDMA) and 3-methacryloxypropyltrimethoxysilane (3-MPS) were obtained from Sigma-Aldrich Chemical Company (Milwaukee, WI, USA). 2,2'-Azobis-(isobutyronitrile) (AIBN) was obtained from Janssen (Geel, Belgium).

MAA was distilled under vacuum before use. EDMA was washed with 1 M aqueous sodium hydroxide for 3 times, dried over Na_2SO4 and distilled under vacuum before use.

3.3.2. Apparatus

UV absorbance measurements were recorded using a Hewlett-Packard diode array spectrophotometer Series 8452A (CS, USA).

The elemental analysis was performed by using a JSM-5800 LV electron microscope (Jeol, MA, USA) equipped with an Oxford Instruments LINK-ISIS 30 X-ray detector and microanalysis system.

The morphology of membranes was examined by using a Jeol series JSM 5800LV, CA, USA.

The atomic force microscopic images were performed by using a Digital Instruments NanoScope IIIa scanning probe microscope (Veeco Instruments GmbH, Germany).

The weights of the membranes were measured by using a Precisa 300 A microbalance (USA: capacity 305 g, readability 0.1 mg).

The membrane resistance was studied by using a Revision G Voltage-Current Clamp, Model VCC 600 (Harvard Apparatus, CA, USA).

The mechanical strength of the membranes was measured using a Universal testing machine (Lloyd, UK) with an operating head load of 100 N.

The receptor fluid of the Franz diffusion cells was stirred by using a Variomag magnetic multipoint submergible stir plate (Variomag®, FL, USA)

The concentrations of the propranolol enantiomers were analyzed by chiral-HPLC method using a Chiralcel OD-R column connected with a Shimadzu HPLC system (Shimadzu Corporation, Kyoto, Japan).

3.3.3. Bacterially derived cellulose membrane

Cellulose membrane was obtained by incubating *A. xylinum* TISTR 975 which was obtained from the Thailand Institute of Scientific and Technological Research. The protocol of bacterial cellulose membranes preparation was modified from the described method of Wanichapichart et al. (2002). *A. xylinum* TISTR 975 was cultured in a pre-culture medium, Buffered Schamm and Hestrin's medium (BSH medium) which composed of 2.0% (w/v) glucose, 0.5% (w/v) yeast extract, 0.5% (w/v) peptone, 0.033% (w/v) $Na_2HPO_4 \cdot 2H_2O$ and 0.011% (w/v) citric acid$\cdot H_2O$. The bacteria were grown in 50 ml of pre-culture medium at 30°C. After 3 days, the pellicle of bacterial cellulose obtained from the surface of the medium bacteria was inoculated into the culture medium in a stainless steel round shallow tray of 39 cm diameter. The culture medium was coconut juice supplemented with 4% sucrose (w/v) at pH 5.0. The culture volume was 500 ml and the cellulose producing bacteria was incubated at 30°C for 1 day under static conditions. The pellicles of bacterial cellulose (0.01 mm thickness) formed on the surface of this medium were harvested aseptically.

Three types of bacterial cellulose membrane were prepared to find out the appropriate cellulose membrane which had good enantioselective property for *S*-propranolol HCl. The two different bacteria suspensions containing either 1×10^8 or 3×10^8 cfu ml^{-1} from the pre-culture medium were inoculated into the culture medium to make the two 'thin' cellulose membranes. For 'thick' cellulose membrane was prepared by another method. Four pieces of pellicles of bacterial cellulose (1×1 cm) were cut and placed in the tray, approximately 10 cm from the edge of the tray and an equal distance from each other. For cellulose membrane production, the volume of the culture medium was 500 ml and the tray was covered with a linen cloth. After 1 day incubation, to make the more homogeneous cellulose membrane for all sheets, the cellulose pellicle formed on the surface of the media was removed and discarded. The remaining culture was further incubated under the same conditions for one more day. The formed cellulose membrane was harvested and transferred to 1% (w/v) NaOH at 80°C for 24 h and then thoroughly washed with distilled water to remove any remaining associated microorganisms and proteins. The pure cellulose sheets were dried at 37°C overnight and kept in a dust free atmosphere until required for use.

3.3.4. Composite MIP membrane preparation

The three types of composite MIP membranes were prepared from the different bacterial cellulose membranes as for screening the suitable type of cellulose membrane to use as a membrane base. The composite MIP membranes were produced by grafting of ethylene glycol dimethacrylate and methacrylic acid copolymer onto

the pore-containing surface of the bacterially-derived membrane. The chemical structures of the components are shown in Figure 3.4.

Propranolol

Methacrylic acid (MAA)

Ethylene glycol dimethacrylate (EDMA)   2,2'-Azobis(isobutyronitrile) (AIBN)
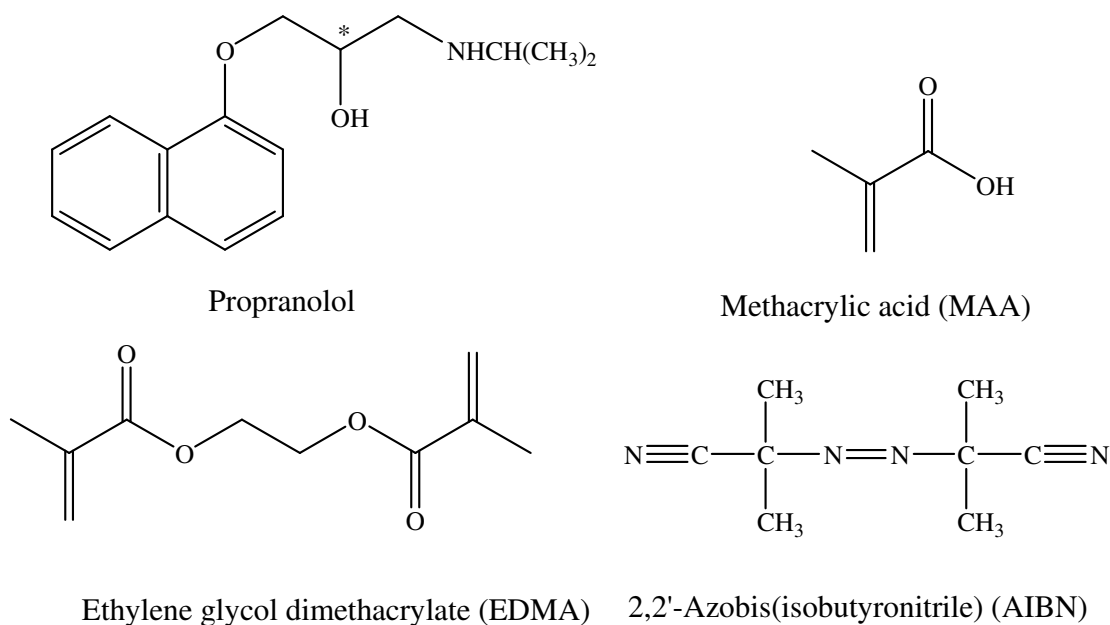
Figure 3.4. Chemical structures of template, functional monomer, crosslinker and initiator.

The grafting was carried out in the presence of the polymeric mixture and propranolol enantiomer template (Figure 3.5). Firstly, the three different types of cellulose membranes were reactivated for changing the -OH group of cellulose membrane to C=C group by reacted with 3-MPS (10% w/w in toluene) at 80 °C for 5 h. The resulting membrane was then thoroughly washed in methanol for eliminating the excess reagent and dried at room temperature overnight. The reacted cellulose membrane was then placed in crystallizing dish, 18 cm in diameter. A polymeric solution contained 12 mmol of MAA as a functional monomer, 0.05 mol of EDMA as

a crosslinking monomer, 2 mmol *S*-propranolol (HCl) or *R*-propranolol (HCl) as template and 0.7 mmol of AIBN as a radical polymerization initiator in DMF (2 ml). The mixture was purged with nitrogen for 2–3 min to remove oxygen (which acts as a radical scavenger) before poured onto the surface of cellulose membranes thoroughly. The polymerization temperature was maintained at 60°C for 18 h. After polymerization, membranes were transferred to a Soxhlet extractor and extracted with 10% (w/v) acetic acid in methanol for at least 72 h before further extraction with methanol for 72 h to remove any non-grafted polymer, monomer, residual initiator and template molecule. The prepared membranes were dried in vacuum overnight.

The membrane prepared with an imprint of *R*-propranolol was referred to as R-MIP membrane and the membrane having the imprint of *S*-propranolol was referred to as S-MIP membrane. Non-imprinted polymer (NIP) cellulose membranes were prepared in the same manner as MIP modified cellulose membrane but with the template molecule omitted for using as control experiments (these membranes were referred to as NIP membranes).

Before using, the MIP composite membrane was tested to confirm the grafting process. The complete removal of the template molecule from the polymer was confirmed by its absence from the methanol extract of the polymer from UV spectroscopy assay compared with the standard propranolol hydrochloride ($\lambda = 254$ nm) and the absence of nitrogen content in elemental analysis results obtained by using a JSM-5800 LV electron microscope.
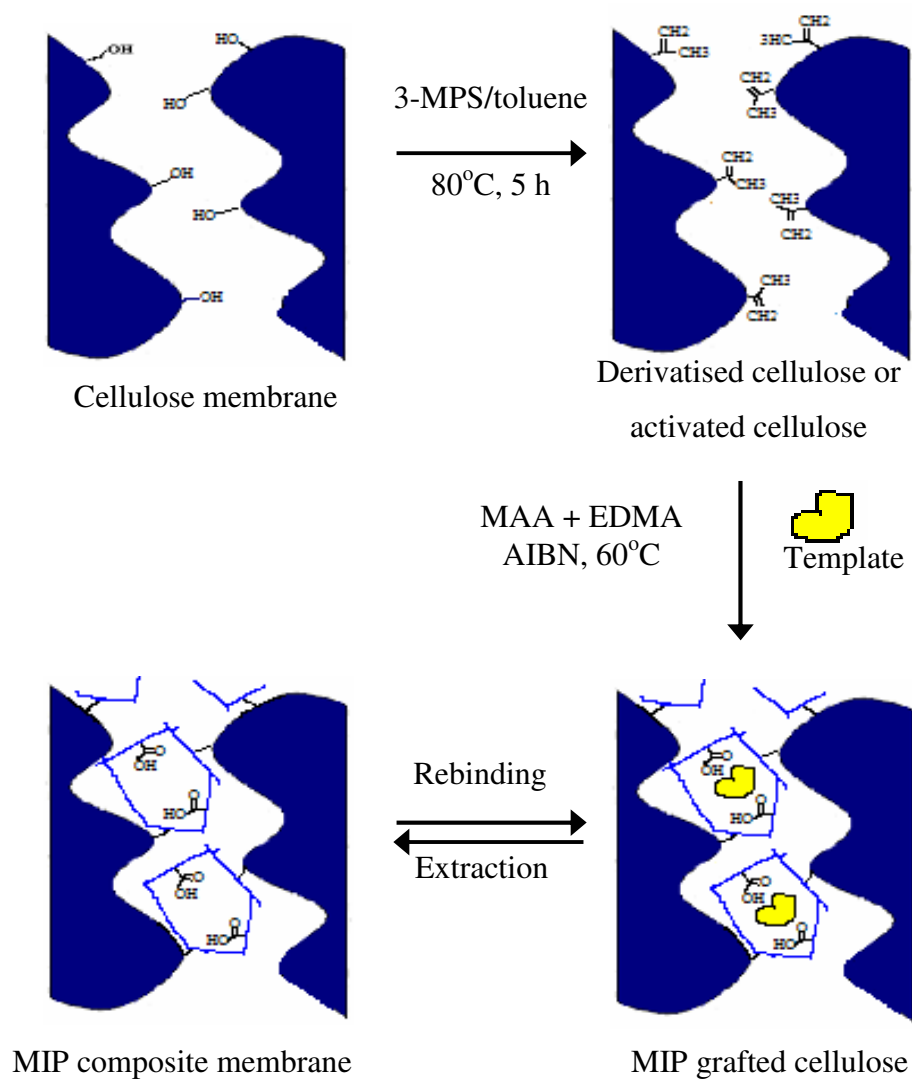
Figure 3.5. Illustration of a surface pore modification of cellulose membrane with a molecularly imprinted polymer against propranolol enantiomer.

3.3.5. Membrane evaluation

3.3.5.1. Surface morphology and cross-section study

The membrane morphology of the initial and modified cellulose was characterized by scanning electron microscope observation of the cross-section and inner and outer surfaces at an accelerating voltage of 15 kV with the samples. For cross-section studies, the membranes were freeze-dried by putting in liquid nitrogen and then torn at room temperature. All membrane samples were sputter-coated with gold before analysis to avoid electrostatic charges and to improve image resolution. The membrane thickness was estimated from SEM cross-section images.

The surface morphology was further examined with an atomic force microscope (AFM) using a Digital Instruments NanoScope IIIa scanning probe microscope. AFM observations were carried out at room temperature without any previous treatment. A rectangular silicon nitride cantilevers with pyramidal tips was used to scan and produce the images.

3.3.5.2. Pore size measurements

The pore size of membranes was estimated from surface pictures of the membrane obtained by SEM with the aid of a Carnoy computer imaging program (Lab of Plant Systemics, Belgium).

3.3.5.3. Degree of modification (DM)

The degree of modification (DM) was calculated from the difference in weight between the sample modified with a deposited MIP layer and the initial unmodified sample. The change in weight of the membrane induced by the grafting procedure was measured using a microbalance.

3.3.5.4.. Electrical resistance measurements

Impedance measurement was used to confirm the deposition of a MIP layer onto the surface of the cellulose membranes and to assess the degree of membrane fibrillation. Electrochemical resistance measurements of membranes were carried out by short-circuit current technique using a Revision G Voltage-Current Clamp. The test membrane was mounted in the measuring cell with an effective area of 1 cm^2 and a current established across it using a potentiostat via an amplifier with high-resistance inputs. The four electrode potentiostat assured a passage of current between the two calomel electrodes in such a manner as to hold constant amplitude of voltage between the two identical reversible silver–silver chloride electrodes and the

intensity and phase of current in the circuit. A 60 μA current was applied and the membrane potential difference, *V* (mV) and the short circuit current, *I* (A or ampere) were recorded simultaneously. The membrane resistance, R_m (Ω cm^2) was calculated from *V/I* based on Ohm's law. These were corrected by eliminating the offset voltage between the electrodes and solution resistance, which was determined prior to each experiment using identical bathing solutions. All experiments were carried out in triplicate at 25±1°C. Ohm's law states that the current *I* flowing in a circuit is proportional to the applied potential difference *V*. The constant of proportionality is defined as the resistance *R*.

3.3.5.5. Mechanical properties measurements

The mechanical strength of the membranes was measured using a Universal testing machine with an operating head load of 100 N. The tensile strength of a material is the maximum amount of tensile stress that it can be subjected to before failure. The membranes were placed between the grips (2.5 cm in length) of the testing machine. The grip length was 2.5 cm and the speed of testing was set at the rate of 30 mm/min. Tensile strength was calculated according to the equation:

$$Tensile\ strength\ (kN/m^2) \quad = \quad \frac{Maxload\ (kN)}{Cross-section\ area\ (m^2)} \qquad (3.1.)$$

3.3.5.6. Degree of swelling of membranes

The degree of swelling of cellulose and modified cellulose membranes was evaluated in pH 5.5 and pH 7.4 buffers, since for some applications membranes were used in these conditions. All polymer membranes were vacuum-dried at room temperature for at least 3 days before testing. The membrane samples were weighed and then soaked in individual tubes containing phosphate buffer pH 7.4 (μ=0.55) or citrate buffer pH 5.5 (μ=0.35) at room temperature (~30°C). The membranes were incubated in the medium until the weight of wet membranes remained stable, which usually occurred after approximately 7 h incubation. Before measuring the weight of the wet membrane, surface water was gently removed with a tissue. The wet films were dried under vacuum at room temperature to a constant weight (over a minimum of 2 days) and stored in a desiccator at room temperature before measurements. The degree of swelling of the membrane (%) was calculated from the equation:

$$\% \ Swelling \ \ = \ \ \frac{(W_{wet}-W_{dry})}{W_{dry}} * 100 \quad\quad\quad (3.2)$$

where W_{dry} and W_{wet} are the weights of dried and wet samples, respectively. Each test was carried out in sets of three.

3.3.5.7. Measurement of partition coefficient

The membrane-pH 7.4 (μ=0.55) buffer partition coefficient was evaluated by equilibrating racemic propranolol HCl solutions with a cellulose membrane. The difference between the initial and equilibrium concentrations of each enantiomer in the aqueous phase was determined and hence the amount of propranolol enantiomer sorbed to the membrane was calculated. In a typical binding assay, the S-MIP membrane having the surface area 1 cm^2 was added to 5 ml of an aqueous solution containing 100 μg ml^{-1} of racemic propranolol HCl in pH 7.4 phosphate buffer solutions, and stirred overnight at room temperature for equilibrium to be established. The partition coefficient (K) was calculated from the equation:

$$K \quad = \quad \frac{C_p}{C_s} \tag{3.3.}$$

where C_p is the concentration of the analyte associated with the membrane, and C_s is the concentration of the analyte in the solution. The selectivity factor representing the effect of the imprinting process was the ratio of K of the S-isomer to K of the R-isomer. The concentration of propranolol enantiomers was analyzed by a chairal-HPLC method (Section 3.3.5.9).

3.3.5.8. Permeation determination

The enantioselective transport of the three different types of cellulose membrane and S-MIP membrane were evaluated by a dialysis method using a vertical Franz-type diffusion cell (Figure 3.6). The diffusion cell composed of two compartments and the studied membranes were sandwiched between the two. The area of diffusion was 0.78 cm^2 and the volume capacity of the donor and receptor compartment were 1 and 2.5 ml, respectively. The studied membrane was mounted between the two chambers of the diffusion cells. The receptor chamber was filled with pH 7.4 phosphate buffer (μ=0.55) solutions. The required amount of racemic propranolol hydrochloride (40 μg ml^{-1}) was dissolved in pH 7.4 phosphate buffer solutions to obtain the donor solutions. The propranolol solution (0.5 ml) was placed evenly on the surface of the membrane. The solubility of propranolol enantiomers in the receiver medium at room temperature (30°C) was 140.8 mg ml^{-1}, the propranolol concentration was typically less than 5% of saturation to maintance the sink condition for the duration of diffusion experiments (Baker and Kochinke, 1988). Drug release was measured by the removal of samples (250 μl) from the receiving chamber at appropriate time intervals over 6 h (15, 30, 60, 90, 120, 180, 240, 300, and 360 min). The volume of the sample withdrawn was replaced by the same volume of the medium. Each test was carried out in sets of four. All experiments were run at room temperature (30°C). The diffusion of each propranolol enantiomer was determined using the chiral-HPLC analytical method outlined in Section 3.3.5.9. The cumulatively permeated amounts (μg) were calculated and plotted as a function of time. The flux J (μg cm^{-2} h^{-1}) is defined by:

$$J = \frac{Q}{A * t} \qquad\qquad (3.4.)$$

where Q (µg) is the amount of analyte permeated, A (cm^2) is the effective membrane

area and t (h) is the time. The selectivity of the membrane was defined as the ratio of

the permeation flux of S-isomer to that of the R-isomer.
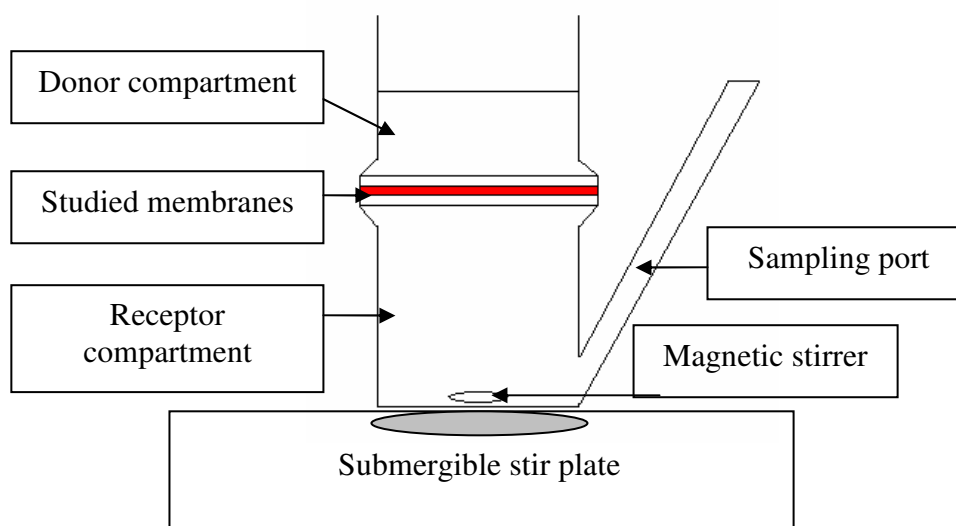
Figure 3.6. Schematic representation of a vertical Franz-type diffusion cell.

3.3.5.9. Stereospecific HPLC method

The analysis of the propranolol enantiomer content of the

samples was performed directly using a chiral-HPLC method. The HPLC system

(Shimadzu Corporation, Kyoto, Japan) comprised a Shimadzu LC-10AD pump, FCL-

10AL gradient valve, DGU-14A in-line solvent degasser, SCL-10A system controller, SIL-10AD auto injector (20 μl injection loop), equipped with a Shimadzu SPD-10A UV–Vis detector set at 290 nm. Data were collected and analysed on a personal computer using Class VP software (version 4.2, Shimadzu). The column employed was a 250×4.6 mm I.D., particle size 10 μm Chiralcel OD-R column (Daicel, Chemical Industries Ltd., Japan). The mobile phase was 60:40 (v/v) 1 N sodium perchlorate:acetonitrile and a flow rate of 1.0 ml/min was employed. The results of the controlled membrane and skin permeation experiments were expressed as a mean±SE. Paired two sided *t-tests* were performed on the data and a significance limit of 5% level was applied, where appropriate.

3.4. Results and discussion

3.4.1. The preparation of the MIP composite membranes

Composite MIP membranes were prepared by reactive filling of the pores of the bacterial cellulose membranes with MIPs having recognition sites for the *S*-propranolol enantiomer. In order to achieve an additional anchor for the MIP, asymmetric porous cellulose membranes were treated with 3-MPS. Thin layer MIPs were synthesised by a free radical copolymerization of MAA functional monomer with EDMA as a cross-linker in the presence of propranolol enantiomer (as a template molecule) in DMF, and this was followed by subsequent template molecule extraction. MAA was chosen as the functional monomer since the acid group of the monomer had the facility to interact with the amine groups of the print molecule via hydrogen

bonding interaction. The cross-linker EDMA was selected due to the anticipated rigidity and compactness vehicle might confer to the imprinted polymer.

Porous asymmetric cellulose membranes were obtained as a product of *A. xylinum* fermentation. The properties of prepared cellulose membrane such as thickness, degree of fibrillation, porosity and pore size can be adjusted by controlling the loading concentration of bacteria during culture as well as the time of cultivation. Three bacterial cellulose membranes having different thickness and electrical membrane resistance were used in this work for screening experiments to optimise the MIP affinity and distribution of the MIP within the membrane. The three lots of cellulose membrane displayed variation in membrane thicknesses and resistance, respectively as follows: (1) 5 μm/1 Ω cm^2; (2) 10 μm /2 Ω cm^2; (3) 15 μm /4 Ω cm^2. Cellulose membranes were imprinted with *S*-propranolol enantiomer during pore-filling and their stereoselective sorption and transport properties determined. The same polymer mixtures were used in the pore-filling process of all three lots of cellulose membranes. The membrane thickness and pore diameter of cellulose membrane appeared to have no significant effect on degree of modification (DM). The DMs of the three modified membranes or composite MIP membrane (S-MIP) were similar with an average DM of 0.80 mg/cm^2. The variation in the DM of individual membranes was found to be less than 10%. The increase of membrane resistance (R_m) after the modification was found to be 0.7 Ω cm^2 for the 5 μm membrane, 1.3 Ω cm^2 for the 10 μm membrane and 2.2 Ω cm^2 for the 15 μm membrane. The tensile strengths of the cellulose membranes were found to increase when each was modified with MIP to form composite membranes. An increase from

3.16 to 7.20 kN/m^2 occurred for the 5 μm membranes, from 6.60 to 8.78 kN/m^2 for

the 10 μm membranes and from 8.83 to 21.45 kN/m^2 for the 15 μm membrane.

SEM cross-sectional images of initial and modified cellulose membranes show the different membrane thicknesses (Figure 3.7). The cross-sectional view shows an array of closely packed MIP domains in the cellulose membranes. The thickness of the deposited MIP layer tends to increase as the thickness of cellulose membrane increases. Even so the relatively small thickness of the MIP layer might be expected to allow relatively high fluxes through the MIP composite cellulose membranes. The cellulose membranes varied in the degree of porosity and fibrillation (Figure 3.8). Fibers were still apparent after modification of the thinnest membrane (5 μm) with MIP but when the same amount of MIP was applied to the 15 μm membrane, it did not penetrate as effectively into the tighter meshed polymer chains (see Figure 3.8), presenting a smoother, but thicker layer with a fibrous surface. The SEM micrographs would suggest that a greater amount of MIP is coupled to the outer surface of the 15 μm membrane compared to the 5 μm membrane.
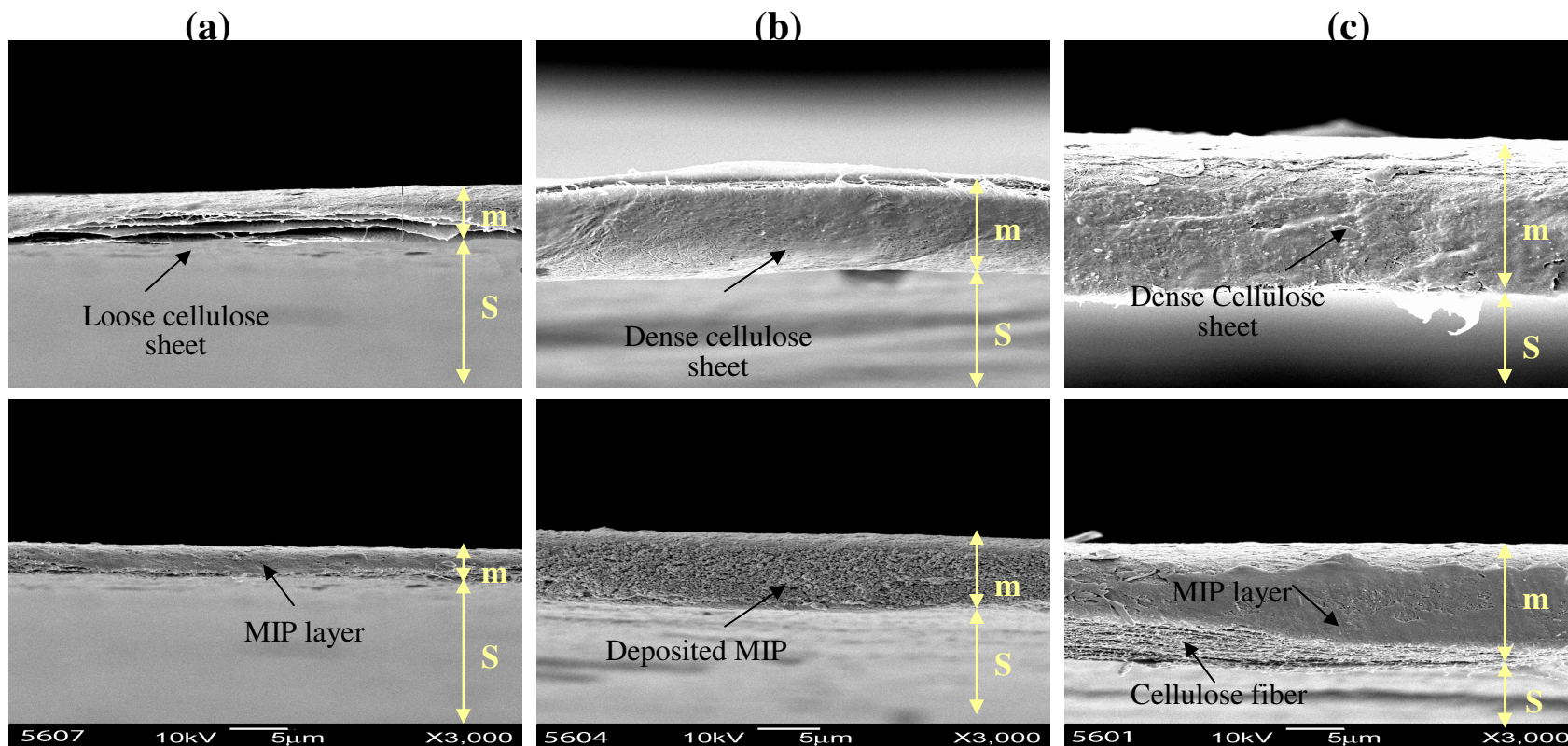
Figure 3.7. SEM-cross-section images of the initial cellulose membrane (top) and the MIP modified membranes (bottom), showing the different membrane thickness with differed membrane resistance. (a) 5 μm/1 Ω cm^2 membrane, (b) 10 μm/2 Ω cm^2 membrane and (c) 15 μm/4 Ω cm^2 membrane. Picture designation: s = stub, m = membrane.
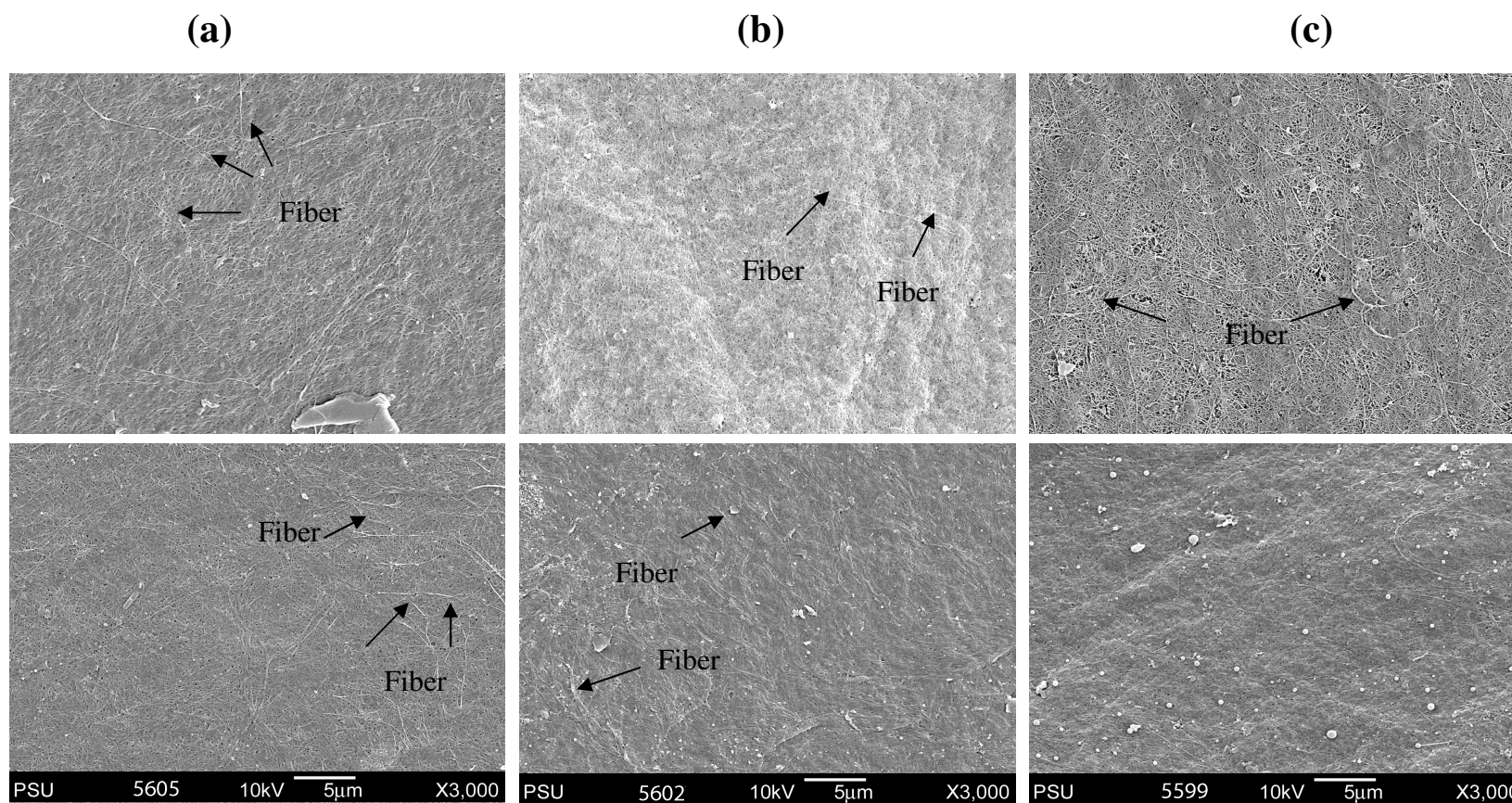
Figure 3.8. SEM images showing the surface morphology of the initial cellulose membrane (top) and the MIP modified membranes (bottom), showing the different membrane thickness with differed membrane resistance. (a) 5 μm/1 Ω cm^2 membrane, (b) 10 μm/2 Ω cm^2 membrane and (c) 15 μm/4 Ω cm^2 membrane.

The AFM images of the membrane (Figure 3.9) show the vertical profile of the sample with the light regions representing the highest points and the darkest regions showing the pores. The pore size obtained from the AFM images of the MIP membrane indicated that this was smaller than that of the parent nonmodified membrane.
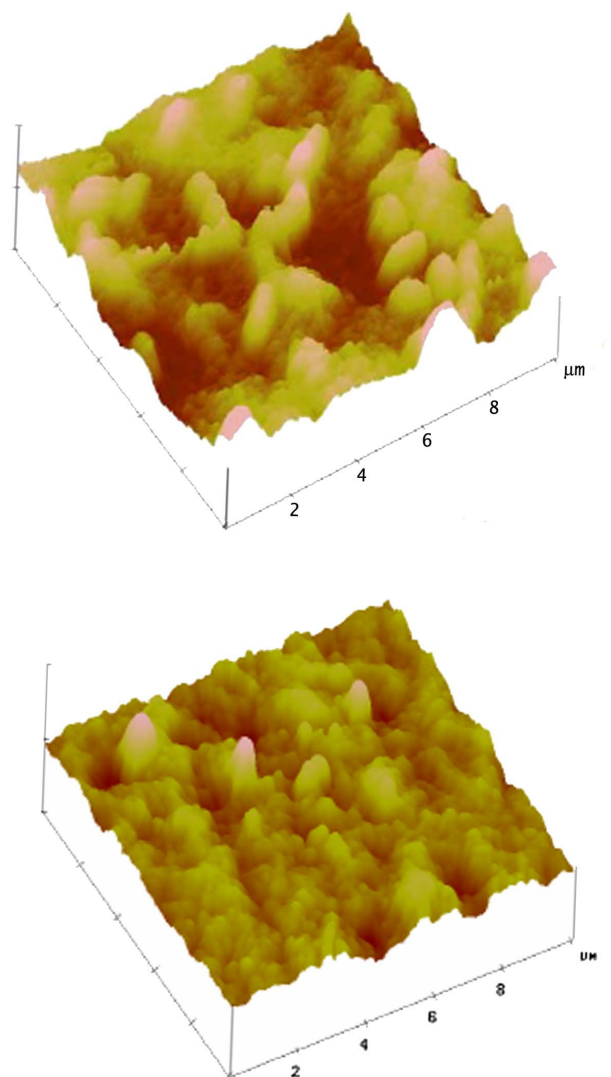
Figure 3.9. Three-dimensional AFM image of (a) 5 μm cellulose membrane and (b) 5 μm S-MIP membrane.

Table 3.2 shows that the partitioning of the propranolol enantiomers between S-MIP membranes and pH 7.4 buffer decreased with increase in the membrane thickness. The differences in the partition coefficients of *S*-enantiomer and *R*-enantiomer were greatest when the thickness of the composite membrane was smallest. Differential transport of the template enantiomer significantly increased with a decrease in the thickness of the membrane. The increase in the thickness of membrane resulted in a reduction in the specificity of S-MIP membrane. This phenomenon may be attributed to the effects of a gradient in DMF concentration being established in the monomer mixture near the surface of the membrane during the imprinting process. Such a gradient would be expected to lead to an alteration in the density of the created polymer network dependent upon depth of the grafted MIP layer. Supporting evidence for this can be seen from the SEM images (Figure 3.7) with much of the MIP not fully penetrating into the membrane pores of the thickest (15 μm) membrane but accumulating at the surface. Since the 5 μm MIP membrane enabled the highest diffusion rates of the enantiomers to be obtained with the greatest imprinting effect, this membrane was selected for further study as a basic membrane for the development of a composite MIP membrane, which might be applied to transdermal delivery. It was necessary to confirm that the basic cellulose membrane prepared with the method described in Section 3.3.3 each time provided similar appearances and release properties. Therefore the thinnest cellulose membranes were prepared on a number of occasions and their morphology examined and the mechanical strength determined. The percentage coefficient of variation (CV) for the thickness of the non-modified cellulose membranes was found to be 5% (n=6). Membrane porosity was found to vary from 1.4% to 2.4%, with the average pore size

170 nm. The %CV of the partition coefficients and enantioselectivity of the modified cellulose membranes obtained for three different batches of the initial membrane were found to be 5.0% and 10.0%, respectively. The mechanical stability of the cellulose membranes was not damaged during grafting process. The stability of cellulose membrane after modification was good, since the membrane could be reused after washing and similar release characteristics and selectivity were obtained.

From the results, S-MIP membrane obtained from 5-μm thin cellulose membrane showed the highest enantioselectivity. Therefore, in the further experiments, the 5-μm thin cellulose membrane was chosen as a membrane base for preparation of the MIP composite membrane.

Table 3.2. Partition (K) and diffusion coefficient of propranolol into/through MIP modified cellulose membranes (S-MIP) of different thicknesses and membrane resistances at room temperature (mean $\pm$ SE, n=3)

Solute	5 μm Membrane		10 μm Membrane		15 μm Membrane	
	K x 10^3	Diffusion coefficient x 10^{-2} (cm h^{-1})	K x 10^3	Diffusion coefficient x 10^{-2} (cm h^{-1})	K x 10^3	Diffusion coefficient x 10^{-2} (cm h^{-1})
R	1.01$\pm$0.22	0.70$\pm$0.26	1.59$\pm$0.18	3.46$\pm$0.41	0.37$\pm$0.20	6.11$\pm$1.23
S	1.79$\pm$0.32	30.84$\pm$2.51	1.56$\pm$0.38	8.10$\pm$1.82	0.29$\pm$0.16	6.62$\pm$0.73
S/R ratio	1.77$\pm$0.58	44.06$\pm$2.96	0.98$\pm$0.25	2.32$\pm$0.42	0.78$\pm$0.12	1.08$\pm$0.09

3.4.2. Characterisation of composite MIP membranes

The general properties of 5 μm S-MIP membranes were compared with those of NIP membrane and R-MIP membranes, which were all produced from the same basic cellulose membrane (Table 3.3). The values obtained for the electrical resistance of membranes provided an indication of the leakage of membrane and it was found that the electrical resistance of the cellulose membrane increased upon modification. This was presumably a consequence of the potential occlusion of the pores due to modification with the copolymer. An increase in the tensile strength of the membranes after modification was also found, possibly as a consequence of the introduction of a rigid copolymer of MAA/EDMA within the pores of cellulose membrane. The average pore diameters obtained by SEM, however, proved to be very similar, within the range 150–200 nm. The results presented in Table 3.3 indicated that cellulose membranes swelled greatly in aqueous solvent confirming the hydrophilic and highly porous nature, which promotes water absorption capacity. Swelling of the non-modified cellulose membranes in citrate buffer (pH 5.5) is clearly inherently greater than when they are placed in phosphate buffer (pH 7.4). The greater swelling of cellulose membrane in acidic pH might be explained by the hydronium ion (H_3O^+) could be formed the hydrogen bonding with the hydroxyl group of cellulose membrane resulting in the more swelling of the membrane than that at basic pH. When EDMA-MAA based polymers are bound at the pore surface, this causes a decrease in the degree of swelling. It might also have been expected that the introduction of ionizable carboxylic acid groups would have resulted in an increased swelling of the composite membrane at the higher pH. However the (modified)

cellulose membrane still shows a greater swelling at pH 5.5 than at pH 7.4. This suggested that the pH-dependency in the swelling of the MIP composite cellulose membranes is governed predominantly by the cellulose membrane.

Table 3.3. Characteristics of cellulose membrane and modified cellulose membrane (5 µm thickness membrane)

Membrane	Membrane resistance (Ω cm^2)	Tensile strength (kN/m^2)	Pore size (nm)[a]	Degree of swelling (%)[b]	
				pH 5.5	pH 7.4
Cellulose	1.11	3.16	177.92$\pm$35.38	101.25$\pm$9.21	55.57$\pm$5.72
NIP	1.71	7.20	146.30$\pm$36.54	74.30$\pm$9.94	34.01$\pm$3.30
R-MIP	1.71	7.20	176.91$\pm$47.76	77.61$\pm$8.62	33.41$\pm$3.82
S-MIP	1.71	7.20	198.27$\pm$4.22	72.36$\pm$3.81	44.44$\pm$9.84

[a] Refer to average pore size estimated from surface pictures of membrane obtained by SEM (n = 10)

[b] Mean $\pm$ SE, n = 3

CHAPTER 4

ENANTIOSELECTIVE PROPERTY OF THE MIP

COMPOSITE MEMBRANE

4.1. Selective transport of molecularly imprinted membrane (MIM)

Major mechanisms for selectivity in biological membranes are transported *via* carriers and through channels, both controlled by receptor-mediated signals, while the mechanisms of synthetic polymer membrane are different. Synthetic membranes (with non recognition) are either non-porous polymer, microporous (pore diameter ≤ 2 nm) or macroporous. Solution-diffusion mechanism governs transport through non-porous membrane. In the later two cases, transport and separation of substances are determined by sieving. For MIMs, template-specific cavities in the volume of a non-porous polymer are not accessible resulting in the low flux. With porous membranes, besides sieving, two different mechanisms for selective transport can be regarded:

• Facilitated permeation driven by preferential sorption of the template together with the better diffusion path availability (non or slow transport of non-specific solutes).

• Retarded permeation due to affinity binding (non or slow transport of the template) (Piletsky et al., 1999).

In case of facilitated permeation, depending on the membrane structure as well as MIP site concentration and distribution, transport can occur via carrier-mediated ("facilitated") transport, in real membranes coupled with diffusion (Ulbricht, 2004). Facilitated permeation mechanism can be found in the other advanced membranes (synthetic membrane with the recognition). A reversible complexation between the solutes and the carriers, which are embedded within polymer matrix, plays an important role for facilitated transport (Figure 4.1) (Sungpet et al., 2002). Two of the most likely mechanistic possibilities of the facilitated transport are carrier-diffusion and fixed-site jumping. With the fixed-site jumping mechanism, the transporter molecules act as "step stones" and the solute moves through the membrane by jumping from one fixed-site to another. For carrier-diffusion, the expected profile transport is a linear plot passing through the origin. For fixed-site jumping, the profile do not exhibit the linear relationship (Munro and Smith, 1997 and Riggs and Smith, 1997).
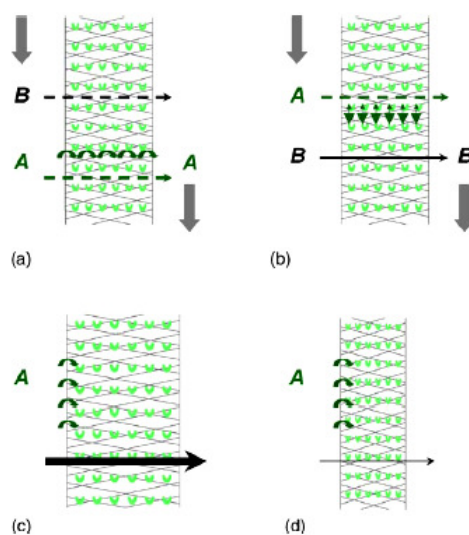
Figure 4.1. Separation mechanisms for MIM as a consequence of the binding selectivity obtained by imprinting for a substance A.

Figure 4.1. is the illustration of the selective separation of the MIM for the substance A : (a) transport of A driven by a concentration gradient is facilitated via binding/desorption to neighbored MIP sites, while the non-specific transport of another substance B by diffusion is hindered by the micropore structure of the membrane ("fixed carrier" membrane), (b) transport of A is retarded either by binding or binding/desorption to MIP sites on the surface of trans-membrane pores, while another substance B which has no specific interactions with the membrane surface will be transported by diffusion or convection (membrane absorber), (c) the MIM permeability is increased, e.g. due to an increase of membrane (barrier) swelling as a

consequence of A binding to MIP sites, (d) the MIM permeability is deceased, e.g. due to a decrease of membrane (barrier) swelling as a consequence of A binding to MIP sites (Ulbricht, 2004).

Some studies indicated an alteration of MIM permeability/conductivity due to binding of the template (Yoshimi et al., 2001 and Hattori et al., 2004). The nature of the gate effects might be explained assuming that interactions between the template molecules with polymeric domain (containing the selective cavities) result in the alteration of surface charge and cause subsequent conformational re-organization of the polymeric structure (Piletsky et al., 1999).

4.2. The objective of the study

The purpose of the study is to identify the effect of imprinting on the enantioselective property of the composite MIP membrane. For this, MIP membranes obtained from different template molecules (i.e. *R*-propranolol and *S*-propranolol) were determined upon comparison with the corresponding non-imprinted polymer (NIP) membranes.

4.3. Experimental

4.3.1. Chemicals and reagents

The NIP, R-MIP and S-MIP membrane were prepared form the 5-μm cellulose membrane with the membrane resistance of 1 Ω cm^2 and the tensile strength of 3.16 kN/m^2 were the same batch as prepared in Chapter 3.

4.3.2. Apparatus

The concentrations of the propranolol enantiomers were analyzed by chiral-HPLC method using a Chiralcel OD-R column connected with a Shimadzu HPLC system (Shimadzu Corporation, Kyoto, Japan).

4.3.3. Membrane evaluations

4.3.3.1. Measurement of partition coefficient

The partition coefficient of the membrane-buffer solution was evaluated according to the method described in the previous chapter. The pH of the buffer solution was 5.5 and 7.4 that represent to the pH of the skin (stratum corneum) and physiological pH. The membrane- pH 5.5 (μ=0.35) and pH 7.4 (μ=0.55) buffer partition coefficient was evaluated by equilibrating racemic propranolol solutions with

a membrane. The difference between the initial and equilibrium concentrations of each enantiomer in the aqueous phase was determined and hence the amount of propranolol enantiomer sorbed to the membrane was calculated. In a typical binding assay, the studied membrane (cellulose, NIP, R-MIP and S-MIP membrane which being 1 cm^2) was added to 5 ml of an aqueous solution containing 100 μg ml^{-1} of racemic propranolol in either pH 5.5 or citrate buffer or pH 7.4 phosphate buffer solutions, and stirred overnight at room temperature for equilibrium to be established. The selectivity factor representing the effect of the imprinting process was the ratio of K of the S-isomer to K of the R-isomer.

4.3.3.2. Permeation determination

The enantioselective transport of the cellulose and modified cellulose membrane (NIP, R-MIP and S-MIP membranes) were evaluated by a dialysis method using a vertical Franz-type diffusion cell as described in previous studied. The area of diffusion was 0.78 cm^2 and the volume capacity of the donor and receptor compartment were 1 and 2.5 ml, respectively. The studied membrane was mounted between the two chambers of the diffusion cells. The receptor chamber was filled with pH 7.4 phosphate buffer (μ=0.55) solutions. The required amount of racemic propranolol HCl (40 μg ml^{-1}) were dissolved in pH 5.5 or citrate buffer (μ=0.35) or pH 7.4 phosphate buffer solutions to obtain the donor solutions. 0.5 ml of the propranolol solution was placed evenly on the surface of the membrane. The solubility of propranolol enantiomers in the receiver medium at room temperature

(30°C) was monitored to maintance the sink condition for the duration of diffusion experiments. Drug release was measured by the removal of samples (250 μl) from the receiving chamber at appropriate time intervals over 6 h. The volume of the sample withdrawn was replaced by the same volume of the medium. Each test was carried out in sets of six. All experiments were run at room temperature (30°C). The diffusion of each propranolol enantiomer was determined using the chiral-HPLC analytical method outlined in Section 4.3.3.3. The selectivity of the membrane was defined as the ratio of the permeation flux of *S*-isomer to that of the *R*-isomer.

4.3.3.3. Stereospecific HPLC method

The analysis of the propranolol enantiomer content of the samples was performed directly using a chiral-HPLC method as described in section 3.3.5.9.

4.4. Results and discussion

4.4.1. Enantiomer uptake and imprinting effect

The partition coefficient of propranolol enantiomers from aqueous solutions into S-MIP membranes was compared with that for cellulose membrane, NIP membrane and R-MIP membrane in order to determine the effects of the imprinting procedure (Table 4.1). In pH 5.5 citrate buffer, the partition coefficients of

both *R*- and *S*-isomers decreased with the modification of cellulose membrane, while in pH 7.4 buffer the partition coefficients of propranolol enantiomers were generally increased by the modification of the cellulose membrane. The apparent preferential sorption of *S*-propranolol to the non-modified cellulose membrane (NIP membrane) in order to determine the effects of the imprinting procedure (Table 4.1) confirms the potential role of the parent cellulose membrane in the selective sorption of the propranolol enantiomers, even after the original membranes are transformed to MIP composite cellulose membranes. Thus the R-MIP membrane still demonstrated selectivity for the *S*-isomer, rather than the *R*-isomer, due to the properties of the cellulose membrane itself. Nevertheless the imprinting effect i.e. the difference between the *S/R* selectivity of the S-MIP membrane and that of the cellulose and NIP membrane was marked, suggesting that the molecular imprinting procedures have produced cavities with a higher affinity for the *S*-enantiomer of propranolol. At the higher pH the enantioselectivity of the membranes as determined by an increased partition coefficient for the *S*-isomer was not significant in the case of the non-modified cellulose membrane but it was for the S-MIP membrane. The enhanced enantioselectivity at a higher pH must be due to an increased binding of the favoured *S*-propranolol enantiomer at the binding site. This is most likely as a consequence of the higher degree of ionization of the functional monomer residues (pKa of MAA < 4) at the higher pH, resulting in an increased electrostatic interaction with the secondary amine of the propranolol molecule (Haginaka and Sakai, 2000).

Table 4.1. Partition coefficient (K x 10^3) of R- and S-propranolol enantiomers fom different donor pH solutions into cellulose and modified cellulose membrane (5 μm thickness membrane), at room temperature (mean $\pm$ SE, n = 3)

membrane	pH 5.5			pH 7.4		
	R-isomer	*S*-isomer	Ratio *S/R*	*R*-isomer	*S*-isomer	Ratio *S/R*
Cellulose	1.25±0.36	1.38±0.33	1.17±0.14	1.26±0.62	1.53±0.62	1.21±0.01
NIP	0.78±0.28	0.93±0.25	1.19±0.20	1.83±0.95	2.32±0.95	1.27±0.05
R-MIP	1.14±0.25	1.29±0.21	1.14±0.13	1.35±0.34	1.57±0.34	1.16±0.11
S-MIP	0.70±0.20	0.94±0.22	1.35±0.08	1.01±0.22	1.79±0.22	1.74±0.38

4.4.2. Selective transport of composite MIP membranes

Preliminary studies using an initial concentration of 40 μg ml^{-1} racemic propranolol established that a steady state flux was achieved during a period of 2–6 h (Figure 4.2 and 4.3). *R*- and *S*-propranolol enantiomers were transported faster across the unmodified cellulose membranes than those that had been modified, indicating the pore-filling effect of modified cellulose membranes. The faster transport of the *S*-enantiomer in comparison to the *R*-enantiomer confirms the inherent enantioselectivity of the modified cellulose membrane, indicated by the partition data. The S-MIP membrane was found to limit the permeation of *R*-enantiomer, and none was detected in the receptor compartment for at least 6 h, indicating the effects of the imprinting process on the pore structure. However the transport of the *S*-enantiomer through the R-MIP membrane was still faster than that of the *R*-enantiomer. This suggests that the inherent enantioselectivity of the original membrane still dominates the process, despite the modification of some of the pores with polymer synthesised in the presence of the *R*-enantiomer. The *R*-isomer was transported faster through the R-MIP membrane than through either the NIP or S-MIP membranes, as a consequence of the *R*-selectivity conferred on some of the membrane pores. These results suggest that the enantiomers are transported via a number of routes across the composite membranes. The cellulose fibers and/or the unmodified pores appear to have inherent selectivity for *S*-enantiomer whereas the modified pores will display selectivity for the template enantiomer. The pore-filling effects of the polymer do appear to reduce the transport of the *S*-enantiomer across the S-MIP membrane in comparison to the unmodified membrane. However the advantage of employing the S-MIP as opposed

to the unmodified membrane is that transport of the *R*-enantiomer over the 6 h of the study was eliminated in the former. The *S*-isomer/*R*-isomer selectivity of the propranolol enantiomers across the S-MIP membranes from pH 7.4 buffer was ca. 45, while the *S*-isomer/*R*-isomer ratio obtained with cellulose, NIP or R-MIP membranes was below 5 (Figure 4.3). For a donor solution with pH 5.5 (Figure 4.2), the *S*-isomer/*R*-isomer selectivity of S-MIP membrane was ca. 80 (the amount of transported of R-isomer was taken assuming the limit of detection was reached after 6 h) whereas the *S*-isomer/*R*-isomer selectivity of cellulose, NIP and R-MIP membranes was less than 20. It should also be noted that the faster drug transport rate at the lower pH correlates with the higher degree of swelling of the membrane (section 3.4.2). Such a swelling at pH 5.5 might alter the net pore size of cellulose membrane and partially account for the increased transport of the enantiomers. It is apparent also that the transport of *S*-propranolol and the enantioselectivity was higher for the S-MIP membrane at pH 5.5 as compared to pH 7.4.
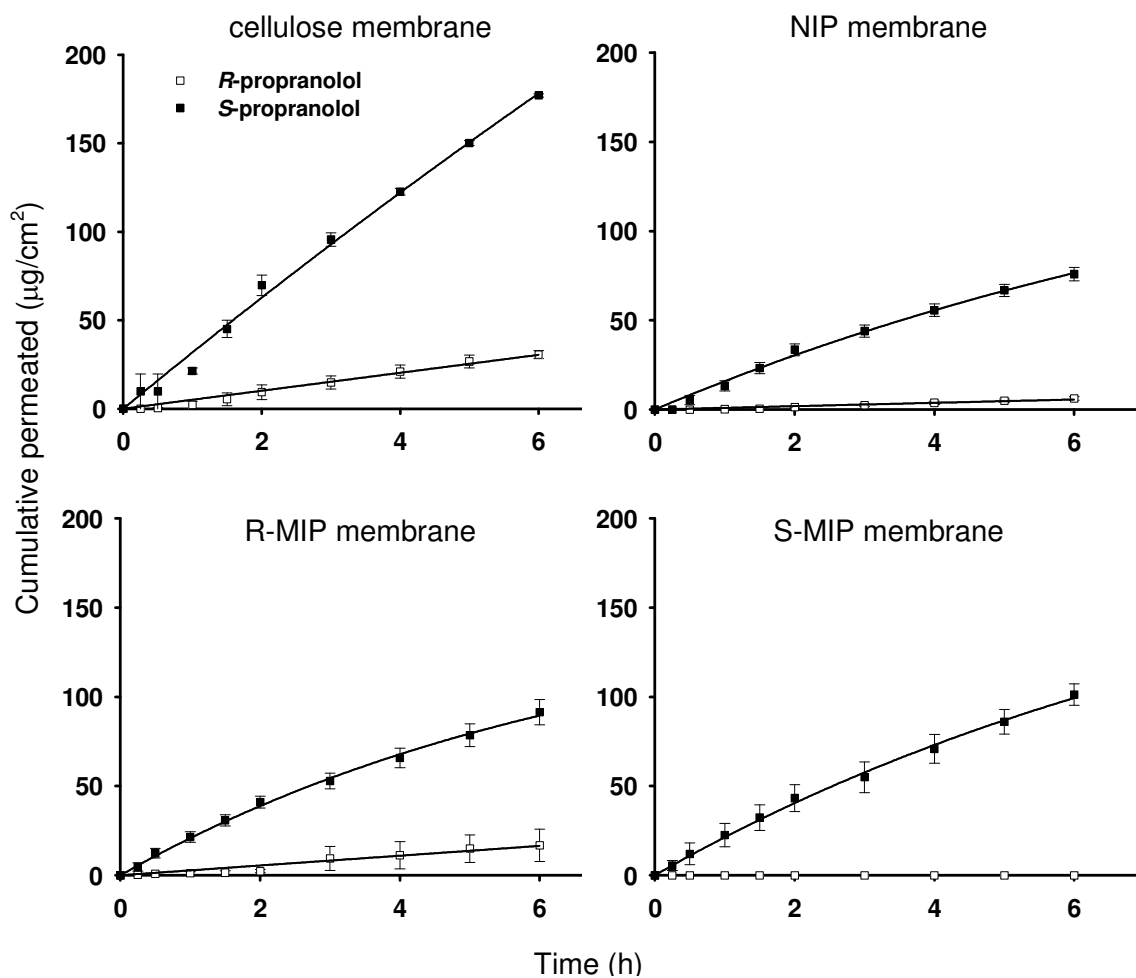
Figure 4.2. The transport of *R*- and *S*-propranolol enantiomers (HCl) as a function of time of various membranes from pH 5.5 citrate buffer.
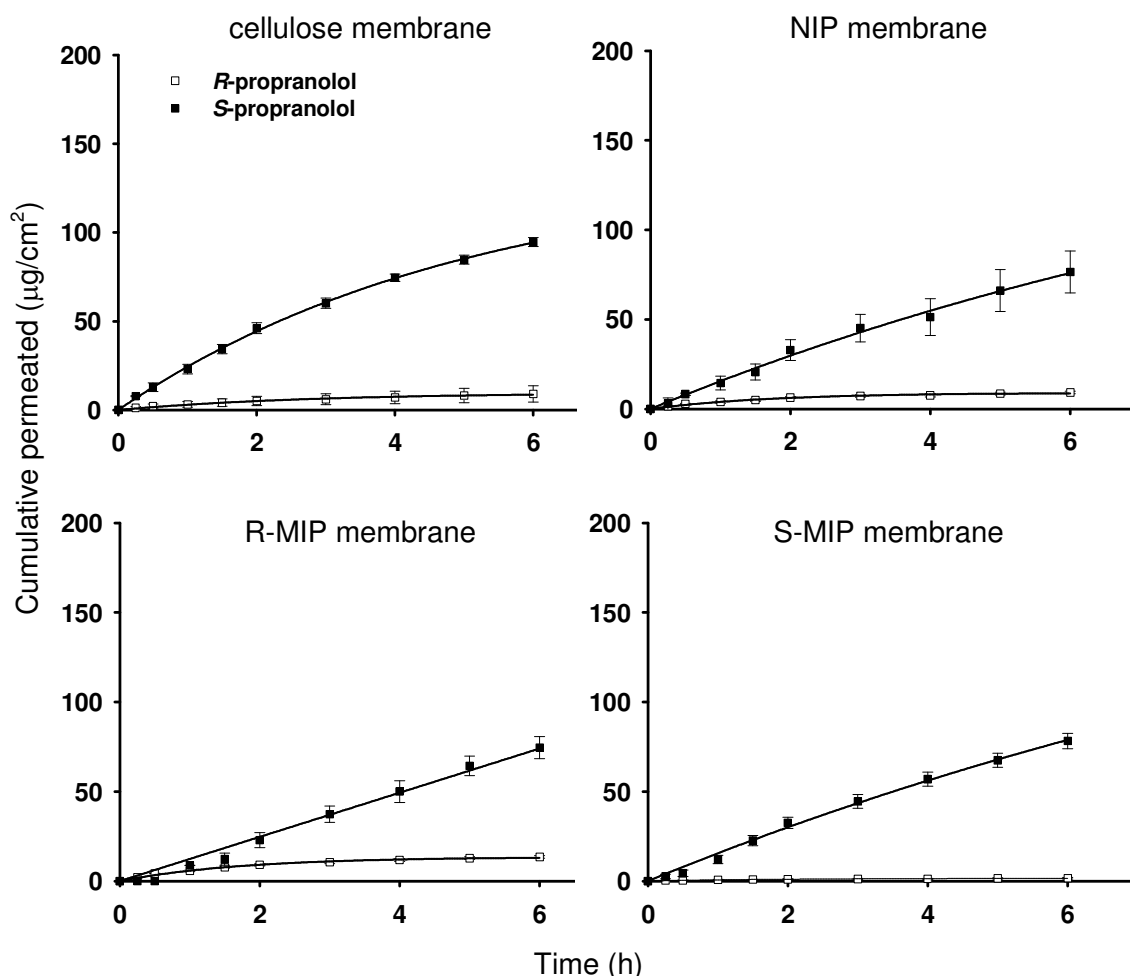
Figure 4.3. The transport of *R*- and *S*-propranolol enantiomers (HCl) as a function of time of various membranes from pH 7.4 phosphate buffer.

Two potentially opposing mechanisms are likely to affect the fluxes of the enantiomers at the two different pH values employed in this study. At the acidic pH, the increased swelling of the basic cellulose matrix would be expected to promote the overall transport of propranolol. However when the pH is raised to 7.4 then the improved MIP recognition, and increased electrostatic binding of the *S*-enantiomers to the S-MIP membrane might reduce the overall transport rate, as a consequence of binding and re-binding at sites within the MIP modified pores (see Figure 4.4). Whilst, at pH 5.5 the release of the *S*-propranolol enantiomer absorbed on the cellulose membrane or the MIP/NIP modified cellulose membranes might be expected to increase with swelling of membrane, which leads to change in the mass transfer rate of the enantiomer and the improved efficiency in enantioselectivity at the lower pH. It is apparent that cellulose membranes provided a degree of enantioselective transport for propranolol, but that this is lower than that achieved using the S-MIP membrane. The preferential sorption of *S*-propranolol to cellulose enhances the transport selectivity of S-MIP composite membranes and limits the involvement of the *R*-enantiomers in such a diffusive pathway. Therefore, although it would appear that the selective transport of *S*-propranolol obtained using a composite cellulose membrane is primarily determined by the parent cellulose membrane, a beneficial contribution is derived from the MIP component. The selective release characteristics of MIP grafted onto the pore surface of the cellulose membrane concurs with the 'fixed-carrier' mechanism that has been proposed for the selective transport achieved via ion-exchange carrier membranes. The facilitated transport conferred by a 'fixed-carrier' site membrane involves adsorption and mobility of the target molecule at the 'fixed-

carried' site. Previous work has shown that MIPs formed as a membrane (Noble, 1992 and Mathew-Krots and Shea, 1996) or prepared into a matrix tablet (Suedee et al., 2000 and Suedee et al., 2002) can provide a facilitated and selective transport of the template molecule. The means of controlled release involves reversible complexation and exchange between the template molecule and sites in the MIP membrane (or the MIP tablet). The *S*-isomer of propranolol binds selectively to the MIP binding sites, with its subsequent reactive diffusion taking place by stepwise dissociation and selective binding to neighboring MIP sites. From the results obtained, it shows that the binding of *S*-propranolol enantiomer to MIP is reversible and fast enough to enable the transport of *S*-enantiomer. The *S*-propranolol complexing to and dissociating from the MIP plays an important role in the enantioselectivity of S-MIP membrane. Any factor that alters in rate of complexation/decomplexation of *S*-propranolol enantiomer with MIP will change the flux and stereoselectivity of the S-MIP composite membrane. In addition as indicated previously, the basic cellulose membrane in the S-MIP membrane plays a crucial role towards the transport of propranolol enantiomers. Macroscopic changes such as degree of hydration and pH of the medium have a marked effect on transport rate through changes in effective pore size and alteration of enantiomer-membrane partition (Table 4.2). Indeed any change in the latter will have a direct effect on transport role, since Fick's first law indicates that the rate is dependent upon partition coefficient.
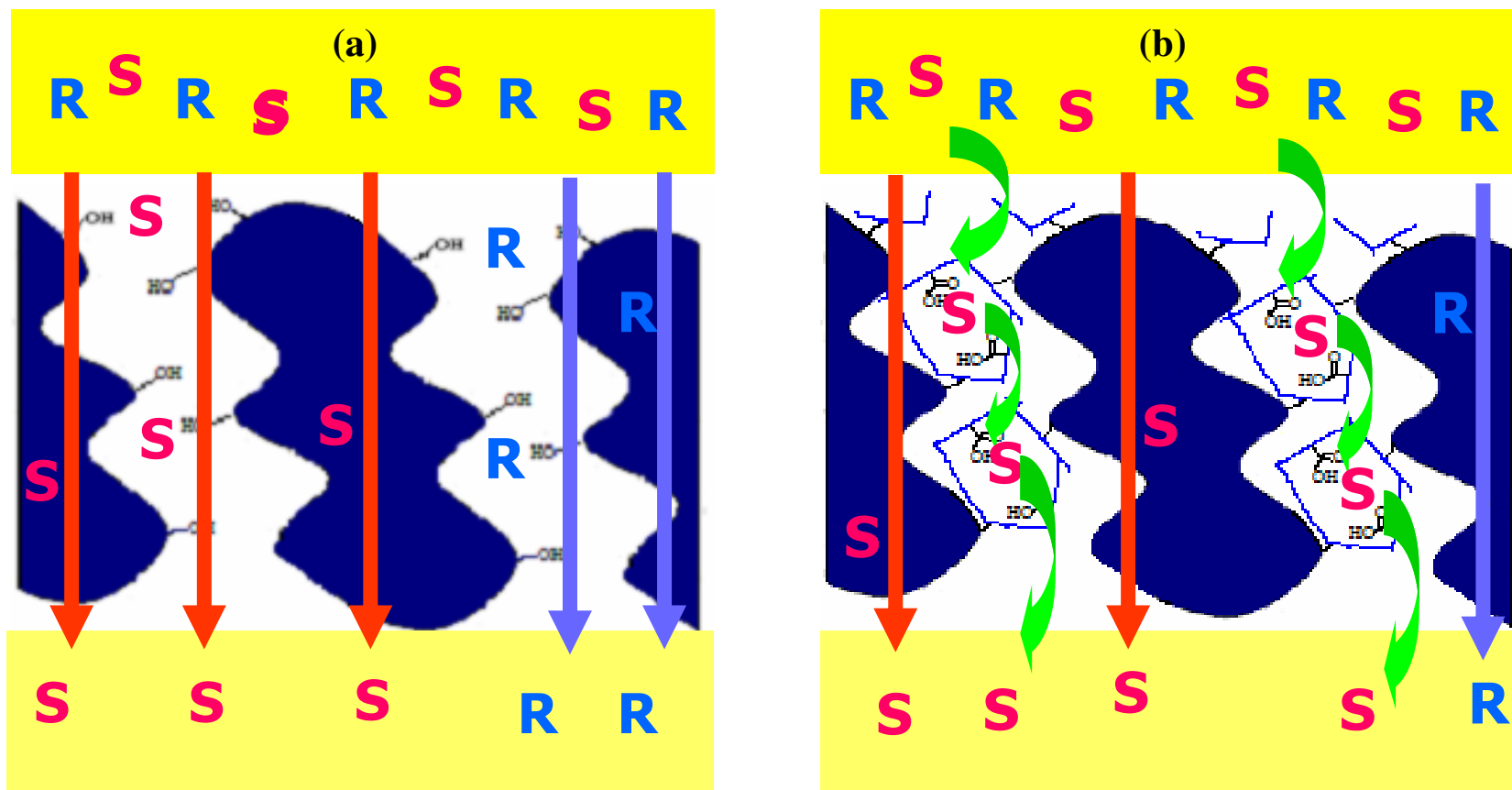
Figure 4.4. Illustration for explanation of the possible selective transport of the (a) cellulose membrane and (b) S-MIP membrane via 'fixed-carrier' mechanism.

CHAPTER 5

SYNTHESIS AND CHARACTERIZATION OF

PRODRUGS

5.1. The objective of the study

The objective of this study was to prepare the propranolol prodrugs for study the enantioselective release property of the MIP composite membrane. This is belived that propranolol prodrugs which have chemical structure similarly to the template, would exhibit the enantioselective transport of *S*-enantiomer through the MIP composite membrane same as propranolol. Apart, the ester prodrugs of propranolol increase the penetration into skin, since they show higher lipophilicity property than the parent compound. For this purpose, three propranolol prodrugs (i.e. valeryl propranolol, cyclopropanoyl propranolol and succinyl propranolol) were synthesized and the physico-chemical properties and hydrolysis of these prodrugs were studied. In addition, the enantioselective release of *S*-isomers of the prodrugs for the MIP composite membrane was studied.

5.2. Prodrug approach

Many drugs are high polarity substances poorly penetrating through the skin by the mechanism of simple diffusion. For this reason, the idea of using the lipophilic prodrugs is justified provided these prodrugs really more rapidly diffuse through the skin (Vasil'ev et al., 2001).

The prodrug approach is to improve the drug delivery by chemical biotransformation of the active drug substances to inactive derivatives (prodrugs) which are converted to the parent compounds within the body. When the parent or active drug is not fully utilized because of poor membrane permeability due to unfavorable physio-chemical properties, theses properties can be altered by attachment of a pro-moiety. This allows the prodrug to bypass the barrier and, once pass the barrier, to revert to the parent compound by a post-barrier enzymatic or non-enzymatic process (Figure 5.1) (Bundgaard, 1989).
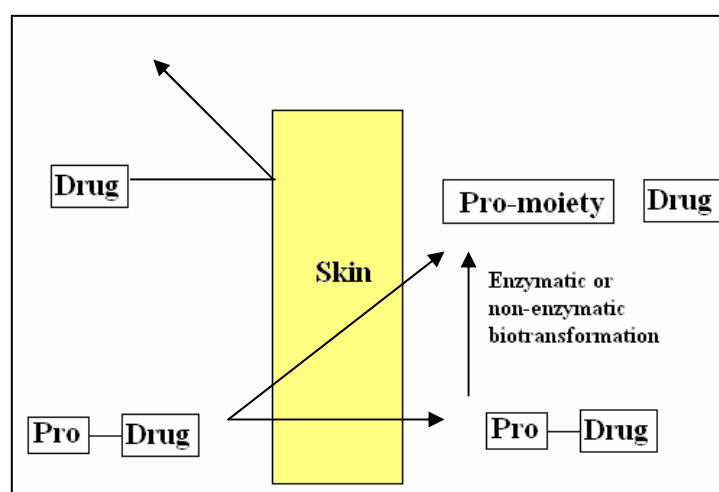
Figure 5.1. The prodrug approach as a means of improving drug absorption (Adapted from Bundgaard, 1989).

Most of the applications of the prodrug approach to date have involved enhancement of bioavailability following various route of administrations such as oral, transdermal, ocular or rectal (Table 5.1). Most prodrugs are in the form of ester compounds which are easily hydrolyzed by esterases present in the skin.

Table 5.1. Examples of β-blocker prodrugs used in drug delivery system.

Delivery system	Drug	Type of prodrugs	References
Oral	Propranolol	O-acetyl propranolol, O-hemisuccinyl propranolol	Anderson et al., 1988
	Propranolol	O-n-acetyl propranolol	Irwin and Belaid, 1988
	Propranolol	butyryl propranolol, isovaleryl propranolol	Yoshigae at el., 1998
	Propranolol	palymitoyl propranolol	Vyas et al., 1999
Transdermal	Propranolol	isovaleryl propranolol, cyclopropanoyl propranolol	Ahmed et al., 1995
	Propranolol	butyryl propranolol, Caproyl propranolol	Ahmed et al., 1997

Table 5.1. Examples of β-blocker prodrugs used in drug delivery system (continued).

Delivery system	Drug	Type of prodrugs	References
Ocular	Timolol	*O-n*-acetyl timolol	Bundgaard et al., 1986
	Propranolol	*O-n*-acetyl propranolol	Buur et al., 1988
		2-oxazolidine propranolol	
	Timolol	*O-n*-acetyl timolol	Bundgaard et al., 1988
	Oxprenolol	*O-n*-acetyl oxprenolol	Jordan et al., 1992
	Propranolol	*O-n*-acetyl propranolol	Quigley et al., 1994
	Timolol	palymitoyl timolol	Pech et al., 1996
	Propranolol	*O-n*-acetyl propranolol	Jordan et al., 1996
	Oxprenolol	*O-n*-acetyl oxprenolol	Jordan et al., 1996

5.3. Skin metabolism

Skin is the outermost layer of human organism separating the internal from the external environment. Hence, the skin is exposed from the external side to numerous substances, cosmetics, topical drugs, chemicals, and environmental pollutants. The skin is capable of metabolizing endogenous and exogenous substances. The biotransformation reactions in the skin comprise functionalization (phase I) and conjugation (phase II) reactions. The biotransformation reactions in the skin include oxidation, reduction, and hydrolysis reaction which have been found likewise as conjugation with glucuronic acid, sulfuric acid, glutathione, and methylation.

Although the skin also shows the metabolic activity likely with liver or plasma, the specific enzyme activities related to milligram of microsomal protein for most enzymes are considerably higher (5-10 fold) in the liver compared to the skin (Täuber, 1989). The metabolic enzymes, including hydroxylases, deethylases, hydrolases, esterases and peptidases, reside in the skin and appendages, mostly at the epidermal layer (Mills and Cross, 2006).

5.4. Experimental

5.4.1. Chemicals and reagents

Racemic propranolol HCl and valeryl chloride were purchased from Aldrich Chemical Company (Milwaukee, WI, USA). Succinic anhydride and cyclopropanecarbonyl chloride were supplied by Fluka ChemieAG (Buchs, Switzerland).

The NIP, R-MIP and S-MIP membrane were prepared form the 5-μm cellulose membrane with the membrane resistance of 1 Ω cm^2 and the tensile strength of 3.16 kN/m^2 were the same batch as prepared in Chapter 3.

5.4.2. Apparatus

IR spectra of the ester prodrugs were recorded on FT-IR spectrophotometer (Perkin Elmer PE1600 FTIR, USA).

^{1}H-NMR spectra were recorded on an INOVA 500 MHz NMR spectrometer (Varian INOVA, Australia) at 25°C. Chemical shifts are referenced to the solvent reference signal TMS (Tetramethylsilane).

Mass spectra were recorded on a MAT 95 XL Mass Spectrometer (Thermofinnigan, Geramany).

UV absorbance measurements were recorded using a Hewlett-Packard diode array spectrophotometer Series 8452A (CS, USA).

The tissue homogenates were prepared by using Ultrasonic Liquid Processing Vibra Cell tissue homogenizer (SONICS, Sonics&Materials, Inc., USA) which the temperature of the operation was controlled at 4°C.

The preparations were centrifuged by HERMLE z 323k centrifuge (Hermile Lobortechnik, Germany) at 15000 rpm for 30 min at 0°C.

The amounts of propranolol enantiomers in the sample obtained in this study were analyzed by chiral-HPLC method using a Chiralcel OD column connected with a shimadzu HPLC system (Shimadzu Corporation, Kyoto, Japan).

5.4.3. Synthesis of propranolol prodrugs

The effect of propranolol prodrug for increasing the permeation of propranolol through the skin was studied. In this study, two lipophilic propanolol prodrugs (valeryl propranolol and cyclopropanoyl propranolol) and one hydrophilic propranolol prodrug (succinyl propranolol), see chemical structure in Figure 5.2 were chosen. The propranolol prodrugs were synthesized from racemic propranolol hydrochloride and fatty acid chlorides by substituting different alkyl groups onto the hydroxyl group, according to the method described previously (Bungraard et al., 1986 and Quigley et al., 1994), replacing timolol HCl with in the same stoichiometric ratios (Figure 5.3).

The propranolol ester prodrugs were prepared by reacting propranolol HCl with the corresponding acid chloride (valeryl chloride or succinic anhydride or cyclopropanecarbonyl chloride). Propranolol hydrochloride (3 mmol) was slurried in 12 ml of benzene. The appropriate acid chloride (10 mmol) was added and the mixture refluxed with stirring for 2 h. After cooling, the mixture was evaporated in vacua. Benzene (10 ml) was added and the mixture evaporated again to remove traces of the acid chloride. The solid residue was slurried in ether, filtered off and washed with ether. The prodrugs were purified by recrystallization from ethanol-ether. IR, ^{1}H-NMR and Mass spectrosmetric analysis were conducted to confirm the synthesis of the propranolol prodrugs.
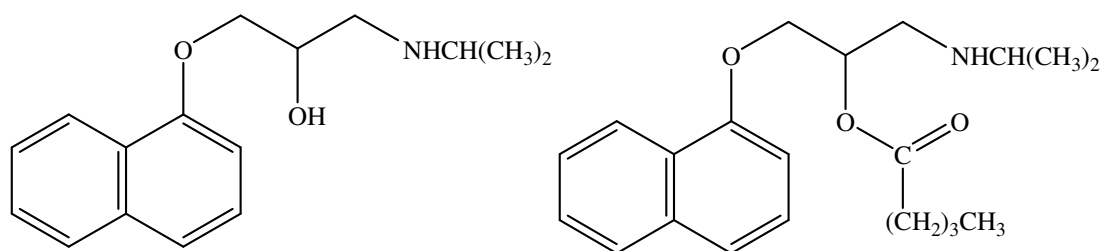
Propranolol

Valeryl propranolol (VL-P)
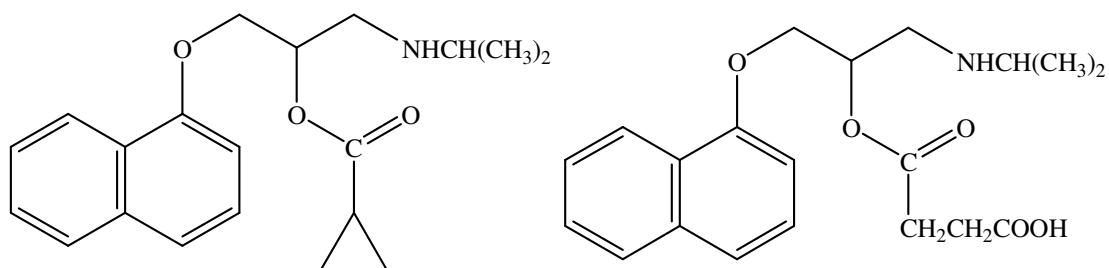
Cyclopropanoyl propranolol (CP-P)

Succinyl propranolol (SN-P)

Figure 5.2. The chemical structure of propranolol and propranolol prodrugs.
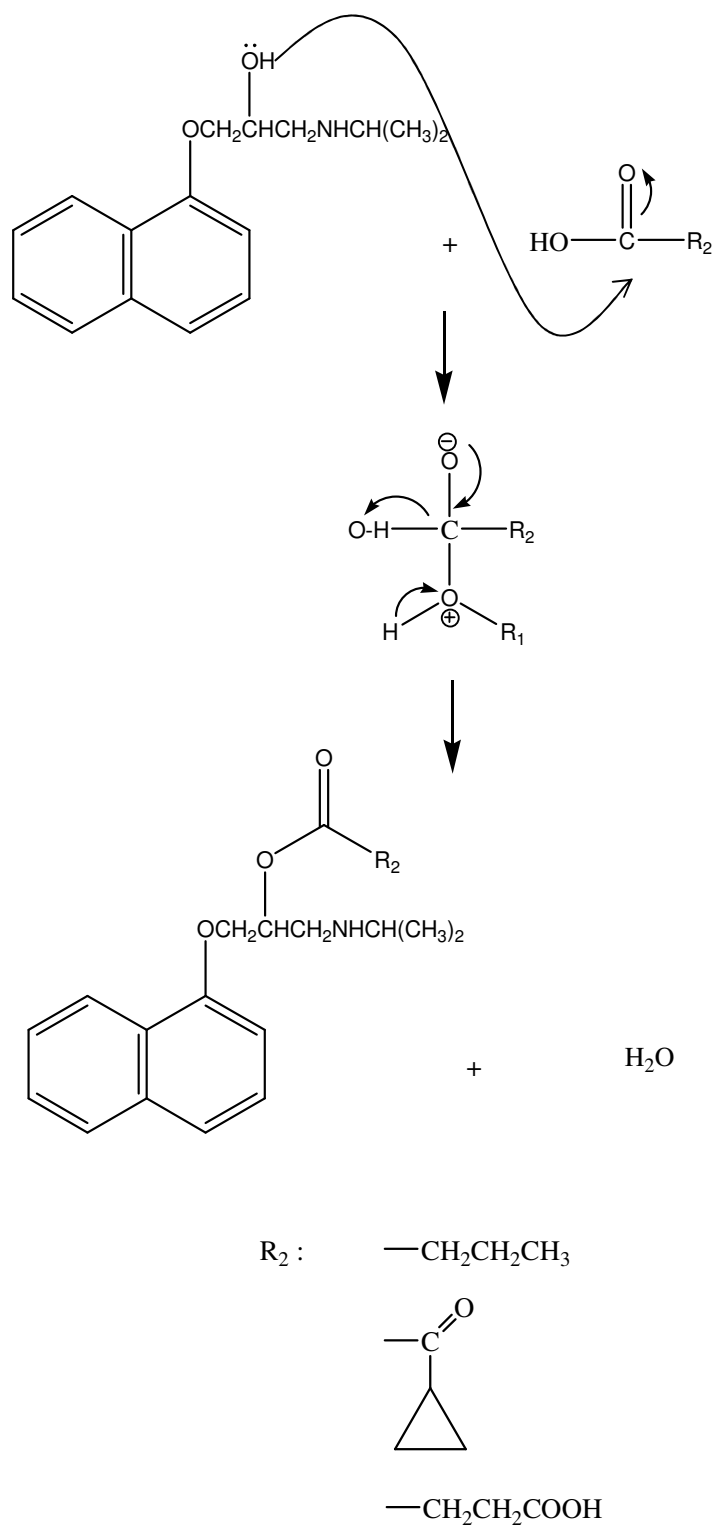
Figure 5.3. Schematic of propranolol prodrug synthesis.

5.4.4. Determination of physical and hydrolysis properties of the propranolol prodrugs

The method for determination in the physical property and hydrolysis of propranolol prodrugs were modified from that described by Ahmed et.al.

5.4.4.1. Solubility determination

An equilibrium solubility determination was undertaken in 0.01 M acetate buffer (pH 4, 37°C). The excess propranolol prodrugs were added to 1 ml of buffer. The samples were shaken mechanically in a temperature-controlled water bath at 37°C for 24 h. The resulting saturated solutions were filtered and the filtrate solutions were diluted. The solubility of each drug was determined by UV-Vis at 290 nm.

5.4.4.2. Measurement of partition coefficient

The partition coefficient of propranolol and the prodrugs were determined in 1-octanol – pH 4 acetate buffer system. The buffer solution and 1-octanol were mixed together and saturated at 25°C before study. Propranolol hydrochloride and propranolol prodrugs were added into the saturated 1-octanol – pH 4 acetate buffer solution. The concentration of each drug in pH 4 buffer was measured by UV-Vis at 290 nm. The partition coefficients were determined as the ratio between the concentration measured in 1-octanol and the concentration measured in the buffer.

5.4.4.3. Hydrolysis studies

1). Animals

Male Wistar rats, weighing 230-250 g, were used for *in vitro* penetration experiments. All the animals were procured from central animal facility of Prince of Songkla University, Songkla, Thailand after clearance from local ethic committee (ST. 0521.05/054). The rats were housed under standard conditions. The temperature was controlled at 25 ± 1°C and the relative humidity was 40-60%. The animals were kept in plastic cages in groups of five per cage. They had access to a commercial diet and tap water ad libitum.

2). Hydrolysis of prodrugs

All of the experiments for homogenate preparations and hydrolysis studies were carried out at 0-4°C to protect the degradation of enzyme. After sacrificing the rats by snapping the spinal cord at the neck, the skin, liver and blood were removed immediately. To prepare the skin or liver homogenate, skin or liver was quickly minced, mixed with cold Tris-HCl buffer (pH 7.4) containing 0.15 M KCl for skin homogenate and cold 0.15 M KCl for liver homogenate. The preparations were bursted by tissue homogenizer for 4 times. Each time the preparations were bursted for 3 minutes and there was a pause of 1 minute between each to permit cooling tissue. The preparations were centrifuged at 15000 rpm for 30

min at 0°C with HERMLE z 323k centrifuge, the supernatant of each preparations were taken and stored at -80°C until use. To prepare plasma for using in hydrolysis study, the collected blood was centrifuged at 3000 rpm and used immediately. The protein contents of the enzyme samples were determined by absorbance assay at 280 nm by using UV-Vis spectroscopy.

All kinetic measurements were carried out at 37°C in a shaking thermostatic water bath. The reaction was initiated by addition the prodrugs to the skin or liver or plasma preparation or buffer, which has been preincubated for 10 min. At appropriate intervals, 100 μl aliquots were withdrawn and then extracted with 1 ml of diethyl ether. The samples were mixed after that the organic phase was collected and dried at room temperature overnight. The samples were reconstituted with 125 μl of mobile phase before injection to HPLC. The residual prodrug was cleaned and analysed by Chiral-HPLC (see Chapter 3, section 3.3.5.9). First order rate constants for the hydrolysis were determined from the slopes of linear plots of the logarithm of residual prodrug against time according to the equation below.

$$\ln[A] = -kt + const. \qquad (5.1)$$

where *[A]* is the concentration of the reactant or prodrug, *t* is time of hydrolysis, *k* is the hydrolysis rate of first order reaction and *const.* is the constant of the reaction.

5.4.5. Measurement of membrane-buffer partition coefficient

The membrane- pH 5.5 (μ=0.35) and pH 7.4 (μ=0.55) buffer partition coefficient was evaluated by equilibrating racemic propranolol prodrugs solutions with a membrane as described previously (see Chapter 3, section 3.3.5.7). The difference between the initial and equilibrium concentrations of each enantiomer in the aqueous phase was determined and hence the amount of propranolol prodrugs enantiomer sorbed to the membrane was calculated. In a typical binding assay, the membrane (cellulose, NIP and S-MIP membrane which being 1 cm^2) was added to 5 ml of an aqueous solution containing 100 μg ml^{-1} of racemic propranolol prodrugs in either pH 5.5 or citrate buffer or pH 7.4 phosphate buffer solutions, and stirred overnight at room temperature for equilibrium to be established. The selectivity factor representing the effect of the imprinting process was the ratio of *K* of the *S*-isomer to *K* of the *R*-isomer.

5.4.6. Permeation determination

The enantioselective transport of the cellulose and modified cellulose membrane (NIP and S-MIP membranes) were evaluated by a dialysis method using a vertical Franz-type diffusion cell as described in the Chapter 3 (see section 3.3.5.8). The diffusion cell composed of two compartments and the studied membranes were sandwiched between the two. The area of diffusion was 0.78 cm^2 and the volume capacity of the donor and receptor compartment were 1 and 2.5 ml, respectively. The studied membrane was mounted between the two chambers of the diffusion cells. The

receptor chamber was filled with pH 7.4 phosphate buffer (μ=0.55) solutions. The required amount of racemic propranolol prodrugs (50 μg ml^{-1}) were dissolved in pH 5.5 or citrate buffer (μ=0.35) or pH 7.4 phosphate buffer solutions to obtain the donor solutions. 0.5 ml of the propranolol prodrugs solution was placed evenly on the surface of the membrane. Drug release was measured by the removal of samples (250 μl) from the receiving chamber at appropriate time intervals over 6 h (15, 30, 60, 90, 120, 180, 240, 300, and 360 min). The volume of the sample withdrawn was replaced by the same volume of the medium. Each test was carried out in sets of four. All experiments were run at room temperature (30°C). The diffusion of each propranolol prodrugs enantiomer was determined using the chiral-HPLC analytical method outlined in Section 3.3.5.9. The selectivity of the membrane was defined as the ratio of the permeation flux of *S*-isomer to that of the *R*-isomer.

5.4.7. Molecular modeling

The 3-D chemical structures of *S*-propranolol and *S*-prodrugs have been modeled with molecular mechanics (Chem3D Ultra 8.0, CambridgeSoft, MA, USA) followed by energy minimization using Truncated Newton (MM2 force field).

5.4.8. Sample preparation

To 'clean-up' the receptor phase samples, a liquid–liquid extraction method was employed. Diethyl ether (2 ml) was added to 250 μl of receptor phase samples. Propranolol prodrug enantiomers were extracted into diethyl ether by shaking for 10 min, using mutually pre-saturated phases. Organic phase (2 ml) was

collected and evaporated to dryness under reduced pressure. The samples were dissolved in 125 µl of HPLC mobile phase, in readiness for assay.

5.4.9. Stereospecific HPLC method

The analysis of the propranolol enantiomer content of the samples was performed directly using a chiral-HPLC method as described in section 3.3.5.9.

5.5. Results and discussion

5.5.1. Physical properties and hydrolysis of the propranolol prodrugs

Table 5.2 shows the physical properties of the propranolol and propranolol prodrugs such as solubility and partition coefficient. These parameters are important for the decision of prodrugs in transdermal delivery system. The solubility studies of the prodrugs were determined in acidic condition (pH 4.1 acetate buffer) for stabilizing the ester prodrugs. SN-P was the highest soluble compared with the other prodrugs because of the hydrophilic group in its molecule (Figure 5.2), while VL-P was the least soluble. The partition coefficient parameter showed the higher log P value of VL-P and CP-P and the lower of SN-P. Partition coefficient is an important parameter for transdermal delivery, the ideal drug for transdermal delivery should have the appropriate partition coefficient value for the ability to penetrate to the lipophilic layer of stratum corneum and hydrophilic layer of dermis. From these

results, the ester prodrugs would be expected to transport through the rat skin more than the parent compound.

Table 5.2. Solubility and Partition coefficient (Log P) of propranolol and propranolol prodrugs

Compounds	Solubility (mg ml^{-1})	Log P
Propranolol	-	2.4
SN-P	598.5	0.68
VL-P	5.15	89
CP-P	8.35	14.4

The hydrolysis of the ester prodrugs in buffer and different tissue preparations exhibited typical first-order kinetics, and the hydrolysis rate constants of the prodrugs are shown in Table 5.3. No stereoselective hydrolysis was observed in the buffer, and this result confirmed the previous study of Takahashi et al. (1991), Ahmed et al. (1995) and Ahmed et al. (1997). All of tissue preparations showed the stereoselectivity hydrolysis and the hydrolysis rate was greater in liver homogenate according with plasma and skin homogenate, respectively. In plasma hydrolysis studies, the VL-P and CP-P showed the R-selectivity, while SN-P showed the S-selectivity. Moreover, in liver and skin hydrolysis studies, the S-enantiomer prodrugs showed the higher hydrolysis rate constant. These results were contrary to the results

reported by Ahmed et al. (1997) when hairless mice were used as models. Ahmed reported that the hydrolysis rates of *R*-enantiomer of the prodrugs for all tissue preparations (plasma, liver and skin homogenate) were higher than *S*-enantiomers. However, Takahashi et al. (1991) showed that plasma had the *R*-selectivity while the liver preparation had the *S*-selectivity, when Wistar rats were used as models. From these results, it indicated that the hydrolysis enzymes are different in various tissue preparations, therefore the different hydrolysis of the prodrugs in different tissue was observed and the hydrolysis properties were effected by the different species of the animal models.

Table 5.3. Stereoselective hydrolysis rate constants of propranolol prodrugs in buffer and different tissue preparations of rats at 37°C.

Prodrugs		Rate constant x 10^3			
		Buffer pH 7.4 (min^{-1})	Plasma(min^{-1} mg^{-1})	Liver Homogenate (min^{-1} mg^{-1})	Skin Homogenate (min^{-1} mg^{-1})
VL-P	(R)	5.5±1.0	2422.8±990.1	1495.8±180.0	149.6±64.4
	(S)	6.1±1.8	2344.6±797.8	1690.4±371.1	189.2±60.5
	R/S	1.0±0.1	1.5±0.7	0.9±0.0	0.8±0.3
SN-P	(R)	6.6±1.0	1307.3±147.3	1970.1±462.0	98.0±16.8
	(S)	6.6±1.1	2188.3±833.8	2103.9±371.1	147.0±6.3
	R/S	1.0±0.1	0.7±0.2	0.9±0.1	0.7±0.2
CP-P	(R)	2.6±1.0	963.9±94.5	462.1±99.6	89.4±29.0
	(S)	2.4±0.8	703.4±26.1	498.6±48.0	252.8±81.0
	R/S	1.1±0.1	1.4±0.4	1.0±0.3	0.4±0.1

5.5.2. Selectivity of the composite MIP membrane for propranolol prodrugs

The propranolol prodrugs employed in this study were valeryl propranolol (VL-P) cyclopropanoyl propranolol (CP-P) and succinyl propranolol (SN-P) (see Figure 5.2), which were synthesized from racemic propranolol hydrochloride and fatty acid chlorides by substituting different alkyl groups onto the hydroxyl group, according to the method described previously (Quigley et al., 1994). The partitioning of racemic prodrugs from saturated solutions was determined at both pH 5.5 and pH 7.4 (Table 5.4). Generally the *S*-enantiomers were sorbed to both the nonmodified and modified cellulose membrane in greater quantities than the *R*-isomer at both pH values. The *S*-enantioselectivity of the unmodified cellulose membrane was apparent for all prodrugs, with the exception of SN-P at the higher pH. As in the case of the parent propranolol molecule, the S-MIP modification of the membrane improved the *S*-enantioselectivity further. Again the enantioselectivity proved to be generally higher at pH 7.4. There are many factors that affect the sorption of propranolol prodrugs on the membranes. Since the ester modification of hydroxyl group increases the hydrophobicity of the propranolol molecule, i.e., in case of VL-P and CP-P, interaction between propranolol enantiomers and cellulose might be expected to be reduced.

Table 5.4. Partition coefficient (K) of propranolol prodrugs into non-modified cellulose and modified cellulose membranes at

different pH values at room temperature (mean±SE, n=3)

		K (x 10³)					
Prodrugs	**Membrane**	**pH 5.5**			**pH 7.4**		
		R	**S**	**S/R**	**R**	**S**	**S/R**
	Cellulose	1.11±0.51	1.35±0.93	1.20±0.39	1.26±0.14	1.63±0.68	1.43±0.69
VL-P	NIP	1.88±0.30	2.10±0.45	1.09±0.07	1.26±0.38	1.67±0.73	1.32±0.12
	S-MIP	0.74±0.21	1.38±0.22	1.71±0.17	0.74±0.29	1.53±0.19	2.11±0.17
	Cellulose	1.30±0.38	1.82±0.53	1.42±0.10	1.03±0.25	0.94±0.30	0.91±0.11
SN-P	NIP	1.61±0.12	1.94±0.38	1.16±0.16	0.26±0.17	0.22±0.18	0.85±0.24
	S-MIP	0.60±0.17	0.74±0.09	1.36±0.17	0.44±0.23	0.60±0.33	1.31±0.11
	Cellulose	0.68±0.12	0.82±0.21	1.20±0.52	0.83±0.02	1.44±0.11	1.73±0.17
CP-P	NIP	1.28±0.23	1.44±0.34	1.12±0.13	0.85±0.07	0.82±0.34	0.98±0.30
	S-MIP	1.02±0.53	1.58±0.23	1.55±0.59	1.59±0.04	2.62±0.20	1.65±0.09

The introduction of different bulkier side chains would be expected to reduce the interaction with any recognition site and the diffusion coefficients of VL-P and CP-P S-isomers through the S-MIP membrane (Table 5.5) were markedly higher than that of *S*-propranolol HCl (see chapter 4). However the diffusion of the *S*-isomer of the most hydrophilic prodrug, SN-P was comparable to that of the parent compound. Since enantioselectivity is preserved when the prodrugs are employed as the diffusing species, this demonstrates that the hydroxyl group, present in propranolol is not crucial. It is apparent that it is the position of the charged nitrogen group within the partitioning and diffusing species, relative to the carboxylic acid residues of MAA that is the dominant mechanism involved in the interaction between the enantiomers and substrate. A preliminary examination of the energy-minimised structures of *S*-propranolol and its prodrugs (Figure 5.4) suggests that VL-P might be expected to adopt a conformation most similar to the parent compound. The principal interaction, as indicated previously, is likely to be between the secondary amine group within the molecule(s) and the carboxylic acid group of the functional monomer. However the pendant groups within VL-P would appear to be most similarly positioned to the parent molecule in comparison to the other prodrug species, such that interaction with active sites in the MIP might occur more readily.

Table 5.5. Diffusion coefficient (D) of propranolol prodrugs through non-modified cellulose and modified cellulose membranes at different pH values at room temperature (mean$\pm$SE, n=3)

| Prodrugs | Membrane | D (x 10^{-6} cm h^{-1}) | | | | | |
| | | pH 5.5 | | | pH 7.4 | | |
		R	*S*	*S/R*	*R*	*S*	*S/R*
VL-P	Cellulose	62.3$\pm$4.52	77.9$\pm$3.84	1.26$\pm$0.07	64.3$\pm$9.74	70.7$\pm$13.7	1.08$\pm$0.06
	NIP	77.8$\pm$4.94	86.8$\pm$5.57	1.12$\pm$0.09	69.8$\pm$5.03	64.4$\pm$7.48	0.94$\pm$0.15
	S-MIP	57.6$\pm$2.57	95.9$\pm$10.5	1.68$\pm$0.22	32.8$\pm$8.61	66.7$\pm$5.81	2.33$\pm$0.56
SN-P	Cellulose	38.8$\pm$8.00	51.3$\pm$8.53	1.32$\pm$0.93	28.7$\pm$4.77	34.1$\pm$9.48	1.25$\pm$0.38
	NIP	29.3$\pm$6.91	42.9$\pm$11.5	1.46$\pm$0.31	23.4$\pm$2.61	26.6$\pm$3.60	1.13$\pm$0.04
	S-MIP	32.8$\pm$3.51	50.5$\pm$7.01	1.57$\pm$0.24	27.1$\pm$4.35	29.5$\pm$5.99	1.23$\pm$0.37
CP-P	Cellulose	69.8$\pm$7.48	73.2$\pm$9.64	1.08$\pm$0.15	38.2$\pm$0.23	44.5$\pm$7.82	1.17$\pm$0.32
	NIP	52.8$\pm$2.64	64.0$\pm$10.4	1.21$\pm$0.17	49.3$\pm$1.53	46.3$\pm$12.2	0.93$\pm$0.23
	S-MIP	59.5$\pm$3.79	68.2$\pm$7.58	1.18$\pm$0.22	49.4$\pm$6.90	61.5$\pm$18.1	1.22$\pm$0.30
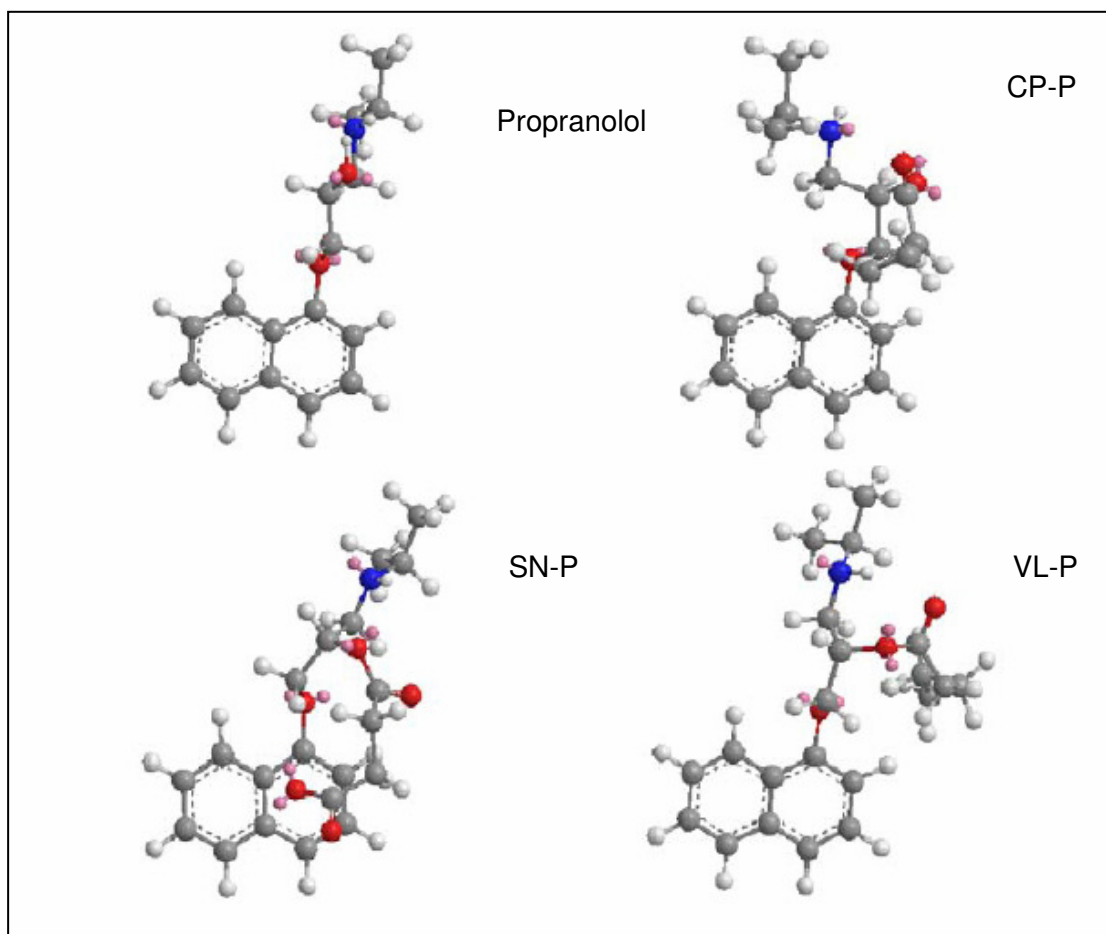
Figure 5.4. The energy-minimized Chem 3D structures of *S*-propranolol and *S*-propranolol prodrugs as calculated by molecular mechanics using MM2 force field (Chem 3D Ultra 8.0, CambridgeSoft, MA, USA).

CHAPTER 6

THE IN VITRO PERCUTANEOUS PERMEATION OF
THE MIP COMPOSITE MEMBRANE

6.1. The objective of the study

The objectives of this work were to study the possibility of using the MIP composite membrane for enantioselective controlled-release of *S*-propranolol through *in vitro* study using excised rat skin, and to study the cross-reactivity of racemic propranolol prodrug for the MIP composite membrane placed on excised rat skin.

6.2. Background

6.2.1. Skin models

During the preclinical development of transdermal devices, it is difficult as well as unethical to test products in humans initially, owing to the potential toxicity of pharmaceutical agents (Ei-Kattan et al., 2000). Therefore, the *in vitro* permeability study is necessary. To evaluated transdermal absorption of a

molecule, the most relevant membrane is human. Skin from various sources, including cosmetic surgery and amputations, has been used for the *in vitro* assessment of percutaneous penetration. However, its availability is limited and animal skin is therefore frequently used (Godin and Touitou, 2007). Practically, it would be advantageous to use human cadaver skin for permeation studies but, for most investigations, human cadaver skin is not readily available. Also, the skin samples are typically obtained from a variety of anatomical sites and after many different diseases states, which might alter the percutaneous permeability of the drug (Ei-Kattan et al., 2000). Hence, a wide range of animal models has been used to evaluate percutaneous permeation of molecules. These include primates, porcine, mouse, rat, guinea pig and snake models (Godin and Touitou, 2007).

The most relevant animal model for human skin is the pig. It is readily available from abattoirs and its histological and biochemical properties have been shown to be similar to human skin (Moser et al., 2001). However, due to its availability, skin of rodents (mice, rats and guinea pigs) is most commonly used in *in vitro* and *in vivo* percutaneous permeation studies. The advantages of these animals are their small size, uncomplicated handling and relative low cost. Except for rat skin, rodent skin generally shows higher permeation rates than human skin. Regarding the rat skin, permeation kinetics parameters are frequently comparable with human skin (Godin and Touitou, 2007).

6.2.2. Quantitating percutaneous absorption

The movement of chemicals across the stratum corneum barrier into the epidermis occurs primarily by passive diffusion driven by the applied concentration of drug on the surface of the skin. This is best expressed using Fick's law of diffusion which states that the steady state of drug flux across a membrane can be expressed as:

$$Flux(J) = \frac{DP}{h}(Concentration\,Gradient)(Surface\,Area) \qquad (6.1)$$

where D is the diffusion coefficient or diffusivity of the drug in the intercellular lipids of the stratum corneum, P is the partition coefficient of the drug between the stratum corneum and the dosing medium on the skin surface, and h is the skin thickness or actual path-length through which the drug diffuses across the diffusion barrier.

The driving force of this process is the concentration gradient that exists between the applied dose and the blood-perfused dermal environment. The term DP/h is often called the permeability coefficient or K_p. Transdermal flux is expressed in terms of skin surface area, making the two important properties of dosage in a transdermal system the concentration of drug applied and the surface area of the application. Finally, Fick's law expresses the steady-state flux of drug that occurs when this rate becomes constant (Riviere and Papich, 2001). In skin diffusion studies, this occurs after passage of a lag time (t_{lag}) which relates inversely to the diffusion coefficient and direct to the diffusion pathlength (h). The use of this extrapolation for

the calculation of diffusion coefficients is common place, although when skin is concerned, the pathlength is unknown, making calculation of absolute values of *D* difficult (Watkinson and Brain, 2002).

$$t_{lag} = \frac{h^2}{6D}$$ (6.2)

6.3. Experimental

6.3.1. Chemicals and reagents

The valeryl ester prodrug of propranolol was synthesized by using the method described in Chapter 5. The NIP, R-MIP and S-MIP membrane employed in this study had the thickness approximately 5 μm, the electric resistance of 1 Ω cm^2 and the tensile strength of 3.16 kN/m^2 (see the preparation procedure in Chapter 3).

6.3.2. Preparation of rat skin

The rats were sacrificed by snapping the spinal cord at the neck. Hair form dorsal side of skin was removed and whole skin was excised by using surgical scissors. The adhering fat and other visceral debris were removed from under surface with tweezers. The skin was rinsed with phosphate buffer solution (pH 7.4). The rat skins were kept at -20°C until use within 2 weeks.

6.3.3. Preparation of racemic propranolol solution for donor solution

In vitro percutaneous penetration study, the concentration of racemic propranolol HCl solution was higher than that used in the release experiments (Chapter 4, section 4.3.3.2). To overcome the skin barrier and reach the high drug concentration in receiver compartment, it was necessary to use the higher drug concentration in the donor. Therefore, the concentrations of racemic propranolol HCl were 100, 200 and 300 μg ml^{-1}. Racemic propranolol hydrochloride was dissolved in phosphate buffer saline (PBS pH 7.4) to produce the required concentration.

6.3.4. *In vitro* percutaneous penetration study of propranolol HCl

The *in vitro* percutaneous penetration study of S-MIP membrane was performed with a Franz-type diffusion cell. The excised skin was mounted between the half-cells, with and without a coupled test membrane (S-MIP or NIP or cellulose membrane), such that the dermal surface was in contact with the receptor fluid and the epidermal side in contact with the test membrane (if present). The receiving compartment was filled with phosphate buffer (pH 7.4). The diffusion cells were placed on a magnetic stirrer submerged in a water bath, such that receptor compartments were immersed in the water. Drug solution (0.5 ml) was applied to the membrane surface and the cell was maintained at 37°C by an external circulating water-bath to represent the vital temperature of *in vivo* and maintain the surface temperature of the skin at 32°C. The receptor phase was stirred constantly at 250 rpm with a magnetic bar. An aliquot (250 μl) of receptor fluid was collected at 0, 6, 12, 18,

24, 30, 36, 42 and 48 h. The receptor medium was replaced with the same volume of fresh PBS (pH 7.4) which equilibrated at 37°C. The collected samples were cleaned up before analysis (see section 5.4.8). The concentration of propranolol in the collected sample was determined by HPLC (see section 6.3.6). The in vitro permeation data were obtained from the equation:

$$J_{ss} = K_p * C_s \qquad (6.3)$$

where J_{ss} is the steady state flux measured as the slope of the profile after regression analysis. K_p is the apparent permeability coefficient through the skin, calculated by dividing J_{ss} by the starting concentration C_s. The x-intercept of the extrapolated linear region of the curve was employed to obtain a lag time (τ).

6.3.5. *In vitro* percutaneous penetration study of valeryl propranolol

The *in vitro* percutaneous penetration study of valeryl propranolol of S-MIP membrane was performed with a Franz-type diffusion cell. The excised skin was mounted between the half-cells, with and without a coupled test membrane (S-MIP or NIP or cellulose membrane), as described in section 6.3.4. The racemic valeryl propranolol prodrug was dissolved in phosphate buffer saline (PBS pH 7.4) to produce the required concentration (400 μg ml^{-1}). The racemic valeryl propranolol solution (0.5 ml) was filled into donor compartment and the cell was maintained at 37°C by an external circulating water-bath. An aliquot (250 μl) of receptor fluid was collected at the appropriate time intervals over 2 days. The collected samples were

cleaned up before analysis (see section 5.4.8). The concentration of propranolol in the collected sample was determined by HPLC (6.3.6).

6.3.6. Stereospecific HPLC method

The analysis of the propranolol enantiomer and valeryl propranolol content of the samples was performed directly using a chiral-HPLC method. The HPLC system (Shimadzu Corporation, Kyoto, Japan) connected with a Chiralcel OD column was used to analyze of both propranolol enantiomer and valeryl propranolol content. The mobile phase was 60:40 (v/v) 1 N sodium perchlorate:acetonitrile and a flow rate of 1.0 ml/min was employed. Typical retention time of valeryl propranolol enantiomers were 7 min for *R*-isomers and 9 min for *S*-isomers. The limit of detection was 1.0 μg ml^{-1}. Correlation coefficients for the calibration curves in the range 1-20 μg ml^{-1} for *R*- and *S*-valeryl propranolol were greater than 0.998.

6.4. Results and discussion

6.4.1. Transdermal enantioselective-controlled release of racemic propranolol HCl of composite MIP membranes

The in vitro percutaneous permeation study of propranolol enantiomers was investigated by applying drug to cellulose, NIP or S-MIP membranes in direct contact with isolated excised rat skin contained in a Franz cell. The initial concentration of racemic propranolol (HCl) in the donor phase was varied from 100 to

400 µg ml^{-1}. Control experiments were also carried out to determine the percutaneous transport of drug across skin alone. The cumulative amounts of propranolol transported across rat skin as a function of time, when drug was applied to the membrane positioned in place on the skin surface are shown in Figure 6.1 and 6.2. The resulting curves indicate that the diffusion of *R*-propranolol across the S-MIP membrane-skin layer is delayed whereas a relatively facilitated transport of *S*-propranolol across S-MIP membrane through the rat skin occurred over the initial 18 h of transport for every donor concentration. The percutaneous transfer of the *S*-enantiomer across cellulose membrane, was less than if the S-MIP membrane was *in situ* and was higher than the *R*-enantiomer across both membrane types. The percutaneous permeation of both *R*- and *S*-enantiomers of propranolol across NIP membranes applied to the skin was initially delayed, which is possibly due to the MAA-EDMA steric hindrances which might occur in the pores of the modified basic cellulose membrane. NIP membranes allowed slightly faster *S*-propranolol enantiomer transport than for the *R*-propranolol enantiomer. There is little facilitated S-propranolol enantiomer transport across NIP membranes and this does not increase markedly as the initially applied concentration of drug is increased.
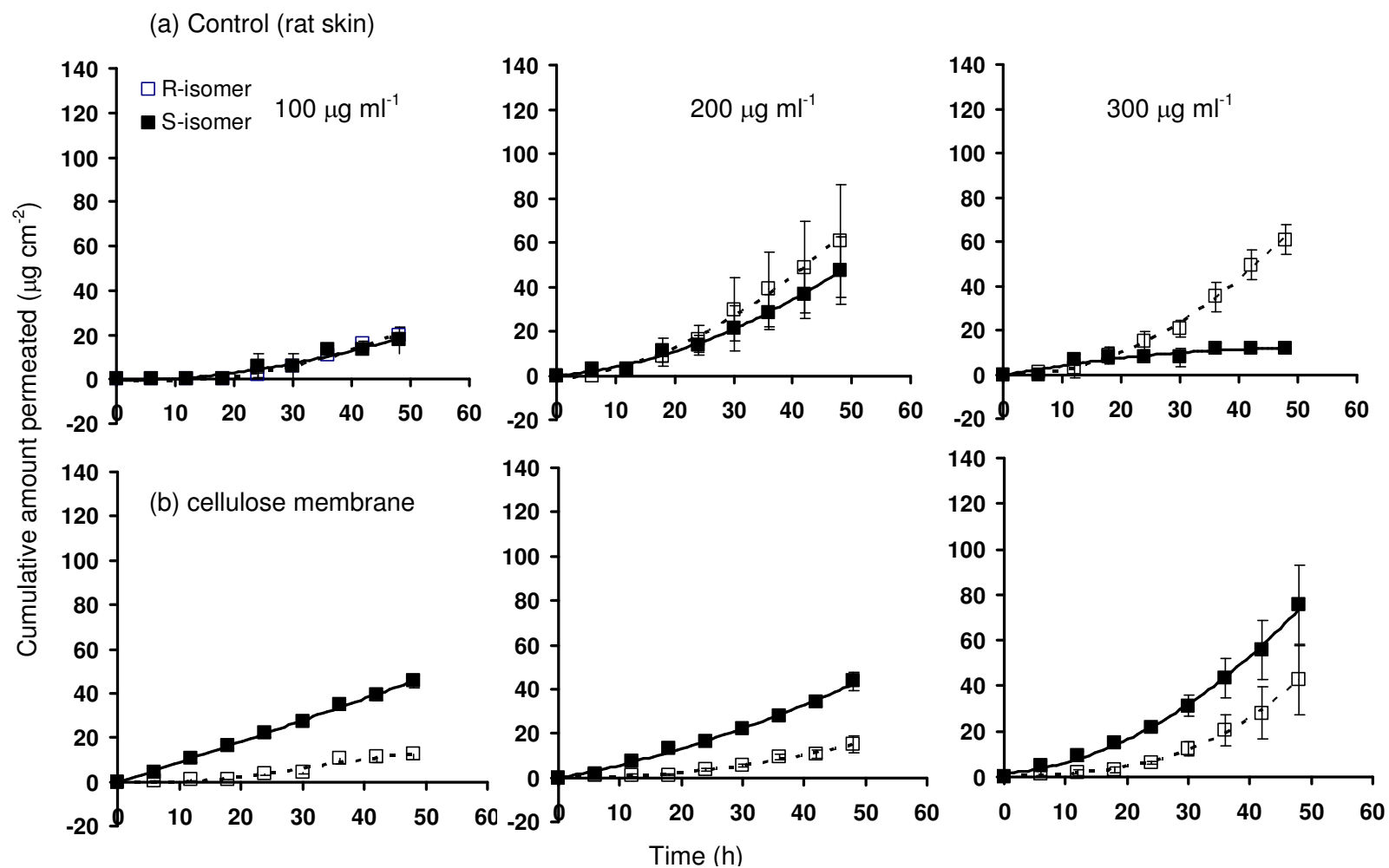
Figure 6.1. The permeation of propranolol enantiomers (HCl) from pH 7.4 buffer solution (a) across full thickness rat skin at 37°C in the absence of the membrane or with (b) cellulose membrane placed on the surface of the skin (mean$\pm$SE, n=6). The initially applied donor concentrations of racemic propranolol were 100, 200 and 300 μg ml^{-1}.
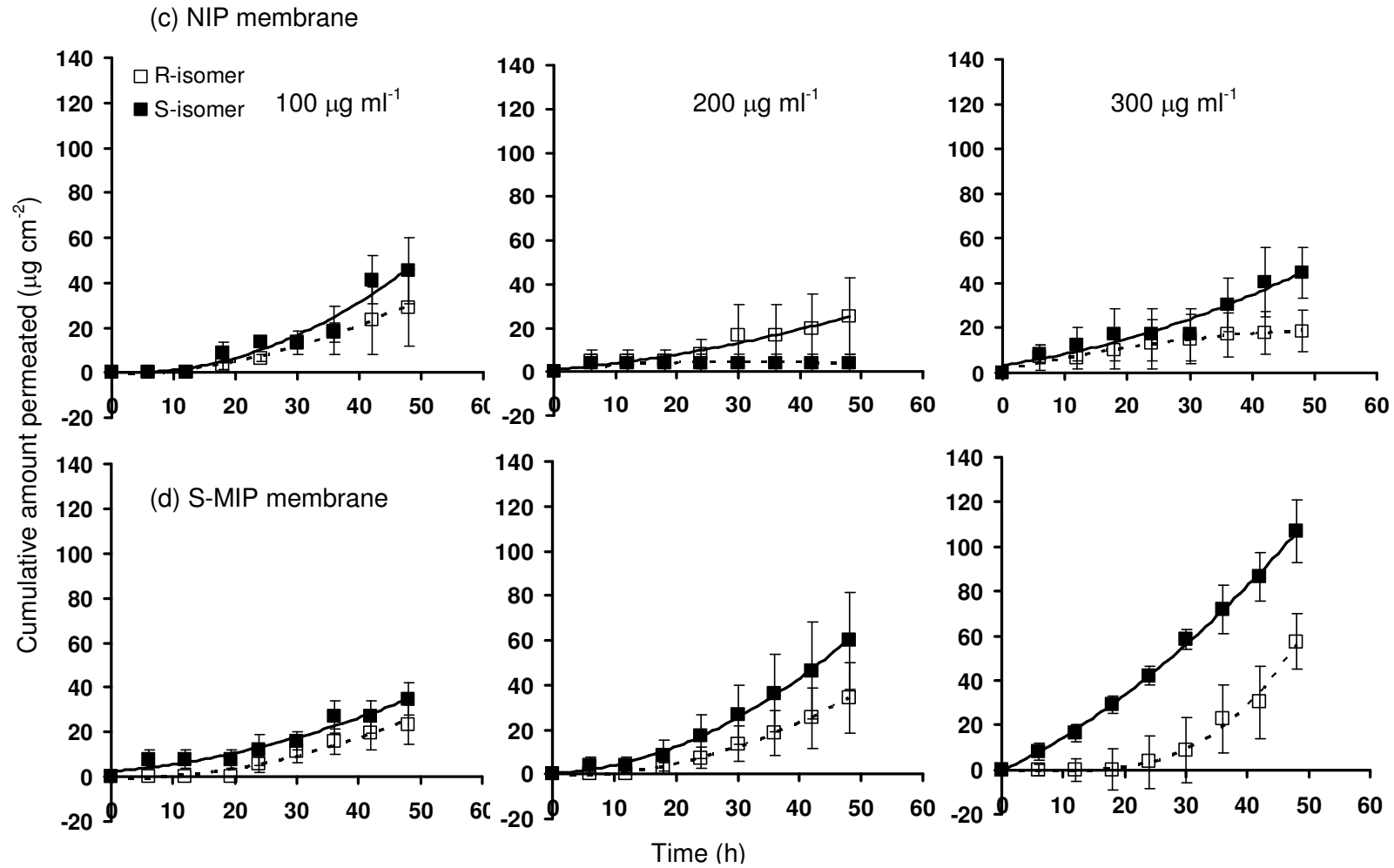
Figure 6.2. The permeation of propranolol enantiomers (HCl) from pH 7.4 buffer solution across full thickness rat skin at 37 °C with (c) NIP or (d) S-MIP membrane placed on the surface of the skin (mean±SE, n=6). The initially applied donor concentrations of racemic propranolol were 100, 200 and 300 μg ml^{-1}

In addition, *S/R* selectivity in terms of the permeability coefficient through NIP membranes is not significantly changed with donor concentration (Table 6.1). At a donor concentration of 100 μg ml^{-1}, the transport of propranolol enantiomers through skin alone was very low and the flux rates of the two enantiomers were found to be similar. Increasing the donor compartment concentrations (to 200 and 300 μg ml^{-1}) resulted in a greater diffusion rate through the skin layer in the absence of membrane, but no enantiomeric differences in transport were observed initially. However, after 12 h the diffusion of *R*-enantiomer across the skin into receptor phase was found to be significantly higher than that of the *S*-enantiomer. The stereoselective penetration of propranolol through excised rat skin has been reported by Miyazaki et al. (1992) who showed that the percutaneous permeation of *S*-propranolol was 4 times higher than that of *R*-propranolol. These latter results were, however, contrary to the results reported by Heard et al. (1993) when the transfer of propranolol from sub-saturated solutions across rat skin was not found to be an enantioselective process. The enantioselective transfer of propranolol across rat skin therefore remains unclear. However, the results obtained in this study indicate that although an enantiomeric difference in the permeation of *R*- and *S*-propranolol through rat skin was shown, particularly after 18 h application, an enantioselective-controlled transport was obtained when the S-MIP membrane was placed in situ on the skin. The flux of *S*-isomer was increased in comparison to the control when the S-MIP membrane was *in situ* for all test concentrations, with enhancement ratios of ca. 2–5 being obtained for the different drug concentrations employed (Table 6.1). The flux of *R*-isomer was reduced with the S-MIP membrane in situ compared with controls at donor concentrations of 200 and 300 μg ml^{-1}. Due to

higher permeability and greater partitioning of *S*-propranolol from S-MIP membrane, the lag time of *S*-isomer was reduced when the membrane was applied as compared to control. However the lag times of the *R*-isomer were found generally to increase in the presence of the S-MIP membrane compared to those obtained in control experiments. Furthermore, the permeability coefficients were greater for the *S*-isomer through the S-MIP membrane and skin than skin alone, whatever the initial donor drug concentration ($p<0.05$). The permeability coefficients of *R*-enantiomer through S-MIP membrane were generally lower when the S-MIP membrane was in situ than through skin alone. The higher permeability coefficients observed for the S-enantiomer would appear to confirm the enantioselective delivery properties of S-MIP membrane. When the concentration of racemic propranolol was increased, the lag time for the permeability of *R*-isomer through the S-MIP membrane and skin appeared to be relatively constant. This was in contrast, to the change in lag times observed when the *S*-isomer was applied since these were reduced, as the initial drug concentration was increased (Table 6.1). This caused the *S/R* ratio of lag time for the transport of propranolol through S-MIP membrane to remain constant or even be reduced as the initial applied concentration was increased. However the results indicated that increasing the donor concentration promoted the stereoselective transport of S-MIP membrane. The results obtained in this study indicate that the enantioselectivity shown with S-MIP membrane placed on rat skin is related to the high combined affinity of cellulose and S-MIP for the *S*-propranolol along with the lesser affinity for *R*-enantiomer inherent in the cellulose and induced in the S-MIP by the imprinting process. The enantioselective-controlled release of S-MIP membrane was clearly apparent when racemic propranolol was placed in the donor compartment at

concentrations up to 300 μg ml^{-1}. Beyond this concentration, i.e., 400 μg ml^{-1}, the stereoselectivity was reduced (data not shown). The reason for this might involve the saturation of binding sites within the excised rat skin.

Table 6.1 Steady state flux (J_{ss}), permeability coefficient (K_p) and lag time (τ) of R- and S-propranolol from pH 7.4 buffer solution containing racemic propranolol at different concentrations through full-thickness rat skin alone or for transport through cellulose, NIP and S-MIP membrane applied to the skin surface (mean$\pm$SE, n=6).

Feed concentration (μg ml^{-1})	Membrane	J_{ss} (μg cm^{-2} h^{-1})		K_p x 10^{-3}			τ (h)		
		R-isomer	*S*-isomer	*R*-isomer	*S*-isomer	selectivity	*R*-isomer	*S*-isomer	selectivity
100	Skin	0.30$\pm$0.04	0.28$\pm$0.01	1.01$\pm$0.13	2.10$\pm$0.15	1.41$\pm$0.38	18.67$\pm$0.67	16.76$\pm$0.38	0.90$\pm$0.05
	Cellulose	0.24$\pm$0.04	0.54$\pm$0.06	2.43$\pm$0.45	5.39$\pm$0.62	2.38$\pm$0.48	12.07$\pm$0.76	1.64$\pm$1.40	0.13$\pm$0.11
	NIP	0.45$\pm$0.05	0.73$\pm$0.07	4.46$\pm$0.49	7.28$\pm$0.65	1.69$\pm$0.29	14.07$\pm$0.67	11.33$\pm$1.33	0.81$\pm$0.02
	S-MIP	0.36$\pm$0.07	0.66$\pm$0.02	3.59$\pm$0.72	6.60$\pm$0.04	2.04$\pm$0.52	18.85$\pm$0.85	5.69$\pm$1.69	0.30$\pm$0.10
200	Skin	0.91$\pm$0.21	0.52$\pm$0.03	4.55$\pm$1.03	2.59$\pm$0.19	0.57$\pm$0.90	10.31$\pm$0.61	8.87$\pm$0.90	0.87$\pm$0.10
	Cellulose	0.24$\pm$0.03	0.48$\pm$0.01	1.20$\pm$0.13	2.39$\pm$0.06	2.07$\pm$0.04	15.72$\pm$3.00	5.90$\pm$0.02	0.44$\pm$0.11
	NIP	0.32$\pm$0.09	0.50$\pm$0.01	1.61$\pm$0.43	2.49$\pm$0.07	1.87$\pm$0.62	8.88$\pm$0.85	10.57$\pm$0.57	1.46$\pm$0.18
	S-MIP	0.49$\pm$0.05	1.10$\pm$0.02	2.46$\pm$0.22	5.50$\pm$0.10	2.27$\pm$0.23	16.23$\pm$1.44	4.65$\pm$0.60	0.30$\pm$0.06

Table 6.1 Steady state flux (J_{ss}), permeability coefficient (K_p) and lag time (τ) of *R*- and *S*-propranolol from pH 7.4 buffer solution containing racemic propranolol at different concentrations through full-thickness rat skin alone or for transport through cellulose, NIP and S-MIP membrane applied to the skin surface (mean±SE, n=6) (Continued).

Feed concentration ($\mu g\ ml^{-1}$)	Membrane	J_{ss} ($\mu g\ cm^{-2}\ h^{-1}$)		K_p x 10^{-3}			τ (h)		
		R-isomer	*S*-isomer	*R*-isomer	*S*-isomer	selectivity	*R*-isomer	*S*-isomer	selectivity
300	Skin	1.00±0.14	0.33±0.16	3.33±0.45	1.09±0.54	0.33±0.18	9.54±1.87	6.00±0.01	0.63±0.13
	Cellulose	0.55±0.26	0.72±0.16	1.84+0.86	2.39±0.52	1.71±0.35	12.45±0.90	9.48±2.90	0.75±0.20
	NIP	0.44±0.12	0.68±0.02	1.48+0.38	2.28±0.07	1.74±0.38	1.33±0.94	1.72±1.30	1.04±0.24
	S-MIP	0.52±0.06	1.73±0.36	1.73+0.19	5.76±1.20	3.50±1.01	17.58±4.46	2.45±1.77	0.11±0.06

The steady-state flux of *R*- and *S*-valeryl propranolol through the full thickness rat skin with and without cellulose membrane, NIP membrane or S-MIP membrane are shown in Table 6.2. The drug concentration of valeryl propranolol at the donor side of the Franz-diffusion cells was 400 μg ml^{-1}. The transport rate of *S*-enantiomer through excised rat skin was slightly higher than the *R*-enantiomer. No enantiomeric differences in transport through excised rat skin were observed initially for cellulose and NIP composite membranes, but after 24 h the transport of *S*-enantiomer across the skin was found to be higher than that of the *R*-enantiomer. In contrast the enantioselective-controlled release of S-MIP membrane placed in situ on skin was apparent after 12 h of the transport testing. The *S*-selectivity of the transport of valeryl propranolol was highest in case of S-MIP and followed with NIP, cellulose membrane and skin (control study), respectively. From these results, it revealed that VL-P did not show the increasing penetration of the enantiomers over propranolol. The transport of the lipophilic VL-P might be affected by the hydrophilic part of dermis layer, therefore the transport of the enantiomer did not increase significantly. The cellulose membrane and modified cellulose membrane permitted the more release of *S*-isomer as found in the study of propranolol. The selectivity of S-MIP membrane for VL-P was found to be decreased when compared with propranolol, it was the same phenomenon as occurred in the previous chapter.

Table 6.2. Steady state flux (J_{ss}), permeability coefficient (K_p) and lag time (τ) of *R*- and *S*-enantiomer from pH 7.4 buffer solution containing racemic valeryl propranolol at the concentration of 400 μg ml^{-1} through full-thickness rat skin alone or for transport through cellulose, NIP and S-MIP membrane applied to the skin surface (mean±SE, n=6).

Feed concentration (μg ml^{-1})	Membrane	J_{ss} (μg cm^{-2} h^{-1})		K_p x 10^{-3}			τ (h)		
		R-isomer	*S*-isomer	*R*-isomer	*S*-isomer	selectivity	*R*-isomer	*S*-isomer	selectivity
400	Skin	0.90±0.02	1.04±0.13	2.26±0.05	2.61±0.05	1.16±0.07	6.12±2.56	9.86±0.99	1.59±0.34
	Cellulose	0.87±0.19	1.12±0.13	2.18±0.48	2.80±0.07	1.44±0.25	7.99±0.90	11.32±2.90	1.40±0.23
	NIP	0.38±0.07	0.58±0.11	0.94±0.17	1.45±0.27	1.78±0.48	7.86±1.21	8.66±1.30	1.10±0.18
	S-MIP	0.28±0.03	0.51±0.05	0.70±0.19	1.27±0.13	1.85±0.13	10.58±4.46	7.45±2.86	0.71±0.34

CHAPTER 7

THE STUDY IN EFFECT OF THE GEL RESERVOIR

7.1. The objective of the study

The aims of this study were to show the potential of the MIP composite membrane for transdermal delivery of *S*-propranolol of either racemic propranolol or racemic propranolol prodrug, and to evaluate the feasibility of poloxamer and chitosan gel for use as a vehicle in the MIP composite membrane transdermal patch.

7.2. Background

The gel formulation can avoid the leaking of the drug from the transdermal patch. In addition, enantioselective permeability might be expected to be particularly sensitive to small changes in molecular environment such as pH and vehicle (Heard et al., 1993). Hence, the release studies of the drug from the gel formulations are considered to be useful in pre-formulation step to predict the best vehicle giving both high permeation and enantioselectivity. The best candidate formulation is particularly crucial in the development of transdermal patch.

7.3. Poloxamer

Poloxamers (or Pluronics) are non-ionic, polyoxyethylene-polyoxypropylene-polyoxyethylene triblock copolymers (PEO_n-PPO_n-PEO_n) that have many pharmaceutical applications (Pandit and Wang, 1998). The poloxamers consist of more than 30 different non-ionic surface-active agents. The poloxamer series covers a range of liquids, pastes, and solids, with molecular weights and ethylene oxide-propylene oxide weight rations varying from 1100 to 14,000 and 1:9 to 8:2, respectively (Ruel-Gariépy and Leroux, 2004). A poloxamer solution of approximately 20% (w/w) or above shows a Newtonian behavior in the sol state but becomes psedoplastic around the gelling point (Moore et al., 2000 and Rhee et al., 2006). The gelation mechanism of poloxamer solutions is still being debated. Many reports suggested that "micellization" may be the important role for their thermoreversible behavior. Poloxamer posses in water the ability to change from individual block copolymer molecules (unimers) to self-assembling micelles. In the low temperature region, poloxamer exists as unimers. These unimers from solutions in water below the critical micelle concentration, while above this concentration, aggregation phenomena occurs giving rise to a micellization process. With increasing temperature, these systems show phase separation, which is due to the complete dehydration of both polypropylene oxide and ethylene oxide. The temperature at which micelles are formed is called the critical micelle temperature. The micelles may have different shapes such as spherical, cylindrical or lamellar morphologies depending on the length of polypropylene oxide and ethylene oxide blocks, but in any case the hydrophobic blocks constitute the core and the hydrophilic blocks from the

external corona. Therefore, the packing of micelles and micelle entanglements may be the mechanism for poloxamer solution gelation with increasing temperature. Both micellization and gelation depend on diffent factors: temperature, polymer concentration and polyethylene oxide block length (Cabana et al., 1997, Moore et al., 2000, Rhee et al., 2006 and Bonacucina et al., 2007).

Poloxamer 407 (Figure 7.1) is a triblock copolymer composed of approximately 70% of ethylene oxide and 30% of propylene oxide with an averaged molecular weight of 115,000 Da. Poloxamer solutions (20-30%) can form a reversible gel at above 4°C (Nair and Panchagnula, 2003 and Pillai and Panchagnula, 2003). Poloxamer 407 are commonly used in cosmetic and pharmaceutical products because of their high stability, biocompatibility with cells and body fluids and low toxicity (Lu and Jun, 1998, Blonder et al., 1999, Ruel-Gariépy and Leroux, 2004 and Ricci et al., 2005). Due to these favorable properties, poloxamer 407 has been used as a vehicle in controlled drug delivery systems.
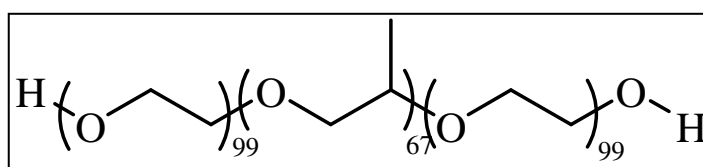
Figure 7.1. The chemical structure of poloxamer 407.

7.4. Chitosan

Chitosan is a naturally occurring polysaccharide whose commercial forms are essentially produced from *N*-deacetylation of chitin. The structure of chitin and chitosan are shown in Figure 7.2.
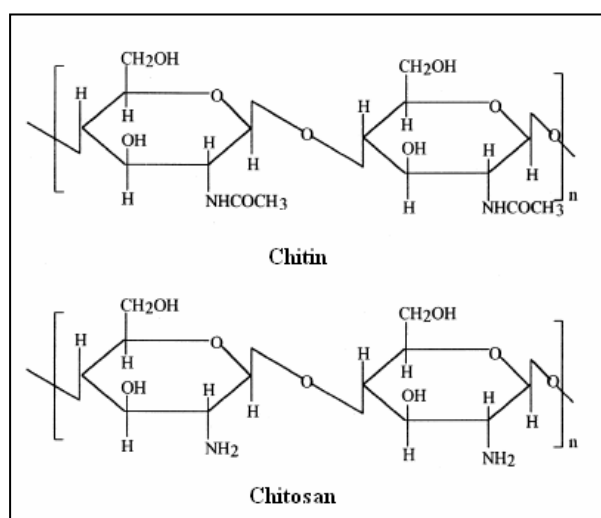
Figure 7.2. The chemical structure of chitin and chitosan (Kumar, 2000).

The word chitosan refers to a large number of polymers which differ in their degree of *N*-deacetylation (40-98%) and molecular weight (50,000-2,000,000 daltons). Chitosan is a weak base with a pK_a value of D-glucosamine of about 6.2-7 and, therefore, insoluble at neutral and alkaline pH values (Hejazi and Amiji, 2002).

Chitosan has favorable biological properties such as biodegradability and biocompatibility therefore, it is suitable for use in biomedical and pharmaceutical formulations (Kumar, 2000). Chitosan has low oral toxicity with an LD_{50} in rats of 16 g/Kg (Hejazi and Amiji, 2002). Chitosan has been shown to possess mucoadhesive

properties due to molecular attractive forces formed by electrostatic interaction between positive charged chitosan and negative charged mucosal surfaces (Sinha et al., 2004). In addition, chitosan has been shown to promote absorption of small polar molecules and peptide/protein drugs through buccal mucosa, nasal mucosa, intestinal mucosa and cultured Caco-2 cells (Senal and Hincal, 2001). These can be explained from the mucoadhesive property of chitosan which can increase the retention time of the drug at the application sites (Bernkop-Schnürch, 2000 and Senal and Hincal, 2001) and the positive charge of chitosan can interact with the epithelial cells resulting in a structural reorganization of tight junction-associated proteins (Schipper et al., 1997). As mentioned above, chitosan and its derivatives are extensively used in pharmaceutical applications especially in drug delivery system such as buccal (Senel et al., 2000, Senal and Hincal, 2001 and Portero et al., 2007), oral (Bernkop-Schnürch, 2000), nasal (Illum et al., 2001), parenteral (Molinaro et al., 2002 and Ruel-Gariépy et al., 2002), and dermal and transdermal delivery (Thacharodi and Rao, 1995, Fang, 1998, Özsoy et al., 2004 and Xie et al., 2005). The non-toxicity of chitosan is insisted by the use of chitosan in tissue engineering (Suh and Matthew, 2000), bone repair (Wang et al., 2002) and skin regeneration (Boucard et al., 2007). Due to these satisfactory properties of chitosan, it was chosen as a vehicle for this study too.

7.5. Experimental

7.5.1. Chemicals and reagents

Racemic propranolol HCl and chitosan (medium molecular weight) were purchased from Aldrich Chemical Company (Milwaukee, WI, USA) and were used as received. Poloxamer 407 was supplied by BASF (Ludwigshafen, USA). Valeryl propranolol was synthesized by using the method described in Chapter 5.

The NIP, R-MIP and S-MIP membrane employed in this study had the thickness approximately 5 μm, the electric resistance of 1 Ω cm^2 and the tensile strength of 3.16 kN/m^2 (see the preparation procedure in Chapter 3).

7.5.2. Apparatus

The pH of the gel formulations was measured by using a Toledo 320 pH meter (Mettler, Bangkok, Thailand).

The viscosity of the gels was measured by using a Rehocal DV-III Ultra Programmable Rheometer (Brookfield Engineering Laboratories, MA, USA) using the smallest spindle (RV 007).

7.5.3. Preparation of racemic propranolol HCl gel and valeryl propranolol HCl gel

7.5.3.1. Preparation of propranolol and valeryl propranolol chitosan gel

In this study, the chitosan gel was prepared using the method reported by Thacharodi and Rao (1995) and the poloxamer gel was prepared by the cold method as reported in the literature (Pandit and Wang, 1998). For the preparation of the chitosan gel, powdered chitosan (2.5 g) was dissolved in 100 ml of 10% (w/w) acetic acid solution, and 10% (w/w) NaOH was added until a white precipitate appeared. This solution was incubated at 37°C in a hot air oven. After 12 h, the chitosan gel solution was washed with three portions of 5 ml distilled water, and left overnight to remove the entrapped air bubbles. To this gel solution, racemic propranolol HCl or racemic valeryl propranolol HCl (to obtain a final concentration of 300 μg ml^{-1} for propranolol and 400 μg ml^{-1} for valeryl propranolol) were added. The resulting mixture of polymer/drug was stirred for 10 min and homogenized for 10 min. For the preparation of the poloxamer gel, 25% (w/w) of powdered poloxamer 407 was dispersed slowly in distilled water under constant stirring at 4°C and kept in a refrigerator until a homogenous solution was obtained. Subsequently, racemic propranolol HCl or racemic valeryl propranolol HCl (to obtain a final concentration of 300 μg ml^{-1} for propranolol and 400 μg ml^{-1} for valeryl propranolol) were added slowly under constant stirring to the cold poloxamer solution, and the resulting

mixture of polymer/drug was then kept refrigerated (2-8 ^{o}C) overnight until polymer had completely hydrated and dispersed.

7.5.3.2. Determination of pH and viscosity of the formulations

The pH of the gel formulations was examined at room temperature (30°C). The viscosity (η) of these two propranolol gel were determined by a Brookfield DV-III Ultra Programmable Rheometer (Brookfield Engineering Laboratories, MA, USA). The viscosity of both gel formulations were measured at room temperature (28°C), 32$°$C and 37$°$C.

7.5.4. *In vitro* drug-release studies

In vitro release studies of propranolol enantiomers and valeryl propranolol enantiomers from the gels across the S-MIP composite membranes, or the NIP composite membranes or the cellulose membranes were conducted with Franz-type diffusion cells. The release experiments were conducted at room temperature (30±1°C). The effective surface area available for permeation was 3.8 cm^2 and the volume of receptor cell was 25 ml. The membrane was mounted between the donor compartment and receptor compartment. A 500 µl of gel was placed into the donor cell. To represent physiological pH the receptor phase used was phosphate buffer at pH 7.4, which was filtered and degassed before use. The receptor medium was stirred constantly at 500 rpm with magnetic bar. Samples (250 µl) were taken periodically from the receptor medium at certain time-intervals and replaced with the same volume

of buffer and analyzed using stereospecific HPLC for propranolol enantiomers or valeryl propranolol enantiomers concentration. To maintain the sink condition throughout the experiments, concentration of propranolol enantiomer in the receptor compartment was monitored. The drug concentration was less than 5% of the solubility of propranolol. Each experiment was repeated three times. The concentration of propranolol in the collected sample was determined by HPLC (Section 7.5.6). In addition, the ratios of the fluxes of the propranolol enantiomers were calculated.

7.5.5. *In vitro* skin permeation study

In vitro percutaneous penetration of propranolol enantiomers and valeryl propranolol enantiomer from the gel formulation containing racemic propranolol (HCl) or racemic valeryl propranolol (HCl) in the donor cell was investigated with vertical Franz diffusion cells (see Section 7.5.3). The full thickness Wistar rat skins were prepared as the same procedure described in section 6.3.2. The S-MIP membrane was attached to the excised rat skin and then the skin was mounted on the donor compartment. The donor compartment was then placed in position such that the surface of dermis side skin just touches the receptor fluid surface. The donor compartment was filled with 500 μl of a 300 μg ml^{-1} racemic propranolol gel or 400 μg ml^{-1} racemic valeryl propranolol gel. The receiving compartment was filled with phosphate buffer (pH 7.4, 25 ml). The diffusion cells were placed on a magnetic stirrer submerged in a water bath, such that receptor compartments were immersed in the water. The water bath was set at 37°C to represent the vital temperature of *in vivo*

and maintain the surface temperature of the skin at 32°C. The receptor solution was stirred constantly at 500 rpm with a magnetic bar. Samples (250 μl) were withdrawn at different time intervals up to 48 h and analyzed for drug content. The receptor phase was replenished with an equal volume of fresh buffer at each time interval.

The collected samples were cleaned up before analysis using the same protocol that in section 5.4.8. The amounts of each propranolol enantiomer were assayed by using a chiral HPLC method outlined in Section 7.5.6. The cumulative amount of each propranolol enantiomer permeated through rat skins was plotted as a function of time. The permeation rate of the propranolol enantiomer at a steady state (J_{ss}, μg cm^{-2} h^{-1}) was calculated from the slope of the linear portion of the cumulative amount of propranolol enantiomer permeated through the rat skins per unit area *versus* time plot. Control permeation studies were performed separately with the NIP membrane, and the cellulose membrane in the same way as for the S-MIP membrane. Complementary control experiments in which the membrane was not used were also undertaken. Each permeation experiment was replicated at least four times.

7.5.6. Stereospecific HPLC method

The analysis of amounts of propranolol enantiomes in the samples obtained from the receptor medium was performed directly by a chiral-HPLC method. The propranolol enantiomers and valeryl propranolol enantiomers were analysed by using AGP column connected with a Shimadzu HPLC system (see section 2.3.3).

7.5.7. Statistical analysis

Differences between the concentration time profiles of the enantiomers and their respective pharmacokinetic parameters within each treatment group were assessed by the Student's *t*-test for pair data. Observed difference in the pharmacokinetic indices between treatment groups were examined using ANOVA. Significance differences were determined at $p<0.05$.

7.6. Results and discussion

7.6.1. Gel formulations

Poloxamer 407 solution of concentration 25% (w/w) in propranolol hydrochloride aqueous solution at $4^{o}C$ was prepared. At this concentration, a stable thermoreversible gel was formed at room temperature ($28\pm1^{o}C$). Poloxamer gel is formed due to the micelle entanglements and packing and it is more entangled at the higher concentration, i.e. 25% (w/w) (Ricci et al., 2002). The viscosity of the poloxamer gel formulations at $37^{o}C$ (18500 cp) was slightly higher than those at room temperature (18000 cp) and $32^{o}C$ (18000 cp) (Table 7.1). The viscosity of the poloxamer gel and chitosan gel were markedly different. The viscosity values of the chitosan gel formulations at room temperature, $32^{o}C$ and $37^{o}C$ were about 500 cp. There was no change in viscosities of the poloxamer gel formulations or chitosan gel formulations when analysed up to 14 days. The pH of the poloxamer and chitosan gel of propranolol was 5.2 and 6.5, respectively, which both pHs were close to the pH of

the skin (~pH 6). Similarly, the poloxamer and chitosan gel of valeryl propranolol was 5.3 and 6.4, respectively.

Table 7.1. The physical properties of prepared propranolol and valeryl propranolol gel.

Drug	Formulation	Color	pH	Viscosity (cp)	
				32°C	37°C
Propranolol	poloxamer gel	White, clear	5.2	18000	18500
	chitosan gel	Yellow, clear	6.5	~500	~450
Valeryl propranolol	poloxamer gel	White, clear	5.3	18000	18500
	chitosan gel	Yellow, clear	6.4	~500	~450

7.6.2. Permeation determinations

The effect of poloxamer and chitosan on the enantioselective release of *S*-propranolol through S-MIP, NIP and cellulose membranes was investigated. The release of *R*- and *S*-propranolol enantiomers, either from the poloxamer gel or the chitosan gel, across the S-MIP composited cellulose membranes and cellulose membranes could be detected within 0.5 h of testing. About 48% and 60% cumulative release of propranolol enantiomers from the poloxamer gel and chitosan gel was observed in 24 h, respectively (Figure 7.3). Table 7.2 shows the release rate of propranolol enantiomers from poloxamer and chitosan gel formulations and transport through S-MIP, NIP and cellulose membranes. Chitosan gel provided relatively faster

release of propranolol enantiomers for all the membranes compared to the poloxamer gel. The faster release of propranolol enantiomers from the chitosan gel may be explained by the repulsive effect between the positive charge of chitosan and propranolol. At high poloxamer concentrations (e.g. 25%, w/w), poloxamer form micelles having a hydrophobic core and a hydrophilic shell (Rhee et al., 2006 and Bonacucina et al., 2007). It is possible that propranolol which is highly hydrophobic, remains associated with the hydrophobic portion of the micelles. Hence the delivery of propranolol enantiomers in poloxamer gel sustains. The enantioselective release of the *S*-isomer of racemic propranolol was shown for all the membranes with chitosan gel as a vehicle in donor phase (*S/R* =1.64±0.15, p =0.001). The poloxamer gel did not affect the enantioselective release of racemic propranolol with any of the three membranes (*S/R* =0.70±0.07, p =0.055). Previously, it was noted in the previous chapter that the higher pH of the media afforded greater enantioselective release of *S*-propranolol by the S-MIP composite cellulose membrane which agrees with the observation that the chitosan gel formulation which has higher pH exhibits greater ability to enantioselective deliver *S*-propranolol. The enhanced enantioselectivity at the higher pH of the S-MIP composite membrane is due to the increase in the degree of ionization of the functional monomer which this increases binding of the favoured *S*-propranolol enantiomer at the binding site. The gel type was found to affect the enantioselective transport of propranolol, with the more rheologically structured poloxamer gel formulation providing no selective release of *S*-propranolol. The greater gel structure of this polymer may interfere with the enantioselective controlled process at the pore surface of the S-MIP membrane.

The NIP composite membranes, which did not have the *S*-propranolol imprinted site, exhibited a release profile of *S*-propranolol that was similar to the non-modified cellulose membranes, but the degree of (*S/R*) selectivity shown with both membrane types was low compared to the S-MIP composited membranes. This is in agreement with the result obtained in the previous study (see Chapter 4, section 4.4.2) that utilized phosphate buffers as vehicles. These results confirmed that the enhanced enantioselective release for *S*-propranolol enantiomer achieved using the S-MIP membrane is due to the presence of the imprinting process in the synthesis that improved the enantioselectivity of the cellulose membrane.

The results of the present study have demonstrated that *S*-propranolol delivery was controlled by the composite S-MIP membrane and the rate of drug release was dependent on the type of gel used. Since the chitosan gel shows the ability to obtain good selectivity for the release of *S*-propranolol from the S-76MIP composite membrane, this gel type was selected as the drug reservoir for the preparation of the transdermal device.

Figure 7.3. Permeability profiles of *R*- and *S*-propranolol enantiomers from gels containing racemic propranolol through S-MIP, NIP and cellulose membranes applied to the skin surface (mean ± SE, n=4).

Table 7.2. Release rate (flux, $\mu g\ cm^{-2}\ min^{-1}$) of *R*- and *S*-propranolol enantiomers released from the gel formulations of racemic propranolol across S-MIP, NIP and non-modified cellulose membrane at room temperature (mean $\pm$ SE, n=3).

Compound/selectivity	Poloxamer gel			Chitosan gel		
	Cellulose	**NIP**	**S-MIP**	**Cellulose**	**NIP**	**S-MIP**
R-propranolol	8.34 ± 0.43	1.76 ± 0.28	1.75 ± 0.04	9.47 ± 0.91	3.12 ± 0.57	3.59 ± 0.23
S-propranolol	7.76 ± 0.60	1.56 ± 0.17	1.87 ± 0.07	13.56 ± 1.73	4.38 ± 0.15	7.08 ± 0.48
S /R ratio	0.94 ± 0.13 (p = 0.625)	0.90 ± 0.06 (p = 0.301)	1.07 ± 0.03 (p = 0.140)	1.43 ± 0.09 (p = 0.017)	1.34 ± 0.19 (p = 0.049)	2.00 ± 0.25 (p = 0.024)

The release of *R*- and *S*-valeryl propranolol enantiomers from the poloxamer and chitosan gel formulations across the cellulose membranes or the modified cellulose membranes could be detected after 2 h of release testing (Figure 7.4). For valeryl propranolol, as shown in Table 7.3 the release rates of *R*- and *S*-enantiomers from the poloxamer and chitosan gel formulations were much lower than those obtained for propranolol (see Table 7.2). The release data showed that the chitosan gel can promote the release of the enantiomers of valeryl propranolol similarly to propranolol. In addition, the chitosan gel provided good *S/R* selectivity for racemic valeryl propranolol for all membranes. In contrast, the poloxamer gel exhibited the modest *S/R* selectivity for enantiomer release of valeryl propranolol in all cases. The results obtained in the current study demonstrate the potential use of the chitosan as vehicle for the enantioselective controlled release of the S-MIP composite membrane.

Figure 7.4. Permeability profiles of *R*- and *S*-valeryl propranolol enantiomers from gels containing racemic valeryl propranolol through S-MIP, NIP and cellulose membranes applied to the skin surface (mean ± SE, n=4).

Table 7.3. Release rate (flux, $\mu g\ cm^{-2}\ min^{-1}$) of *R*- and *S*-propranolol enantiomers released from the gel formulations of racemic valeryl propranolol (VL-P) across S-MIP, NIP and non-modified cellulose membrane at room temperature (mean $\pm$ SE, n=3).

Compound/selectivity	Poloxamer gel			Chitosan gel		
	Cellulose	**NIP**	**S-MIP**	**Cellulose**	**NIP**	**S-MIP**
R-VL-P	2.84 ± 0.12	1.59 ± 0.17	1.43 ± 0.21	3.70 ± 0.21	2.11 ± 0.30	2.67 ± 0.34
S-VL-P	2.88 ± 0.03	2.34 ± 0.67	1.74 ± 0.32	3.88 ± 0.22	2.31 ± 0.35	2.67 ± 0.26
S /*R* ratio	1.02 ± 0.04 ($p = 0.724$)	1.47 ± 0.31 ($p = 0.129$)	1.22 ± 0.03 ($p = 0.150$)	1.05 ± 0.02 ($p = 0.126$)	1.10 ± 0.07 ($p = 0.320$)	1.05 ± 0.02 ($p = 0.233$)

7.6.3. *In-vitro* skin permeation study

The enantioselective transfer of propranolol enantiomers from the chitosan gel across the S-MIP, NIP or cellulose membranes through full thickness rat skin as a permeation barrier was studied, and these permeation profiles are shown in Figure 7.5. There was no enantiomeric difference in the permeation of propranolol enantiomers from chitosan gel containing racemic propranolol through excised rat skin (J_{ss} for S-isomer = 0.20 ± 0.02 µg cm^{-2} h^{-1} and J_{ss} for R-isomer = 0.23 ± 0.03 µg cm^{-2} h^{-1}, p=0.368). The S-MIP composite membranes showed significant difference in percutaneous transfer of propranolol enantiomers over 48 h of permeation (J_{ss} for S-isomer = 0.33 ± 0.05 µg cm^{-2} h^{-1} and J_{ss} for R-isomer = 0.11 ± 0.01 µg cm^{-2} h^{-1}, p=0.013). In addition, the mean ratio (*S/R*) of percutaneous permeation obtained, using Franz diffusion cell with rat skin and S-MIP composite membranes, (3.01 ± 0.42, p=0.013) was relatively higher than that obtained from the cellulose membranes (1.73 ± 0.25, p=0.037). and NIP composite membranes (1.54 ± 0.12, p=0.012). Enantiomeric differences in the percutaneous transfer of the enantiomers of propranolol were not observed initially (0-12 h) for NIP and cellulose membranes placed *in situ* with the skin, which is possibly due to the steric effect of gel reservoir which might occur in the pore of the membranes. However after 12 h, greater amounts of the *S*-propranolol enantiomer in comparison to the *R*-enantiomer were detected in the receptor phase for both membrane types. This low to moderate selectivity after 12 h with these 'control' membranes is probably due to the cellulose membrane, a naturally occurring material that has some recognition ability.
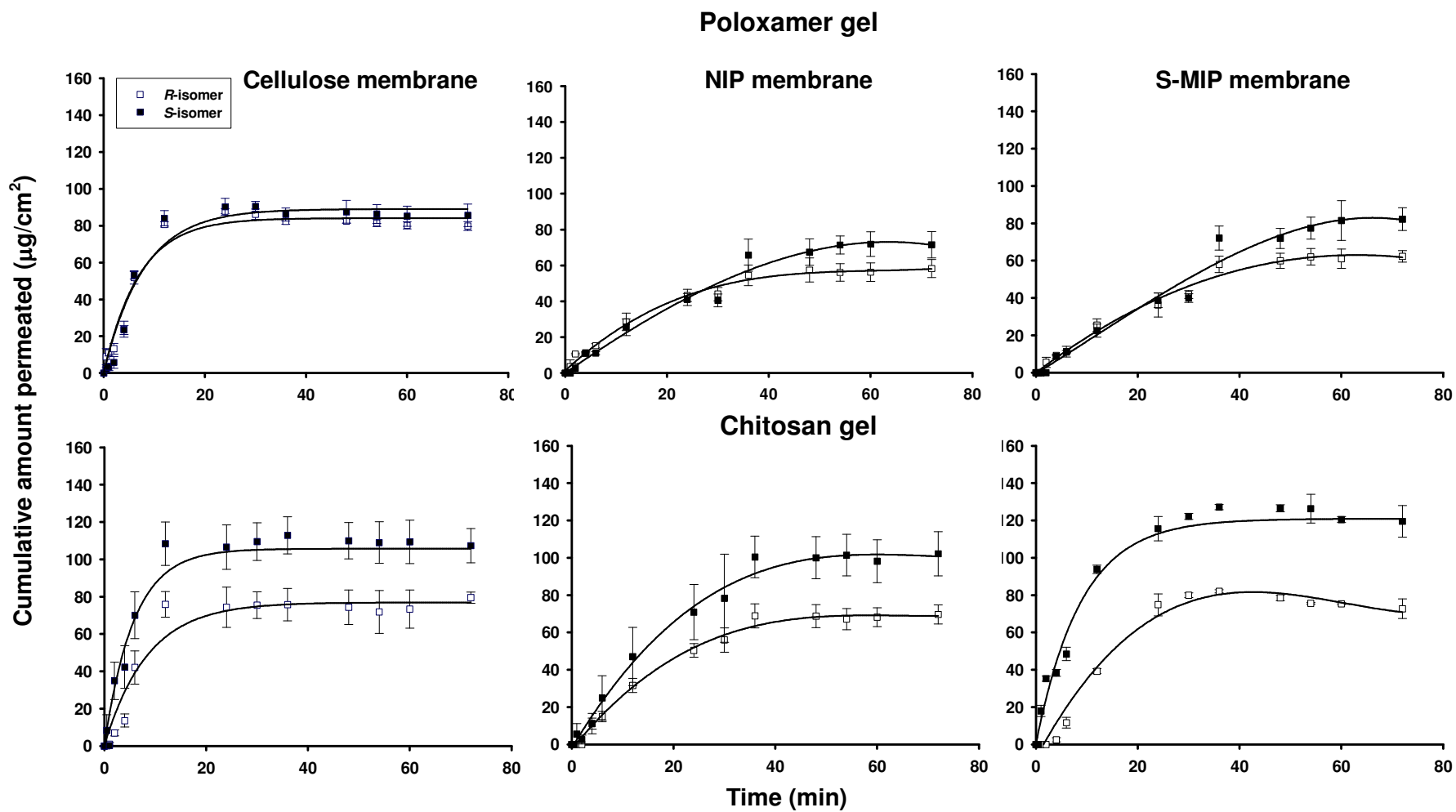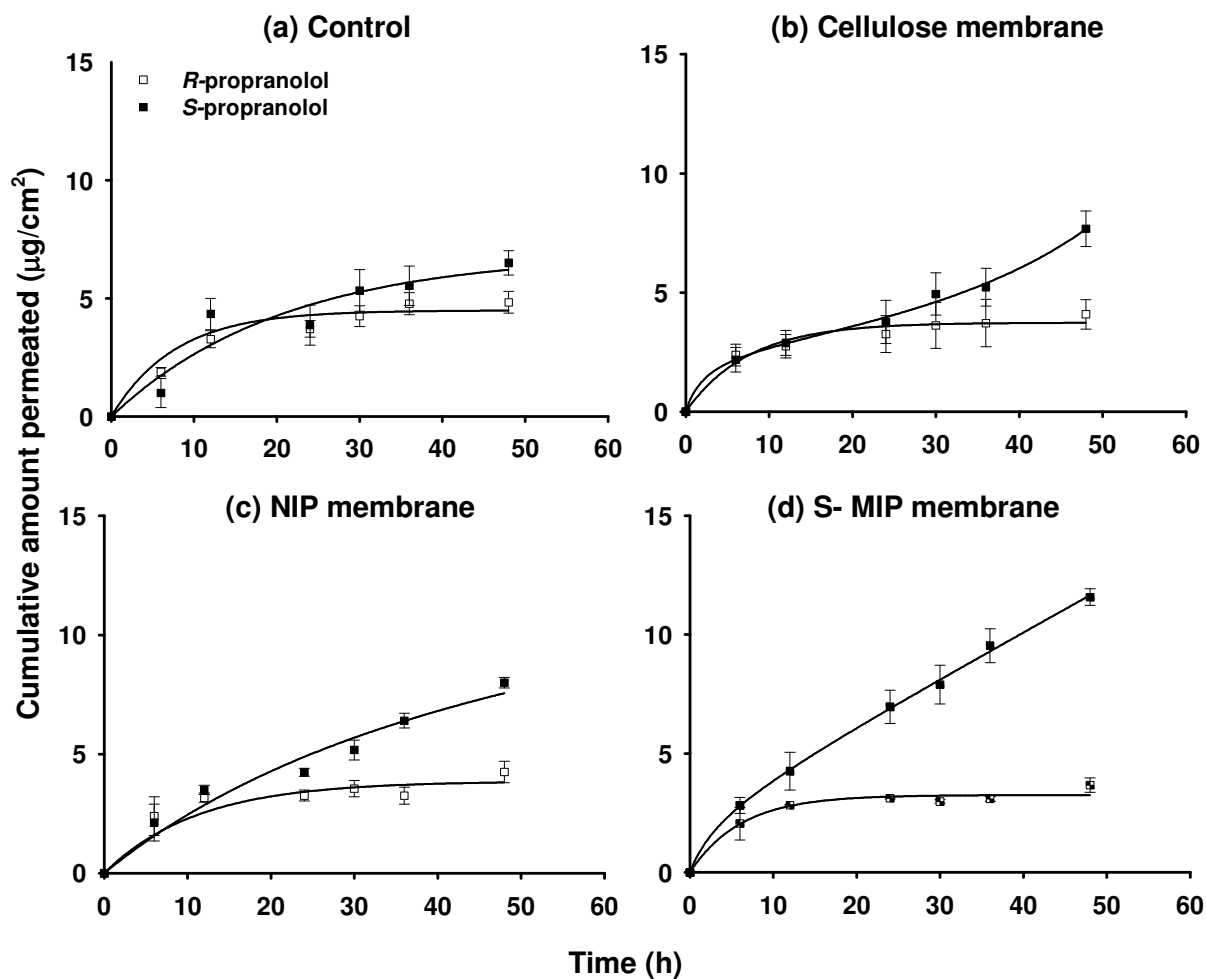
Figure 7.5. Permeability profiles of *R*- and *S*-propranolol enantiomers from gels containing racemic propranolol through full-thickness rat skin alone, or for transport through S-MIP, NIP and cellulose membranes applied to the skin surface (mean ± SE, n=4).

In case of valeryl propranolol gel, the transports of *R*- and *S*-valeryl propranolol from the chitosan gel through the full thickness rat skin with and without cellulose membrane, NIP membrane or S-MIP membrane were increased slightly compared with propranolol (Table 7.4). The increasing of the transport resulted from the increasing of the lipophilicity of the ester prodrug that can penetrate through the lipophilic layer of stratum corneum barrier more than that of propranolol HCl. While the transport of the prodrug increased, the selectivity (*S/R*) decreased. As mentioned in Chapter 5, the ester prodrug with modification of hydroxyl and the high bulky group could not be bound to S-MIP recognition cavity specifically, resulting in lower selectivity of the prodrug to interact with the membrane which has the recognition sites for *S*-propranolol. From these results, it can be indicated that propranolol should be useful for the enantioselective transdermal device more than valeryl propranolol.

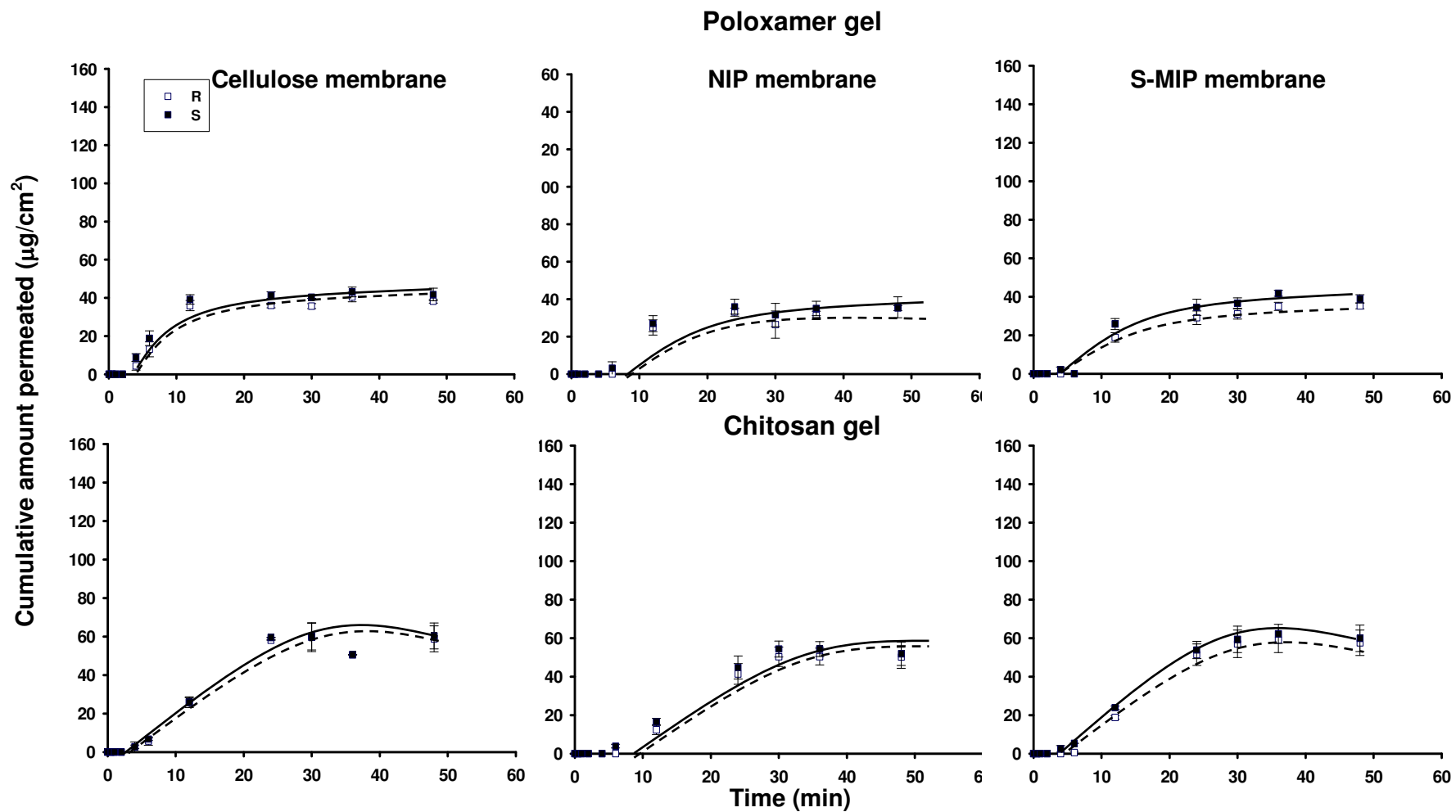Table 7.4. Permeability profiles of *R*- and *S*-valeryl propranolol enantiomers from gels containing racemic valeryl propranolol through full-thickness rat skin alone, or for transport through S-MIP, NIP and cellulose membranes applied to the skin surface (mean $\pm$ SE, n=4).

Membranes	Flux ($\mu g \, cm^{-2} \, h^{-1}$)		*S/R* selectivity
	R-isomer	*S*-isomer	
Skin (control)	0.50$\pm$0.04	0.55$\pm$0.02	1.11$\pm$0.05
Cellulose	0.45$\pm$0.04	0.50$\pm$0.07	1.13$\pm$0.10
NIP	0.43$\pm$0.08	0.49$\pm$0.03	1.21$\pm$0.16
S-MIP	0.41$\pm$0.01	0.55$\pm$0.06	1.55$\pm$0.34

CHAPTER 8

THE IN VIVO EVALUATION OF THE MIP COMPOSITE MEMBRANE

8.1. The objective of the study

The objectives of this study were to prepare the reservoir-type transdermal patch with the use of the MIP composite membrane as the enantioselective controlled release system, and to evaluate *in vivo* permeation of the transdermal patch using Wistar rats.

8.2. Transdermal patch

Transdermal patches are flexible pharmaceutical preparations of varying sizes, containing one or more active substances. They are intended to be applied to the unbroken skin in order to deliver the active substance to the systemic circulation after passing the skin barrier (The United States Pharmacopeia, 2007). From 1979, when the Food and Drug Administration approved the first transdermal drug delivery

system (Transderm Scop® Patch, Alza Corporation), to the current transdermal delivery systems, there evolved a successful alternative to a systemic drug delivery (Degim, 2006). The system was designed to deliver the drug scopolamine to the skin behind the ear for systemic absorption in the control of nausea and vomiting associated with motion sickness.

8.1.1. Transdermal device design

Transdermal devices can be divided into three general types: drug in adhesive, drug in matrix (usually polymer) and drug in reservoir (Figure 8.1) (Walters and Brain, 2002).
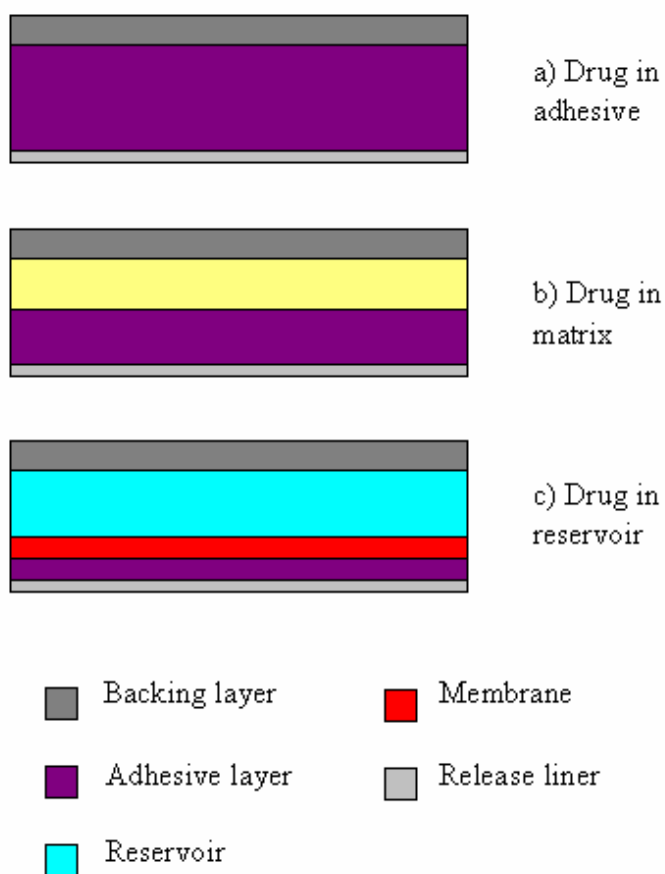
Figure 8.1. Schematic of the typical transdermal drug delivery system designs.

Although there are many differences in the design of the transdermal drug delivery systems, several features are common to all systems including the release liner, the adhesive layer and the backing layer. In the simplest form, the drug in adhesive or adhesive matrix design, the drug is directly loaded or dispersed into the adhesive polymer. The adhesive matrix provides several functions, including skin adhesion, storage of the drug, and control over drug delivery rate. The drug in adhesive matrix is supported on the topside by an impermeable backing film and on the side that faces the skin it is laminated with a removable release liner (Tan and Pfister, 1999). The function of the release liner is to protect and adhesive layer and to prevent drug loss (Vasil'ev et al., 2001). The second type is drug in matrix device, generally incorporating a backing layer, a drug-loaded matrix device, adhesive layer and release liner. The matrix layer is usually a polymeric material in which the solid drug is dispersed, and rate of drug release from the device is controlled by the polymer matrix. With this type, drug release rate falls off with time, as the drug in the skin contracting side of the matrix is depleted. The third type of device is the drug in reservoir. In this case, the drug which usually in liquid and gel form, is contained in a reservoir separated form the skin by a membrane that controls rate of drug release to the skin. This design offers an advantage over monolithic devices in that as long as the drug solution in the reservoir remains saturated, the rate of drug release through the membrane remains relatively constant (Baker and Kochinke, 1989).

8.3. Experimental

8.3.1. Chemicals and reagents

Racemic propranolol HCl and chitosan (medium molecular weight) were purchased from Aldrich Chemical Company (WI, USA) and were used as received. Poloxamer 407 was supplied by BASF (Ludwigshafen, Germany). The backing laminate (Scotchpak™, Polyester Film # 1109), the release liner (Scotchpak™, Low Adhesion Polyester # 1022) and the spacer (Scotchpak™, Polyolefin Foam Tape # 9773) were obtained as gifts from 3M Pharmaceuticals (MN, USA). All solvents used were of either analytical-reagent grade or HPLC grade and were used as received. Working standard solutions were prepared daily.

The NIP, R-MIP and S-MIP membrane employed in this study had the thickness approximately 5 μm, the electric resistance of 1 Ω cm^2 and the tensile strength of 3.16 kN/m^2 (see the preparation procedure in Chapter 3).

8.3.2. Animals

Male Wistar rats, weighing 230-250 g, were used for *in vivo* experiments. All the animals were procured from central animal facility of Prince of Songkla University, Songkla, Thailand after clearance from local ethic committee (ST. 0521.05/054). The rats were housed under standard conditions. The temperature was

controlled at 25±1 °C and the relative humidity was 40-60%. The animals were kept in plastic cages in groups of five per cage. They had access to a commercial diet and tap water ad libitum. There were three rats for each group of the study.

8.3.3. Patch preparation

The component of the transdermal patch includes a backing layer, gel reservoir, MIP membrane and release liner. The effective surface area of the transdermal patch was 16 cm^2. The chitosan gel formulation that gave satisfactory enantioselective delivery of S-propranolol was adopted as the reservoir for the formulation of the transdermal patch. Chitosan gel was prepared by using the method reported by Thacharodi and Rao, 1995 with slightly modification as described in the Chapter 7. The required amount of racemic propranolol HCl (0.75 mg) was added in this gel to obtain the reservoir formulation (0.5 ml). In order to prepare the transdermal patch, a sheet of MIP membrane (20 cm^2) was laminated with the adhesive-coated release liner, thus an 'adhesive-membrane laminate' was obtained. A spacer obtained from the Scotchpak™ foam tape (thickness: 1.0 mm and internal dimension: 4 cm) was used to hold the gel in the device. The capacity of the spacer was 1.5 cm^3. The spacer was attached to the 'adhesive-membrane laminate' to obtain an empty device. The spacer was filled with 0.5 ml of gel reservoir and then the backing laminate was covered onto the spacer with epoxy resin, to obtain the complete device (Figure 8.2).

The backing membrane   The S-MIP membrane

The foam tape   The release liner

The drug reservoir
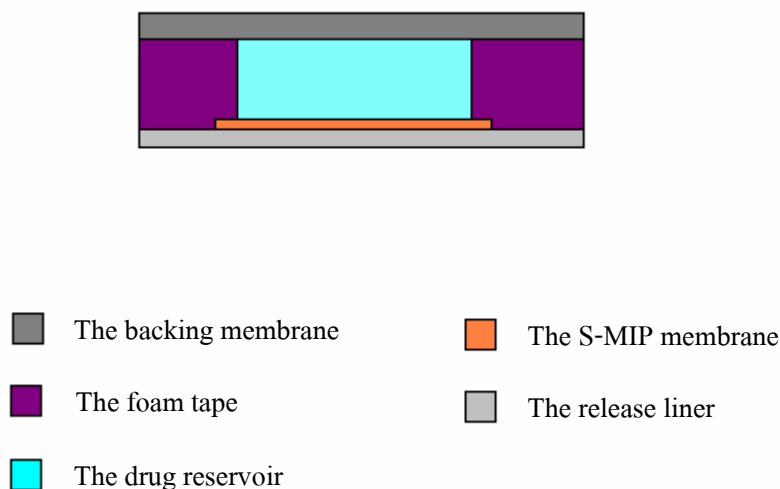
Figure 8.2. Schematic representation of the adhesive device used in this study.

8.3.4. Racemic propranolol and *S*-propranolol chitosan gel preparation for topical administration (control experiments)

The racemic propranolol HCl and *S*-propranolol HCl chitosan gel formulations were prepared to use as a topical gel in control experiments. The effect of the gel formulations in *in vivo* studies was observed. The gels were prepared as the same manner of the drug reservoir as described in section 8.3.3. Racemic propranolol HCl or *S*-propranolol HCl was thoroughly mixed with the viscous gel to achieve the desired concentration (1.5 mg ml^{-1} of racemic propranolol HCl and 0.75 mg ml^{-1} of *S*-propranolol HCl).

8.3.5. *In-vivo* studies

Rats were anaesthetized with urethane 30% (0.9 g/kg, i.p.) and the hairs at dorsal region were removed with an electronic hair clipper. Loss of righting reflex was used to determine the presence of anesthesia. During anesthesia the frequency and ease of breathing was checked every 10 min. The paper liner covering the adhesive layer was peeled off from the transdermal patches (as prepared in Section 8.3.3) and the patches were attached onto the prepared dorsal areas of the rats. For control experiments, the spacers were prepared as for the transdermal patch; after removing the paper liners from the adhesive tape, the spacers were fixed to the hair free dorsal skins, and a fixed amount of the gel formulations, containing the same gel preparation and the same amount of either racemic propranolol (0.75 mg) or the single *S*-enantiomer of propranolol (0.37 mg) as the patch, was dropped into the empty space on the dorsal surfaces. The backing films were then applied onto the spacers, protecting the loss of gel, the evaporation of water from the gel formulation. Each experiment was performed in triplicate. Blood samples (250 μl) were withdrawn from the femoral vein into heparin tubes. Blood samples were collected at zero time, and every 3-6 h during the period of 24 h. Blood samples were centrifuged (3000 x *g* for 10 min) and the plasma was collected and stored in vials at -20°C until analysis. The plasma samples were pretreatmented (see section 8.3.7) before analysis of the amount of propranolol enantiomers. Figure 8.3. shows the situation of the rats for applying the topical gels and the S-MIP patch.
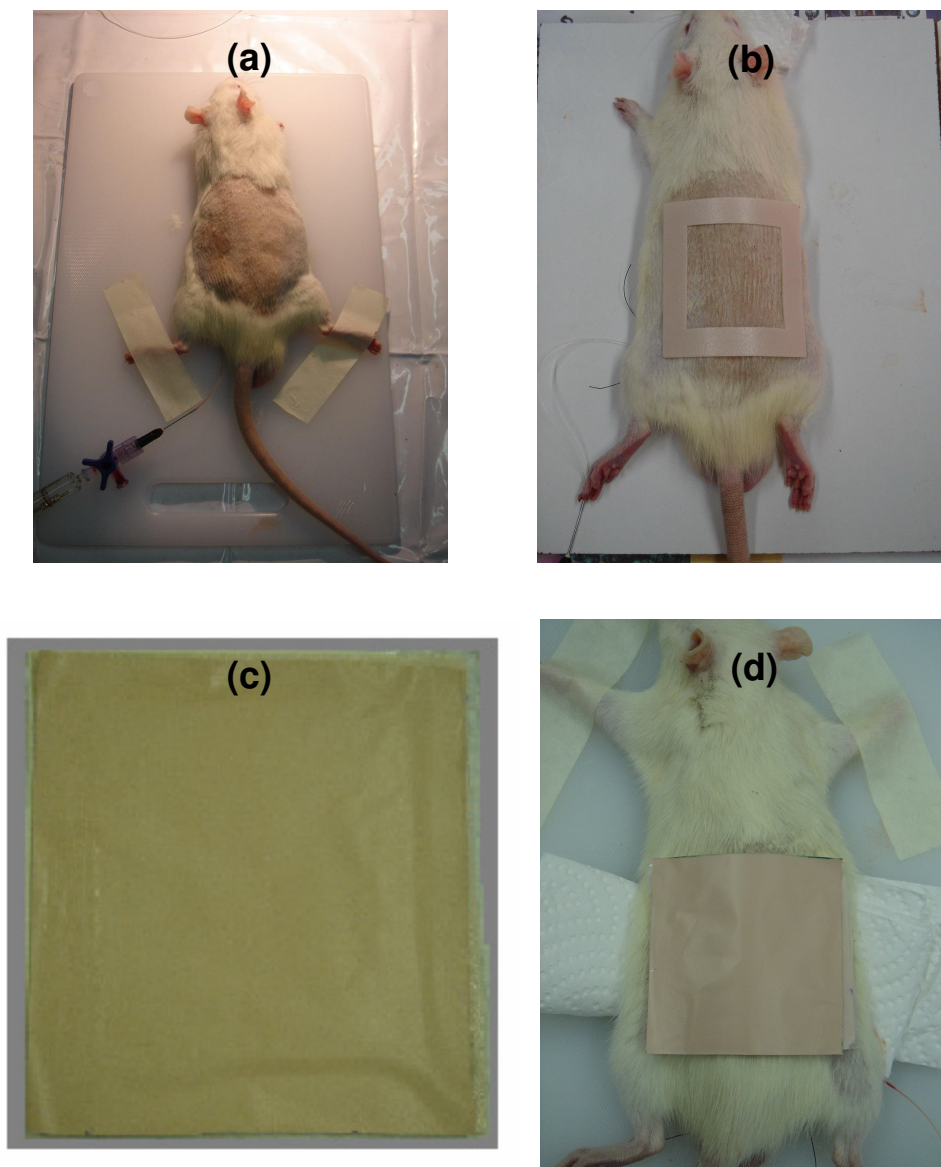
Figure 8.3. The situation of the rat *in vivo* studies: (a) the hair on the dorsal was removed prior the studies, (b) the foam tape was fixed at the dorsal side to act as a spacer for topical gel applications (control experiments), (c) the prepared S-MIP transdermal patch and (d) the S-MIP patch which have the same effective surface area as that of the control experiments was applied on the dorsal of the rats.

8.3.6. Pharmacokinetic analysis

C_{max} and T_{max} were determined from the pharmacokinetic profiles generated by plotting the concentration of propranolol enantiomer in plasma (ng/ml) versus time. The area under the concentration time curves (AUC) was calculated using Prism 4.0 software (GraphPad, CA, USA).

8.3.7. Sample preparation

The blood samples were pretreatmented by a liquid–liquid extraction method as described previously with some modifications. Plasma samples (125μl) were spiked with 50 μl of an aqueous solution of 40 ng ml^{-1} S-phenylephrine (internal standard) and followed by extraction with ether (3 ml). Propranolol enantiomers were extracted into diethyl ether by shaking for 10 min, using mutually pre-saturated phases. Organic phase was collected and evaporated to dryness. The residues were dissolved in 125μl of HPLC mobile phase.

8.3.8. Stereospecific HPLC method

The analysis of amount propranolol enantiomer in samples was performed directly by a chiral-HPLC method. The HPLC system (Shimadzu Corporation, Kyoto, Japan) consisted of a Shimadzu LC-10AD pump, FCL-10AL gradient valve, DGU-14A in-line solvent degasser, SCL-10A system controller, SIL-

10AD auto injector (20 µl injection loop), with a fluorescence spectrophotometer (Shimadzu RF-10A XL fluorescence spectrophotometer, Japan) set at excitation and emission wavelengths of 290 and 340 nm, respectively. Data were collected and analysed on a personal computer using Class VP software version 4.2, (Shimadzu Corporation, Kyoto, Japan). The column employed was a 150×4 mm I.D., particle size 5 µm Chiral-AGP column (CHIRAL-AGP^{TM}, ChromTech Ltd., UK). The lower detection limits for both enantiomers when assayed with the method described above were 5 ng ml^{-1}. Correlation coefficient of 10-50 ng ml^{-1} R- and S-propranolol were greater than 0.995.

8.3.9. Statistical analysis

Differences between the concentration time profiles of the enantiomers and their respective pharmacokinetic parameters within each treatment group were assessed by the Student's t-test for pair data. Observed difference in the pharmacokinetic indices between treatment groups were examined using ANOVA. Significance differences were determined at $p<0.05$.

8.4. Results and discussion

8.4.1. *In-vivo* evaluation of the MIP transdermal patch

Figure 8.4 shows the plasma concentration *versus* time following application of the transdermal patch containing racemic propranolol and direct application of the topical gel formulations containing either racemic propranolol or the pure *S*-propranolol alone (the controls). The plasma concentration levels of *S*-propranolol enantiomer increased markedly and reached the maximum concentration within 8 h after applying the transdermal patches (Figure 8.4c). The absorption rate of the *S*-propranolol enantiomer was lower for both racemic propranolol and *S*-propranolol applied as topical gel formulations, this being reflected by longer T_{max} (~12 h) for *S*-enantiomer as compared to the patch. The transdermal patch containing the MIP composite membrane as the enantioselective-controlled release system differences in plasma concentration of propranolol enantiomers, such that C_{max} of *S*-propranolol enantiomer was about 4 times higher than that of *R*-propranolol enantiomer, and the AUC_{0-24} for *S*-propranolol was about 5 times higher than for *R*-propranolol (Table 8.1). The gel formulation containing racemic propranolol did not show enantiomeric differences in the plasma concentrations and AUC_{0-24}. No apparent differences were observed in the *S*-propranolol plasma concentration between the transdermal patch and gel formulation comprising a single *S*-enantiomer of propranolol (p=0.416). Similarly AUC values for *S*-isomer of propranolol were not significantly different when the transdermal patch was compared to the gel

formulation (p=0.481). The transdermal patch had the capability to selectively regulate the release of *S*-isomer of propranolol with the selectivity of *S*-propranolol enantiomer 4 fold higher than that of *R*-enantiomer. Propranolol possesses one chiral center, and the *S*-enantiomer of propranolol is 100-130 times more pharmacologically active than the *R*-enantiomer (Barett and Cullum, 1968). The degree of stereoselectivity *in vivo* achieved using the reservoir patch containing the MIP composite membrane with chitosan gel as drug reservoir could result in considerably higher therapeutic advantage when considering the differential in pharmacological activities of the two enantiomers of propranolol. Inspection of the patch application site did not reveal any significant erythema.
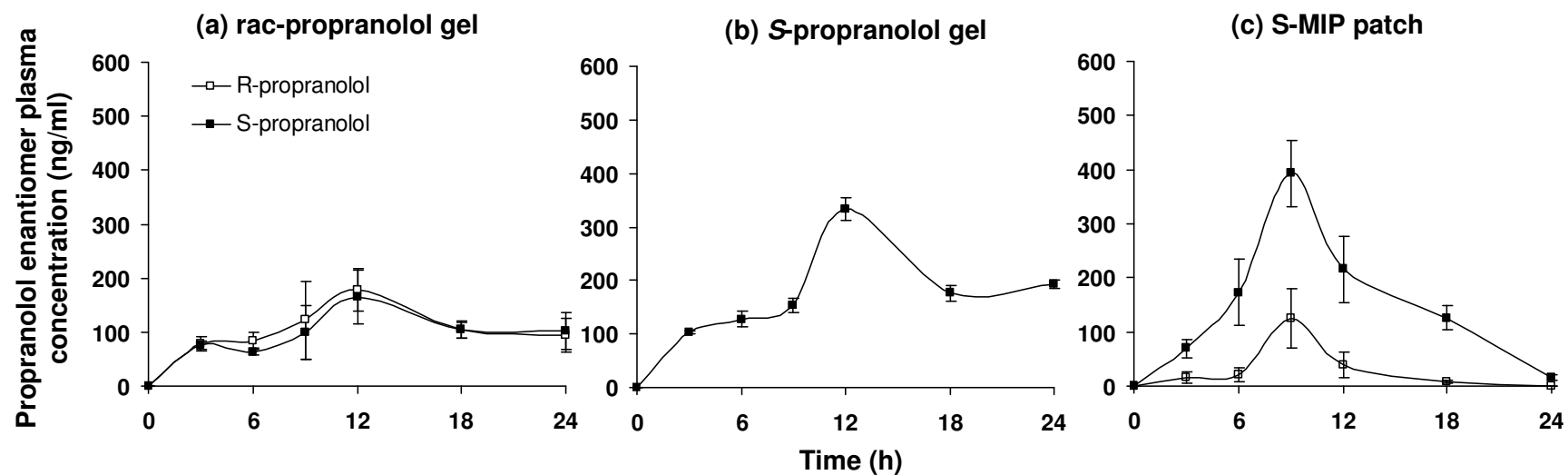
Figure 8.4. Plasma concentration versus time profiles of propranolol enantiomers in rats following transdermal application of: (a) gel formulation containing 1.5 mg ml^{-1} racemic propranolol, (b) gel formulation containing 0.75 mg ml^{-1} *S*-propranolol, and (c) the S-MIP patch containing 1.5 mg ml^{-1} racemic propranolol (mean $\pm$ SE, n=3).

Table 8.1. Pharmacokinetic parameters of propranolol enantiomers in rats following transdermal application of the gel formulation containing racemic propranolol or the single S-propranolol enantiomer, and the application of the S-MIP patch containing racemic propranolol (mean $\pm$ SE, n=3).

		rac-propranolol gel	P value	S-propranolol gel	S-MIP patch	P value
T_{max}(h)	R	11.2$\pm$1.0		-	8.0$\pm$1.0	
			0.983			0.892
	S	11.1$\pm$1.0		12.0$\pm$0.0	8.1$\pm$1.0	
C_{max} (ng.ml^{-1})	R	178$\pm$40		-	123$\pm$18	
			0.368			0.049
	S	165$\pm$50		333$\pm$21	391$\pm$53	
AUC_{0-24} (ng ml^{-1} h)	R	2568$\pm$69		-	715$\pm$80	
			0.118			0.034
	S	2394$\pm$98		4235$\pm$147	3928$\pm$536	
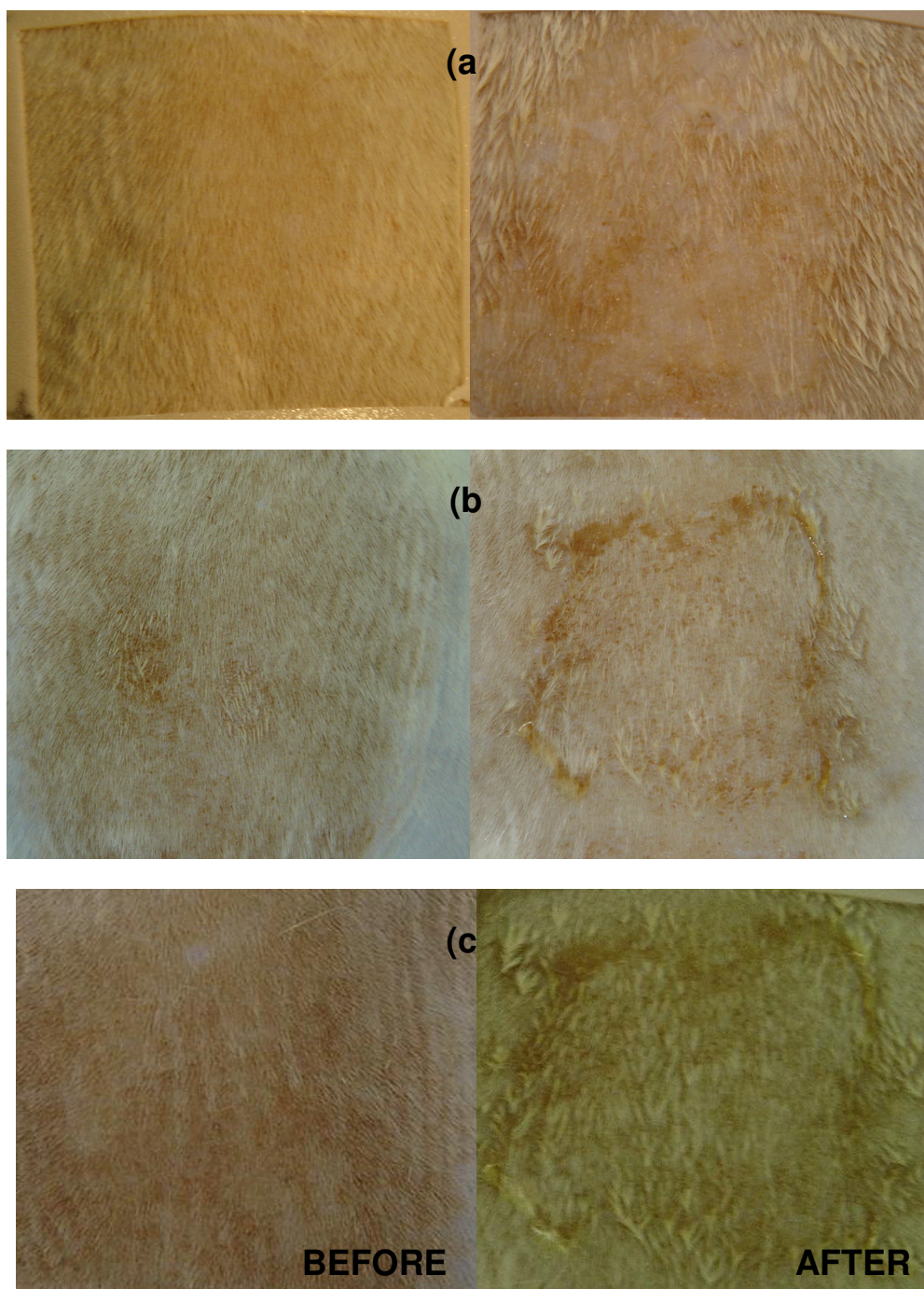
Figure 8.5. The pictures of the rat skin before and after 24 h of application: (a) gel formulation containing 1.5 mg ml^{-1} racemic propranolol, (b) gel formulation containing 0.75 mg ml^{-1} S-propranolol, and (c) the S-MIP patch containing 1.5 mg ml^{-1} racemic propranolol.

CHAPTER 9

CONCLUSION

In this thesis, a composite membrane of bacterially-derived cellulose and molecularly imprinted polymer (MIP) as an enantioselective-controlled release membrane was developed for transdermal delivery of S-propranolol. The composite MIP membrane was synthesized by pore filling of an asymmetric porous cellulose membrane with a MIP thin-layer. Two step grafting procedure was used to yield a MIP by in situ copolymerization of MAA and EDMA within the thin layer of the base material. The effect of cultured condition of the bacterial cellulose membranes on the enantioselective property of cellulose membrane was studied. The different types of bacterial cellulose membranes from various cultured conditions were prepared and these membranes were used as membrane bases for the production of the composite MIP membranes. The MIP composite membrane with selective for S-propranolol, with 5 μm thickness and 1.7 Ω cm^2 exhibited the highest he highest enantioselective release of S-propranolol enantiomer.

The results from release study showed that the mechanism underlying the release of *S*-propranolol and *S*-propranolol prodrugs for the S-MIP membrane involve adsorption and mobility of this enantiomer at the binding site in the MIP. The selective release behavior of the MIP composite membrane concurs with the 'fixed-[192] carrier' mechanism.

The available form of propranolol is hydrochloride salt resulting in the low penetration through the skin. Thus, the lipophilic propranolol prodrugs were aimed to increase the permeation of the drug. Three propranolol prodrugs were synthesized by substituting different alkyl groups onto the hydroxyl group of propranolol. The *S*-enantioselectivity is generally appeared when the prodrugs are employed as the diffusion species for the cellulose membrane and modified cellulose membranes. Valeryl propranolol (VL-P) shows the highest enantioselectivity release across S-MIP membrane. The penetration of valeryl propranolol (HCl) enantiomers through the Wistar rat skins (*in vitro*) with and without cellulose membrane and the composite MIP membrane were compared with that of propranolol (HCl). Unfortunately, VL-P did not improve the permeation of the enantiomers of propranolol as expected objective. Also the selectivity of the S-MIP membrane was reduced in case of VL-P. However, S-MIP membrane shows the potential in controlling the release of the *S*-propranolol into Wistar rat skin.

Polxamer 407 and chitosan gel were studied as a vehicle for propranolol and valeryl propranolol in the release experiments. The drugs were retained in the hydrophobic core of poloxamer 407 resulting in the lower flux and selectivity of the membranes, where the repulsive effect between the positive charge of chitosan and propranolol leading the higher flux and selectivity. The propranolol, the template, is preserved the highest *S*-enantioselectivity of S-MIP membrane for both release experiments and penetration through rat skin (*in vitro*) studies over the VL-P.

The enantioselective-controlled release devices as the transdermal patches were prepared from the S-MIP membrane. The S-MIP devices expressed the *S*-enantioselectivity, C_{max} and AUC_{0-24} of the *S*-propranolol was higher than that of *R*-propranolol (about 4 times), whereas the topical application of the racemic propranolol gel did not show the differences of the enantiomers. In addition, the S-MIP patch showed the high concentration of *S*-propranolol in plasma similarly as the topical application of the pure *S*-propranolol gel. The degree of stereoselectivity demonstrated would result in considerably higher therapeutic advantage when considering the different pharmacological activities of the two enantiomers of propranolol.

The positive finding of the *in vivo* studies of the S-MIP membrane suggest that transdermal delivery in rats using the transdermal reservoir patch containing molecularly imprinted polymer composite membrane with chitosan gel as a drug reservoir could result in *S*-propranolol enantiomer (the eutomer) in blood levels similar to those seen after transdermal delivery by gel formulation containing a single

S-propranolol. Thus, the S-MIP device should be a therapeutic advantage delivery system by increasing the transport of the eutomer (*S*-propranolol) as well as reducing the release of the distomer (*R*-propranolol) leading to reduce the chance of the side effect or toxicity of the drug.

REFERENCES

Aboul-Enein, H.S. and Basha L.I. 1997. Chirality and drug hazards, in: Aboul-Enein, Wainer, I.W. (Eds), The impact of stereochemistry on the drug development and use, John Wiley & Sons, Inc, New York, p. 1-19.

Aboul-Enein, H. Y. 2001. High-performance liquid chromatographic enantioseparation of drugs containing multiple chiral centers on polysaccharide-type chiral stationary phases, *Journal of Chromatography A*, 906: 185-193.

Ahmed, S., Imai, T. and Otagiri, M. 1995. Stereoselective hydrolysis and penetration of propranolol prodrugs: *In vitro* evaluation using hairless mouse skin, *Journal of Pharmaceutical Science*s, 84: 877-883.

Ahmed, S., Imai, T., Yoshigae, Y. and Otagiri, M. 1997. Stereospecific activity and nature of metabolizing esterases for propranolol prodrug in hairless mouse skin, liver and plasma, *Life Sciences*, 61: 1879:1887.

Ahuja, S. 1991. Chiral separations: an overview, in Ahuja, S. (Ed), Chiral separations by liquid chromatography, American Chemical Society, Washington, DC, p. 1-26.

Ahuja, S. 1997a. Chiral separations and technology: an overview, in Ahuja, S. (Ed), Chiral separations: Applications and technology, American Chemical Society, Washington, DC, p.1-7.

Ahuja, S. 1997b. The importance of chiral separations in pharmaceuticals, in: Aboul-Enein, Wainer, I.W. (Eds), The impact of stereochemistry on the drug development and use, John Wiley & Sons, Inc, New York, p. 287-315.

Allender, C. J., Richardson, C., Woodhouse, B., Heard, C. M. and Brain, K. R. 2000. Pharmaceutical applications for molecularly imprinted polymers, *International Journal of Pharmaceutics*, 195: 39-43.

Alvarez-Lorenzo, C. and Concheiro, A. 2004. Molecularly imprinted polymers for drug delivery, *Journal of Chromatography B*, 804: 231-245.

Alvarez-Lorenzo, C., Yañez, F., Barreiro-Iglesias, R. and Concheiro, A. 2006. Imprinted soft contact lenses as norfloxacin delivery systems, *Journal of Controlled Release*, 113: 236-244.

Amnuaikit, C., Ikeuchi, I., Ogawara, K., Higaki, K. and Kimura, T. 2005. Skin permeation of propranolol from polymeric film containing terpene enhancers for transdermal use, *International Journal of Pharmaceutics*, 289: 167-178.

Andersson, B. D., Chu, W. W. and Galinsky, R. E. 1988, Reduction of first-pass metabolism of propranolol after oral administration of ester prodrugs, *International Journal of Pharmaceutics*, 43: 261-265.

Andersson, L. I., O'shannessy, D. J. and Mosbach, K. 1990. Molecular recognition in synthetic polymers: preparation of chiral stationary phases by molecular imprinting of amino acid amides, *Journal of Chromatography*, 513: 167-179.

Andersson, L. I. 2000. Molecular imprinting: developments and applications in the analytical chemistry field, *Journal of Chromatography B*, 745: 3-13.

Ansel, H.C., Popovich, N.G. and Allen, L.V. (Eds.). 1995. Pharmaceutical dosage forms and drug delivery systems, Williams & Wilkins, Malvern, PA.

Ansell, R. J. 2005. Molecularly imprinted polymers for the enantioseparation of chiral drugs, *Advanced Drug Delivery Reviews*, 57: 1809-1835.

Baker, R. and Kochinke, F. 1988. Transdermal drug delivery system, in: Rossoff, M. (Ed.), Controlled release of drugs: Polymers and aggregate systems, VCH Publishers, Inc, New York, p 277-305.

Barrett, A. M. and Cullum, V.A. 1968. The biological properties of the optical isomers of propranolol and their effects on cardiac arrythemias, *British Journal of Pharmacology*.34: 43–55.

Barnwell, S. G., Burns, S. J., Higginbottom, S., Whelan, I., Corness, D., Hay, G., Rosenberg, E. and Attwood, D. 1996. Demonstration of the importance of biphasic oleic acid delivery for enhancing the bioavailability of propranolol in healthy volunteers, *International Journal of Pharmaceutics*, 128: 145-154.

Barry, B. W. 1983. Structure, function, diseases, and topical treatment of human skin, in Barry, B. W. (Ed), Dermatological formulations, Marcel Dekker, Inc, New York, p.1-48.

Barry, B. W. 2001a. Novel mechanisms and devices to enable successful transdermal drug delivery, *European Journal of Phrmaceutical Sciences*, 14: 101-114.

Barry, B. W. 2001b. Is transdermal drug delivery research still important today?, *Drug Discovery Today*, 19: 967-971.

Barry, B. W. 2002. Drug delivery routes in skin: a novel approach, *Advanced Drug Delivery Reviews*, 54: S31-S40.

Bernkop-Schnürch, A. 2000. Chitosan and its derivatives: potential excipients for peroral peptide delivery systems, *International Journal of Pharmaceutics*, 194: 1-13.

Bhatnagar, S. and Vyas, S. P. 1994. Organogel-based system for transdermal delivery of propranolol, *Journal of Microencapsulation*, 11: 431-438.

Blonder, J., Baird, L., Fulfs, J. C. and Rosenthal, G. J. 1999. Dose dependent hyperlipidemia in rabbits following administration of poloxamer 407 gel, *Life Sciences*, 65: 261-266.

Bonacucina, G., Spina, M., Misici-Falzi, M., Cespi, M., Pucciarelli, S., Angeletti, M. and Palmieri, G. F. 2007. Effect of hydroxypropyl β-cyclodextrin on the self-assembling and thermogelation properties of poloxamer 407, *European Journal of Pharmaceutical Sciences,*

Bonato, P. S., Bortocan, R., Gaitani, C. M., Paias, F. O., Iha, M. H. and Lima, R. P. 2002. Enantiomeric resolution of drugs and metabolites in polysaccharide- and protein-based chiral stationary phases, *Journal of the Brazilian Chemical Soci*ety, 13: 1900-199.

Boucard, N., Viton, C., Agay, D., Mari, E., Roger, T., Chancerelle, Y. and Domard, A. 2007. The use of physical hydrogels of chitosan for skin regeneration following third-degree burns, *Biomaterials*, 28: 3478-3488.

Brown, R. M. Jr., Saxena, I. M. and Kudicka, K. 1996. Cellulose biosynthesis in higher plants, *Trends in Plant Science*, 1: 149-156.

Brüggemann, O., Haupt, K., Ye, L., Yilmaz, E. and Mosbach, K. 2000. New configurations and applications of molecularly imprinted polymers, *Journal of Chromatography A*, 889: 15-24.

Brun, P. P. H. L., Fox, P. L. A., de Vries, M. E, and Boddé, H. E. 1989. In vitro penetration of some β-adrenoreceptor blocking drugs through porcine buccal mucosa, *International Journal of Pharmaceutics,* 49: 141-145.

Bundgaard, H., Buur, A., Chang, S. and Lee, V. H. L. 1986. Prodrugs of timolol for improved ocular delivery: synthesis, hydrolysis kinetics and lipophilicity of various timolol esters, *International Journal of Pharmaceutics*, 33: 15-26.

Bundgaard, H., Buur, A., Chang, S. and Lee, V. H. L. 1988, Timolol prodrugs: synthesis, stability and lipophilicity of various alkyl, cycloalkyl and aromatic esters of timolol, *International Journal of Pharmaceutics*, 46: 77-88.

Bundgaard, H. 1989. The prodrug approach for improved rectal delivery, in: Prescott, L. F. and Nimmo, W. S. (Eds), Novel drug delivery and its therapeutic application, John Wiley & Sons, Inc, New York, p. 193-208.

Bures, P., Huang, Y., Oral, E. and Peppas, N. A. 2001. Surface modifications and molecular imprinting of polymers in medical and pharmaceutical applications, *Journal of Controlled Release*, 72: 25-33.

Buur, A., Bundgaard, H. and Lee, V. H. L. 1988, Prodrugs of propranolol: hydrolysis and intramolecular aminolysis of various propranolol esters and an oxazolidine-2-one derivative, *International Journal of Pharmaceutics*, 42: 51-60.

Cabana, A., Aït-Kadit, A. and Juhász, J. 1997. Study of the gelation process of polyethylene oxide$_a$-polypropylene oxide$_b$-polyethylene oxide$_a$ copolymer (poloxamer 407) aqueous solutions, *Journal of Colloid and Interface Science*, 190: 307-312.

Campo, C.del, Llama, E. F. and Sinisterra, J. V. 1996. Design, synthesis and evaluation of a chiral propranolol selector, *Tetrahedron-Asymmetry*, 7: 2627-2631.

Chao, Y., Ishida, T., Sugano, Y. and Shoda, M. 2000. Bacterial cellulose production by *Acetobacter xylinum* in a 50-L internal-loop airleft reactor, *Biotechnology and Bioengineering*, 68: 345-352.

Chaplin, M. (May 12, 2008). Water structure and sciences : cellulose. Retrived: May 14, 2008, from: http://www.lsbu.ac.uk/water/hycel.html.

Chen, C., Chen, Y., Zhou, J. And Wu, C. 2006. A 9-vinyladenine-based molecularly imprinted polymeric membrane for the efficient recognition of plant hormone [1]H-indole-3-acetic acid, *Analytica Chemica Acta*, 569: 58-65

Chen, W. and Hwang, G. C. 1992. Adhesive and *in vitro* release characteristics of propranolol bioadhesive disc system, *International Journal of Pharmaceutics*, 82: 61-66.

Chesnoy, S., Durand, D., Doucet, J. and Couarraze, G. 1999. Structural parameters involved in the permeation of propranolol HCl by iontophoresis and enhancers, *Journal of Controlled Release*, 58: 163-175.

Ching, C. B., Fu, P., Ng, S. C. And Xu, Y. K. 2000. Effect of mobile phase composition on the separation of propranolol enantiomers using a perphenylcarbamate β-cyclodextrin bonded chiral stationary phase, *Journal of Chromatography A*, 898: 53-61.

Crossley, R. 1995. Chirality and the biological activity of drugs, CRC Press, Florida. p 1-35

Czaja, W., Romanovicz, D. and Brown, R. M. Jr. 2004. Structural investigations of microbial cellulose produced in stationary and agitated culture, *Cellulose*, 11: 403-411.

Czaja, W., Krystynowicz, A., Bielecki, S. and Brown, R. M. Jr. 2006. Microbial cellulose-the natural power to heal wounds, *Biomaterials*, 27: 145-151.

Davies, A. M. and Teng, X. W. 2003. Importance of chirality in drug therapy and pharmacy practice: Implications for psychiatry, *Advances in Pharmacy*, 1:242-252.

Degim, I. T. 2006. New tools and approaches for predicting skin permeability, *Drug Discovery Today*, 11: 517-523.

Donato, L., Figoli, A. and Drioli, E. 2005. Novel composite poly (4-vinylpyridine)/ polypropylene membranes with recognition properties for (*S*)-naproxen, *Journal of Pharmaceutical and Biomedical Analysis*, 37: 1003-1008.

Drayer, D.E. 1988. The history of stereochemistry, in: Wainer, I.W., Drayer, D.E (Eds), Drug stereochemistry: Analytical methods and pharmacology, Marcel Dekker, Inc, New York, p. 3-29.

Dubey, V., Saxena, C., Singh, L., Ramana, K. V. and Chauhan, R. S. 2002. Pervaporation of binary water–ethanol mixtures through bacterial cellulose membrane, *Separation and Purification Technology*, 27: 163-171.

Dyas, A. M. 1992. The chiral chromatographic separation of β-adrenoreceptor blocking drugs, *Journal of Pharmaceutical and Biomedical Analysis*, 10: 383-404.

El-Kattan, A., Asbill, C. S. and Haidar, S. 2000. Transdermal testing: practical aspects and methods, *PSTT*, 3: 426-430.

Ellwanger, A., Owens, P. K., Karlsson, L., Bayoudh, S., Cormack, P., Sherrington, D. and Sellergren, B. 2000. Application of molecularly imprinted polymers in supercritical fluid chromatography, *Journal of Chromatography A*, 897: 317-327.

Evans, B. R., O'Neill, H. M., Malyvanh, V. P., Lee, I. and Woodward, J. 2003. Palladium-bacterial cellulose membranes for fuel cells, *Biosensors and Bioelectronics*, 18: 917-923.

Facklam, C. and Modler, A. 1994. Separation of some enantiomers and diasteromers of propranolol derivatives by high-performance liquid chromatography, *Journal of Chromatography A*, 664: 203-211.

Fang J., Huang, Y., Lin, H. And Tsai, Y. 1998. Transdermal iontophoresis of sodium noninvamide acetate. IV. Effect of polymer formulations, *International Journal of Pharmaceutics*, 173: 127-140.

Fishman W. H. and Jorde, U. 2000. β-adrenergic blockers, in: Oparil, S. and Weber, M. A., Hypertension: A comparison to Brenner and Rector's The kidney, W.B. Saunders Company, Pensylvania, p. 590-595.

Flynn, G.L. 1995. Cutaneous and transdermal delivery: Processes and systems of delivery, in: Banker G.S. and Rhodes C.T. (Ed.), Drugs and the Pharmaceutical Sciences vol. 72 Modern Pharmaceutics, Marcel Dekker, Inc, New York, p 239-298.

Food and Drug Administration. 1992. Policy statement for the development of new stereoisomeric drugs. Available from: CDER Executive Secretariat Staff Center for Drug Evaluation and Research (HFD-8), FDA, USA.

Franco, P., Senso, A., Oliveros, L. and Minguillón, C. 2001. Covalently bonded polysaccharide derivatives as chiral stationary phases in high-performance liquid chromatography, *Journal of Chromatography A*, 906: 155-170.

Francotte, E. R., Enantioselective chromatography as a powerful alternative for the preparation of drug enantiomers, *Journal of Chromatography A*, 906: 379-397.

George, J., Ramana, K. V., Sabapathy, S. N., Jagannath, J. H. and Bawa, A. S. 2005. Characterization of chemically treated bacterial (*Acetobacter xylinum*) biopolymer: Some thermo-mechanical properties, *International Journal of Biological Macromolecules*, 37: 189-194.

Godin, B. and Touitou, E. 2007. Transdermal skin delivery: Predictions for humans from *in vivo*, *ex vivo* and animal models, *Advanced Drug Delivery Reviews*, 59: 1152-1161.

Götmar, G., Fornstedt, T., Andersson, M. and Guiochon, G. 2001. Influence of the solute hydrophobicity on the enantioselective adsorption of β-blockers on a cellulose protein used as the chiral selector, *Journal of Chromatography A*, 905: 3-17.

Gray, J., The world of skin care, Retrieved: April 04, 2008, from: http://www.pg.com/science/skincare/Skin_tws_9.htm.

Gumí, T., Valiente, M. and Palet, C. 2005a. Elucidation of *S/R*-propanolol transport rate and enantioselectivity through chiral activated mambranes, *Journal of Membrane Science*, 256: 150-157.

Gumí, T., Minguillón C. and Palet, C. 2005b. Separation of propranolol enantiomers through membranes based derivatized polysulfone, *Polymer*, 46: 12306-12312.

Guyot, M. and Fawaz, F. 2000. Design and *in vitro* evaluation of adhesive matrix for transdermal delivery of propranolol, *International Journal of Pharmaceutics*, 204: 171-182.

Hadgraft, J. and Lane, M. E. 2005. Skin permeation: The years of enlightenment, *International Journal of Pharmaceutics*, 305: 2-12.

Haginaka, J. and Sakai, Y. 2000. Uniform-sized molecularly imprinted polymer material for (*S*)-propranolol, *Journal of Pharmaceutical and Biomedical Analysis*, 22: 899-907.

Haginaka, J. 2002. Pharmaceutical and biomedical applications of enantioseparations using liquid chromatographic techniques, *Journal of Pharmaceutical and Biomedical Analysis*, 27: 357-372.

Hakinaka, J. and Kagawa, C. 2004. Retentivity and enantioselectivity of uniformly sized molecularly imprinted polymers for *d*-chlopheniramine and – brompheniramine in hydro-organic mobile phases, *Journal of Chromatography B*, 804: 19-24.

Hattori, K., Hiwatari, M., Iiyama, C., Yoshimi, Y., Kohori, F., Sakai, K. and Piletsky, S. A. 2004. Gate effect of theophylline-imprinted polymers grafted to the cellulose by living radical polymerization, *Journal of Membrane Sciences*, 233: 169-173.

Heard, C. M., Watkinson, A. C., Brain, K. R. and Hadgraft, J. 1993. *In vitro* skin penetration of propranolol enantiomers, *International Journal of Pharmaceutics*, 90: R5-R8.

Heard, C. M. and Suedee, R. 1996. Stereoselective adsorption and trans-membrane transfer of propranolol enantiomers using cellulose derivatives, *International Journal of Pharmaceutics*, 139: 15-23.

Hejazi, R. and Amiji. 2002. Chitosan-based delivery systems: Physicochemical properties and Pharmaceutical applications, in: Dumitriu, S. (Ed), Polymeric Biomaterials 2nd edition, revised and explanded, Marcel Dekker, Inc, New York, p.213-237.

Hilal, N. and Kochkodan, V. 2003. Surface modified microfiltration membranes with molecularly recognizing properties, *Journal of Membrane Sciences*, 213: 97-113.

Hilal, N., Kochkodan, V., Busca, G., Kochkodan, O. And Atkin, B. P. 2003. Thin layer composite molecularly imprinted membranes for selective separation of cAMP, *Separation and Purification Technology*, 31: 281-289.

Hillberg, A. L., Brain, K. R. and Allender, C. J. 2005. Molecular imprinted polymer sensors: Implications for therapeutics, *Advanced Drug Delivery Reviews*, 57: 1875-1889.

Hiratani, H. and Alvarez-Lorenzo, C. 2002. Timolol uptake and release by imprinted soft contact lenses made of *N,N*-diethylacrylamide and methacrylic acid, *Journal of Controlled Release*, 83: 223-230.

Hiratani, H., Fujiwara, A., Tamiya, Y., Mizutani, Y., Alvarez-Lorenzo, C. 2005. Ocular release of timolol from molecularly imprinted soft contact lenses, *Biomaterials*, 26: 1293-1298.

Hori, M., Satoh, S., Maibach, H. I. and Guy, R. H. 1989. Enhancement of propranolol hydrochloride and diazepam skin absorption *in vitro*: Effect of enhancer lipophilicity, *Journal of Pharmaceutical Sciences*, 80: 32-35.

Huang, X., Qin, F., Chen, X., Liu, Y. and Zou, H. 2004. Short columns with molecularly imprinted monolithic stationary phases for rapid separation of diastereomers and enantiomers, *Journal of Chromatography B*, 804: 13-18.

Illum, L., Jabbal-Gill, I., Hinchcliffe, M., Fisher, A. N. And Davis, S. S. 2001. Chitosan as a novel nasal delivery system for vaccines, *Advanced Drug Delivery Reviews*, 51:81-96.

Irwin, W. J. and Belaid, K. A. 1988, Drug-delivery by ion-exchange. Hydrolysis and rearrangement of ester prodrugs of propranolol, *International Journal of Pharmaceutics*, 46: 57-67.

Jiang, Z., Yu, Y. and Wu, H. 2006. Preparation of CS/GPTMS hybrid molecularly imprinted membrane for efficient chiral resolution of phenylalanine isomers, *Journal of Membrane Science*, 280: 876-882.

Jonas, R. and Farah, L. F. 1998. Production and application of microbial cellulose, *Polymer Degradation and Stability*, 59: 101-106.

Jordan, C. G. M., Quigley, J. M. and Timoney, R. F. 1992. Synthesis, hydrolysis kinetics and lipophilicity of *O*-acyl esters of oxprenolol, *International Journal of Pharmaceutics*, 84: 175-189.

Jordan, C. G. M., Davis, G. W. and Timoney, R. F., 1996. Studies showing the effect of enzymes on the stability of ester prodrugs of propranolol and oxprenolol in biological samples, *International Journal of Pharmaceutics*, 141: 125-135.

Kafková, B., Bosáková, Z., Tesařová, E. and Coufal, P. 2005. Chiral separation of beta-adrenergic antagonists, profen non-steroidal anti-inflammatory drugs and chlorophenoxypropionic acid herbicides using tricoplanin as the chiral selector in capillary liquid chromatography, *Journal of Chromatography A*, 1088: 82-93.

Kalim, R., Schoäcker, R., Yüce, S. And Brüggemann,O. 2005. Catalysis of a β-elimination applying membranes with incorporated molecularly imprinted polymer particles, *Polymer Bulletin*, 55: 287-297.

Kaplan, N. M. and Lieberman, E. (Eds). 1998. Clinical hypertension, Williams & Wilkins a Waverly Company, Maryland, p. 205-206.

Kempe, M. and Mosbach, K. 1995a.Receptor binding mimetics: A novel molecularly imprinted polymer, *Tetrahedron Letters*, 36: 3563-3566.

Kempe, M. and Mosbach, K. 1995b. Molecularly imprinting used for chiral separations, *Journal of Chromatography A*, 694: 3-13.

Kielczyński, R. and Bryjak, M. 2005. Molecularly imprinted membranes for cinchona alkaloids separation, *Separation and Purification Technology*, 42: 231-235.

Kochkodan, V, Weiged, W. and Ulbricht, M. 2001. Thin layer molecularly imprinted microfiltration membranes by photofunctionalization using a coated α-cleavage photoinitiator, *Analyst*, 126: 803-809.

Komiyama, M., Takeuchi, T., Mukawa, T. and Asanuma, H. 2003. Molecular Imprinting: From Fundamentals to Applications, Willey-Vch Verlag GmbH & Co. KGaA, Weinheim, p. 9-20.

Kondo, Y., Yoshikawa, M. and Okushita, H. 2000. Molecularly imprinted polyamide membranes for chiral recognition, *Polymer Bulletin*, 44: 517-524.

Krishna, R. and Pandit, J. K. 1996. Carboxymethylcellulose-sodium based transdermal drug delivery system for propranolol, *Journal of Pharmacy and Pharmacology*, 48: 367-370.

Krystynowicz, A., Koziołkiewicz, M., Wiktorowska-Jezierska, A., Bielecki, S., Klemenska, E., Masny, A. and Płucienniczak, A. 2005. Molecular basis of cellulose biosynthesis disappearance in submergedculture of *Acetobacter xylinum*, *Acta Biochemica Polonica*, 52: 691-698.

Ktistis, G. and Niopas, I. 1998. A study on the *in vitro* percutaneous absorption of propranolol from disperse systems, *Journal of Pharmacy and Pharmacology*, 50: 413-418.

Kumar, M. N. V. R. 2000. A review of chitin and chitosan applications, *Reactive & Functional Polymer*, 46: 1-27.

Kunta, J. R., Goskonda, V. R., Brotherton, H. O., Khan, M. A. and Reddy, I. K. 1997. Effect of Menthol and related terpenes on the percutaneous absorption of propranolol across excised hairless mouse skin, *Journal of Pharmaceutical Sciences*, 86: 1369-1373.

Lacy, C. F., Armstrong, L. L., Goldman, M. P. and Lance, L.L (Eds.). 2007. Drug Information Handbook 15th edition, Lexi-Comp, Ohio, p. 1446-1449.

Landoni, M. F., Soraci, A. L., Delatour, P. and Lees, P. 1997. Enantioselective behaviour of drugs used in domestic animals: a review, *Journal of Veterinary Pharmacology and Therapeutics*, 20: 1-16.

Lu, G. and Jun, H. W. 1998. Diffusion studies of methotrexate in carbopol and poloxamer gels, *International Journal of Pharmaceutics*, 160: 1-9.

Maier, N. M., Franco, P. And Lindner, W. 2001. Separation of enantiomers: needs, challenges, perspectives, *Journal of Chromatography A*, 906: 3-33.

Malaisamy, R. and Ulbricht, M. 2004. Evaluation of molecularly imprinted polymer blend filtration membranes under solid phase extraction conditions, *Separation and Purification Technology*, 39: 211-219.

Marier, J., Pichette, V. and du Souich, Patrick, 1998. Stereoselective disposition of propranolol in rabbits, *Drug Metabolism and Disposition*, 26: 164-169.

Masqué N., Marcé, R. M. and Borrull, F. 2001. Molecularly imprinted polymers: new tailor-made materials for selective solid-phase extraction, *TRENDS in Analytical Chemistry*, 20: 477-486.

Mathew-Krotz, J. and Shea, K. J. 1996. Imprinted polymer membranes for selective transport of targeted neutral molecules, *Journal of the American Chemical Society*, 118: 8154-8155.

Mayes, A. and Mosbach, K. 1997. Molecularly imprinted polymers: useful materials for analytical chemistry?, *TRENDS in Analytical Chemistry*, 16: 321-322.

Mayes, A. G. and Whitcombe, M. J. 2005. Synthetic stratergies for the generation of molecularly imprinted polymers, *Advanced Drug Delivery Reviews*, 57: 1742-1778.

Mehvar, R. and Brocks, D. R. 2001. Stereospecific pharmacokinetics and pharmacodynamics of Beta-adrenergic blockers in humans, *Journal of Pharmacy and Pharmaceutical Sciences*, 4: 185-200.

Melendres, J. L., Nangia, A., Sedik, L., Hori, M. and Maibach, H. I. 1993. Nonane enhancers propranolol hydrochloride penetration in human skin, *International Journal of Pharmaceutics*, 92: 243-248.

Mills, P. C. and Cross, S. E. 2006. Transdermal drug delivery: Basic principles for the veterinarian, *The Veterinary Journal*, 176: 218-233.

Miyazaki, K., Kaiho, F., Inagaki, A., Dohi, M., Hazemoto, N., Haga, M., Hara, H. and Kato, Y. 1992. Enantiomeric difference in percutaneous penetration of propranolol through rat excised skin, *Chemical and Pharmaceutical Bulletin*, 40: 1075-1076.

Molinaro, A., Leroux, J., Damas, J. and Adam, A. 2002. Biocompatibility of thermosensitive chitosan-based hydrogels: an in vivo experimental approach to injectable biomaterials, *Biomaterials*, 23: 2717-2722.

Moore, T., Croy, S., Mallapragada, S. and Pandit, N. 2000. Experimental investigation and mathematical modeling of Pluronic® F127 gel dissolution: drug release in stirred systems, *Journal of Controlled Release*, 67: 191-202.

Morimoto, K., Fukanoki, S., Morisaka, K., Hyon, S. H. and Ikada, Y. 1989. Design of polyvinyl alcohol hydrogel as a controlled-release vehicle for rectal administration of dl-propranolol HCl and atenolol, *Chemical and Pharmaceutical Bulletin*, 75: 7-10.

Mosbach, K. and Ramström, O. 1996. The emerging technique of molecular imprinting and its future impact on biotechnology, *Biotechnology*, 14: 163-170.

Moser, K., Kriwet, K., Naik, A., Kalia, Y. N. And Guy, R. H. 2001. Passive skin penetration enhancement and its quantification *in vitro*, *European Journal of Phrmaceutics and Biopharmaceutics*, 52: 103-112.

Munro, T. A. and Smith, B. D. 1997. Facilitated transport of amino acids by fixed-site jumping, *Chemical Communications*, 2167-2168.

Na, N., Hu, Y., Ouyang, J., Baeyens, W. R. G., Delanghe, J. R. and Beer, T. D. 2004. Use of polystyrene nanoparticles to enhance enantiomeric separation of propranolol by capillary electrophoresis with Hp-beta-CD as chiral selector, *Analytica Chemica Acta*, 527: 139-147.

Nair, V. and Panchagnula, R. 2003. Poloxamer gel as vehicle for transdermal iontophoretic delivery of arginine vasopressin: evaluation of in vivo performance in rats, *Pharmacological Research*, 47: 555-562.

Nishi, Y., Uryu, M., Yamanaka, S., Watanabe, K., Kitamura, N., Iguchi, M. and Mitsuhashi, S. 1990. The structure and mechanical properties of sheets prepared from bacterial cellulose: Part 2 Improvement of the mechanical properties of

sheets and their applicability to diaphragms of electroacoustic transducers, *Journal of Materials Science*, 25: 2997-3001.

Noble, R.D. 1992. Generalized microscopic mechanism of facilitated transport in fixed site carrier membranes, *Journal of Membrane Sciences*, 75: 121–129.

Nostrum, C. F. van. 2005. Molecular imprinting: A new tool for drug innovation, *Drug Discovery Today*, 2: 119-124.

Okamoto, Y., Kawashima, M., Aburatani, R., Hatada, K., Nishiyama, T. and Masuda, M. 1986a. Optical resolution of β-blockers by HPLC on cellulose triphenylcarbamate derivatives, *Chemistry Letters*, 1237-1240.

Okamoto, Y., Aburatani, R., Kawashima, M., Hatada, K. and Okamura, N. 1986b. Resolution of 4-hydroxy-2-cyclopentenone derivatives by HPLC on cellulose triphenylcarbamate derivatives, *Chemistry Letters*, 1767-1770.

O'shannessy, D. J., Ekberg, B., Andersson, L. I. and Mosbach, K. 1989. Recent advances in the preparation and use of molecularly imprinted polymers for enantiomeric resolution of amino acid derivatives, *Journal of Chromatography*, 470: 391-399.

Owens, P. K., Karlsson, L., Lutz, E. S. M. and Andersson, L. I. 1999. Molecular imprinting for bio- and pharmaceutical analysis, *TRENDS in Analytical Chemistry*, 18: 146-154.

Özsoy, Y., Güngör, S. and Cevher. 2004. Vehicle effects on *in vitro* release of triaprofenic acid from different topical formulations, *Il Farmaco*, 59: 563-566.

Pandit, N.K. and Wang, D. 1998. Salt effects on the diffusion and release rate of propranolol from poloxamer 407 gels, *International Journal of Pharmaceutics*, 167: 183-189.

Pandey, L. K., Saxena, C. and Dubey, V. 2005. Studies on pervaporative characteristics of bacterial cellulose membrane, *Separation and Purification Technology*, 42: 213–218.

Pasetto, P. Maddock, S. C. and Resmini, M. 2005. Synthesis and characterization of molecularly imprinted catalytic microgels for carbonate hydrolysis, *Analytical Chemica Acta*, 542: 66-75.

Pech, B. Duval, O., Richomme, P. and Benoit, J. 1996. A timolol prodrugs for improved ocular delivery: synthesis, conformational study and hydrolysis of palmitoyl timolol malonate, *International Journal of Pharmaceutics*, 128: 179-188.

Piletsky, S. A., Panasyuk, T. L., Piletskaya, E. V., Nicholls, I. A. and Ulbricht, M. 1999, Receptor and transport properties of imprinted polymer membranes – a review, *Journal of Membrane Sciences*, 157: 263-278.

Piletsky, S. A., Alcock, S. and Turner, A. P. F. 2001. Molecular imprinting: at the edge of the third millennium, *TRENDS in Biotechnology*, 19: 9-12.

Pillai, O. and Panchagnula, R. 2003. Transdermal delivery of insulin from poloxamer gel: ex vivo and in vivo skin permeation studies in rat using iontophoresis and chemical enhancers, *Journal of Controlled Release*, 89: 127-140.

Plunkett, S. D. and Arnold, F. H. 1995. Molecularly imprinted polymers on silica: selective supports for high-performance ligand-exchange chromatography, *Journal of Chromatography A*, 708: 19-29.

Pogorelova, A. P., Kharitonov, A. B., Willner, I., Sukenik, A. N., Pizem, H. and Bayer, T. 2004. Development of ion-sensitive field-effect transistor-based sensors for

benzylphosphonic acids and thiophenols using molecularly imprinted TiO$_2$ films, *Analytica Chemica Acta*, 504: 113-122.

Pongpibul, Y. and Whitworth, C. W. 1986. Preparation and *in vitro* dissolution characteristics of a propranolol microcapsules, *International Journal of Pharmaceutics*, 33: 243-248.

Porter, W. H. 1991. Resolution of chiral drugs, *Pure and Applied Chemistry*, 63: 1119-1122.

Portero, A., Teijeiro-Osorio, A., Alonso, A. J. and Remuñán-López. 2007. Development of chitosan sponges for buccal administration of insulin, *Carbohydrates Polymers*, 68:617-625.

Powel, J. R., Ambre, J. J. and Ruo, T. I. 1988. The efficacy and toxicity of drug stereoisomers, in Wainer, I.W., Drayer, D.E (Eds), Drug stereochemistry: Analytical methods and pharmacology, Marcel Dekker, Inc, New York, p. 244-270.

Production of biocellulose (bacterial cellulose). Retrieved: April 04, 2008, from: http://www.res.titech.ac.jp/~junkan/english/cellulose/.

Quigley, J. M., Jordan, C. G. M. and Timoney, R. F. 1994. The synthesis, hydrolysis kinetics and lipophilicity of *O*-acyl esters of propranolol, *International Journal of Pharmaceutics*, 101: 145-163.

Ramachandran, C. and Fleisher, D. 2000. Transdermal delivery of drugs for the treatment of bone diseases, *Advanced Drug Delivery Reviews*, 42: 197-223.

Rezaee, A., Solimani, S. and Forozandemogadam, M. 2005. Role of plasmid in production of *Acetobacter Xylinum* Biofilms, *American Journal of Biochemistry and Biotechnology*, 1: 121-124.

Rhee, Y., Shin, Y., Park, C., Chi, S. and Park, E. 2006. Effect of flavors on the viscosity and gelling point of aqueous poloxamer solution, *Archives of Pharmaceutical Research*, 29: 1171-1178.

Ricci, E. J., Lunardi, L. O., Nanclares, D. M. A. and Marchetti, J. M. 2005. Sustained release of lidocain from Poloxamer 407 gels, *International Journal of Pharmaceutics*, 288: 235-244.

Riggs, J. A.and Smith, B. D. 1997. Facilitated transport of small Carbohydrates through plasticized cellulose triacetate mambranes. Evidence for fixed-site jumping transport mechanism, *Journal of the American Chemical Society*, 119: 2765-2766.

Riviere J. E. and Papich, M. G. 2001. Potential and problems of developing transdermal patches for veterinary applications, *Advanced Drug Delivery Reviews*, 50: 175-203.

Roberts, M. S., Cross, S. E. and Pellett, M.A. 2002. Skin Transport, in: Walters, K. A. (Ed), Dermatological and transdermal formulations, Marcel Dekker, Inc, New York, p. 89-195.

Rolland, A. 1993. Particulate carriers in dermal and transdermal drug delivery: Myth or reality?, in Rolland, A.(Ed), Pharmaceutical Particulate Carriers, Marcel Dekker, Inc, New York, p. 367-399.

Ruel-Gariépy, E., Leclair, G., Hildgen, P., Gupta, A. and Leroux, J.. 2002. Thermosensitive chitosan-based hydrogel containing liposomes for the delivery of hydrophilic molecules*, Journal of Controlled Release*, 82: 373-383.

Ruel-Gariépy, E. and A. and Leroux. 2004. In situ forming hydrogels – review of temperature-sensitive systems, *European Journal of Pharmaceutical Sciences,* 58: 409-426.

Scheindlin, A. 2004. Transdermal drug delivery: Past, present, future, *Molecular Interventions*, 4: 308-312.

Schipper, N. G., Olsson, S., Hoogstraate, J. A., deBoer, A G., Vårum, K. M. and Artursson, P. 1997. Chitosan as absorption enhancers for poorly absorbable drugs 2: mechanism of absorption enhancement, *Pharmaceutical Research*, 14: 923-929.

Schweitz, L., Andersson, L. I. and Nilsson, S. 1998. Molecular imprint-based stationary phases for capillary electrochromatography, *Journal of Chromatography A*, 817: 5-13.

Sekine, S., Watanabe, Y., Yoshimi, Y., Hattori, K. and Sakai, K. 2007. Influence of solvents on chiral discriminative gate effect of molecularly imprinted poly(ethylene glycol dimethacrylate-*co*-methacrylic acid), *Sensors and Actuators B*, 127: 512-527.

Sellergren, A. 2001. Imprinted chiral stationary phases in high-performance liquid chromatography, *Journal of Chromatography A*, 906: 227-252.

Sellergren, A. and Allender, C. J. 2005. Molecularly imprinted polymers: A bridge to advanced drug delivery, *Advanced Drug Delivery Reviews*, 57: 1733-1741.

Senel, S., Ikinci, G., Kas, S., Yousefi-Rad, A., Sargon, M. F. and Hincal., A. A. 2000. Chitosan films and hydrogels of chlorhexidine gluconate for oral mucosal delivery, *International Journal of Pharmaceutics*, 193: 197-203.

Senel, S. and Hincal, A. A. 2001. Drug permeation enhancement via buccal route: possibilities and limitations, *Journal of Controlled Release*, 72: 133-144.

Sergeyeva, T. A., Piletsky, S. A., Brovko, A. A., Slinchenko, E. A., Sergeeva, L. M. and El'skaya, A. V. 1999. Selective recognition of atrazine by molecularly imprinted polymer membranes. Development of conductometric sensor for herbicide detection, *Analytica Chemica Acta*, 392: 105-111.

Sergeyeva, T. A., Matuschewski, H., Piletsky, S. A., Bendig, J., Schedler, U. and Ulbricht, M. 2001. Molecularly imprinted polymer membranes for substance-selective solid phase extraction from water by surface photo-grafting polymerization, *Journal of Chromatography A*, 907: 89-99.

Shah, J. and Brown, R. M. 2004. Towards electronic paper displays made from microbial cellulose, *Applied Microbilogy and Biotechnology*.

Sheldon, R.A. 1993. Chirotechnology: Industrial synthesis of optical active compounds, Marcel Dekker, Inc, New York, p. 1-37.

Shivanand, P. and Sprockel, O. M. 1993. Release of propranolol HCl from a tablet coated with a macroporous membrane, *International Journal of Pharmaceutics*, 92: 35-45.

Sinha, V. R., Singla, A. K., Wadhawan, S., Kaushik, R., Kumria, R., Bansal, K. and Dhawan, S. 2004. Chitosan microspheres as a potential carrier for drugs, *International Journal of Pharmaceutics*, 274: 1-33.

Sowinski, K. M., Lima, J. J., Burlew, B. S., Massie, J. D. and Johnson, J. A. 1996. Racial differences in propranolol enantiomer kinetics following simultaneous i.v. and oral administration, *British Journal of Pharmacology*, 42: 339-346.

Stott, P. W., Williams, A. C. and Barry, B. W. 2001. Mechanistic study into the enhanced transdermal permeation of a model β-blocker, propranolol, by fatty acids: a melting point depression effect, *International Journal of Pharmaceutics*, 219: 161-176.

Suedee, R., Brain, K. R. and Heard, C. M. 1998. Enantioselective retardation of rac-propranolol from matrices containing cellulose derivatives, *Chirality*, 9: 307-312.

Suedee, R., Srichana, T. and Martin G. P. 2000. Evaluation of matrices containing molecularly imprinted polymers in the enantioselective-controlled delivery of β-blockers, *Journal of Controlled Release*, 66: 135-147.

Suedee, R., Srichana, T., Chotivatesin, R. and Martin G. P. 2002. Stereoselective release behaviors of imprinted bead matrices, *Drug Development and Industrial Pharmacy*, 28: 545-554.

Suedee, R., Srichana, T., Sangpagi, C., Tunthana, C. and Vanichapichat, P. 2004. Development of trichloroacetic acid sensor based on molecularly imprinted polymer membrane for the screening of complex mixture of haloacetic acids in drinking water, *Analytica Chemica Acta*, 504: 89-100.

Suh, J.-K., F., Matthew, H. W. T. 2000. Application of chitosan-based polysaccharide biomaterials in cartilage tissue engineering: a review, *Biomaterials*, 21: 2589-2598.

Sungpet, A., Wongjirung, S., Sriaramrungraung, V. and Kampangseri, N. 2002. Facilitated transport near the carrier saturation limit, *Songklanakarin Journal of Science and Technology*, 24: 908-913.

Takahashi, K., Tamagawa, S., Haginaka, J., Yasuda, H., Katagi, T. and Mizuno, N. 1992. Stereoselective hydrolysis of *O*-acetyl propranolol as prodrug in rat tissue homogenates, *Journal of Pharmaceutical Sciences*, 81: 226-227.

Takeuchi, T. and Haginaka, J. 1999. Separation and sensing based on molecular recognition using molecularly imprinted polymers, *Journal of Chromatography B*, 728: 1-20.

Tan, H. S. and Pfister, W. R. 1999. Pressure-sensitive adhesives for transdermal drug delivery systems, *PSTT*, 2: 60-69.

Täuber, U. 1989. Drug Metabolism in the skin: advantages and disadvantages, in: Hadgraft, J. and Guy, R. H. (Eds), Transdermal Drug Delivery: developmental issues and research initiatives, Marcel Dekker, Inc, New York, p. 99-112.

Taylan, B., Capan, Y., Güven, O., Kes, S. and Hincal, A. A. 1996. Design and evaluation of sustained-release and buccal adhesive propranolol HCl tablets, *Journal of Controlled Release*, 38: 11-20.

Thacharodi, D. and Rao, K. P. 1995. Development and *in vitro* evaluation of chitosan-based transdermal drug delivery systems for the controlled delivery of propranolol hydrochloride, *Biomaterials*, 18: 145-148.

The United States Pharmacopeia: Asian Edition. 2007, The United States Pharmacopeial Convention, MD, p. 3057-3063.

Thomas, B. J. and Finnin, B. C. 2004. The transdermal revolution, *Drug Discovery Today*, 9: 697-703.

Touitou, E., Chow, D. D. and Lawter, J. R. 1994. Chiral β-blockers for transdermal delivery, *International Journal of Pharmaceutics*, 104: 19-28.

Ulbricht, M. 2004. Membrane separations using molecularly imprinted polymers, *Journal of Chromatography B*, 804: 113-125.

Ulbricht, M. 2006. Advanced functional polymer membranes, *Polymer*, 47: 2217-2262.

Vasil'ev, A. E., Krasnyuk, I. I., Ravikumar, S. and Tokhmakhchi, V. N. 2001. Drug synthesis methods and manufacturing technology: Transdermal therapeutic systems for controlled drug release (a review), *Pharmaceutical Chemistry Journal*, 35: 613-626.

Vandamme, E. J., Baets, S. D., Vanbaelen, A., Joris, K. and Wulf, P. D. 1998. Improved production of bacterial cellulose and its application potential, *Polymer Degradation and Stability*, 59: 93-99.

Venkatesh,S., Siezemore, S. P. and Byrne, M. E. 2007. Biomimetic hydrogels for enhanced loading and extended release of ocular therapeutics, *Biomaterials*, 28: 717-724.

Viegas, R. M. C., Afonso, C. A. M., Crespo, J. and Coelhoso, I. M. 2007. Modelling of the enantioselective extraction of propranolol in a biphasic system, *Separation and Purification Technology*, 53: 224-234.

Vyas, S. P. Jaitely, V. and Kanaujia, P. 1999. Synthesis and characterization of palmitoyl propranolol HCl auto-lymphotrophs for oral administration, *International Journal of Pharmaceutics*, 186: 177-189.

Walshe, M., Howarth, J., Kelly, M. T., O'Kennedy, R. and Smyth, M. R. 1997a. The preparation of a molecular imprinted polymer to 7-hydroxycoumarin and its used as a solid-phase extraction material, *Journal of Pharmaceutical and Biomedical Analysis*, 16: 319-325.

Walshe, M., Garcia, E., Howarth, J., Smyth, M. R. and Kelly, M. T. 1997b. Separation of the enantiomers of propranolol by incorporation of molecularly imprinted polymer particles as chiral selectors in capillary electrophoresis, *Analytical Communications*, 34: 119-122.

Walters, K. A. and Brain, K. R. 2002. Dermatological formulation and transdermal systems, in: Walters, K. A. (Ed), Dermatological and transdermal formulations, Marcel Dekker, Inc, New York, p.319-399.

Walters, K.A. and Roberts, M.S. 2002. in: Walters, K.A. (Ed.), Dermatological and transdermal formulations, Marcel Dekker, Inc, New York, p. 1-31.

Wang, X., Ma, J., Wang, Y. and He, B. 2002. Bone repair in radii and tibias of rabbits with phosphorylated chitosan reinforced calcium phosphate cements, *Biomaterials*, 23: 4167-4176.

Wang, X., Liu, Y. and Ching, C. B. 2006. Kinetic and equilibrium study of enantioseparation of propranolol in preparative scale chromatography, *Separation and Purification Technology*, 50: 204-211.

Wanichapichart, P., Kaewnopparat, S., Buaking, K. and Puthai, W. 2002. Characterization of cellulose membranes produced by *Acetobacter xylinum*, *Songklanakarin Journal of Science and Technology*, 24: 855-862.

Watanabe, M., Akahoshi, T., Tabata, Y. and Nakayama, D. 1998. Molecular specific swelling change of hydrogels in accordancewith the concentration of guest molecules, Journal of American Chemical Society, 120: 5577–5578.

Watkinson A. C. and Brain, K. R. 2002. Dermatological formulation and transdermal systems, in: Walters, K. A. (Ed), Dermatological and transdermal formulations, Marcel Dekker, Inc, New York, p. 61-88.

Welch, C. J. and Perrin, S. R. 1995. Improved chiral stationary phase for β-blocker enantioseparations, *Journal of Chromatography A*, 690: 218-225.

Wickett, R. R. and Visscher, M. O. 2006. Structure and functional of the epidermal barrier, *American Journal of Infection Control*, 34: S98-S110.

Wulff, Günter. 1995. Molecularly imprinting in cross-linked materials with the aid of molecular templates-A way towards artificial antibodies, *Angewandte Chemie-International Editio*n, 34: 1812-1832.

Xie, Y., Xu, B., Gao, Y. 2005. Controlled transdermal delivery of model drug compounds by MEMS microneedle array, *Nanomedicine: Nanotechnology, Biology, and Medicine*, 1: 184-190.

Yashima, E. 2001. Polysaccharide-based chiral stationary phases for high-performance liquid chromatographic enantioseparation, *Journal of Chromatography A*, 906: 105-125.

Yin, J., Yang, G. and Chen, Y. 2005. Rapid and efficient chiral separation of nateglinide and its L-enantiomer on monolithic molecularly imprinted polymers, *Journal of Chromatography A*, 1090: 68-75.

Yoshigae, Y., Imai, T., Aso, T. and Otagiri, M. 1998. Species differences in the disposition of propranolol prodrugs derived from hydrolase activity in intestinal mucosa, *Life Sciences*, 62: 1231-1241.

Yoshikawa, M. 2002. Molecularly imprinted polymeric membranes, *Bioseparations*, 10: 277-286.

Yoshimi, Y., Ohdaira, R., Iiyama, C. and Sakai, K. 2001; "Gate effect" of thin layer of molecularly-imprinted poly(methacrulic acid-co-ethyleneglycol dimethacrylate), *Sensors and Actuators B*, 73: 49-53.

Zhang, Y., Wu, D., Wang-Iverson, D. B. and Tymiak, A. A. 2005. Enantioselective chromatography in drug discovery, *Drug Discovery Today*, 10: 571-577.

Zhao, K. and Singh, 1999. In vitro percutaneous absorption enhancement of propranolol, hydrochloride, through porcine epidermis by terpenes/ethanol, *Journal of Controlled Releas*e, 62: 359-366.

APPENDIX

1. The absence of nitrogen content in elemental analysis results obtained by using a JSM-5800 LV electron microscope.
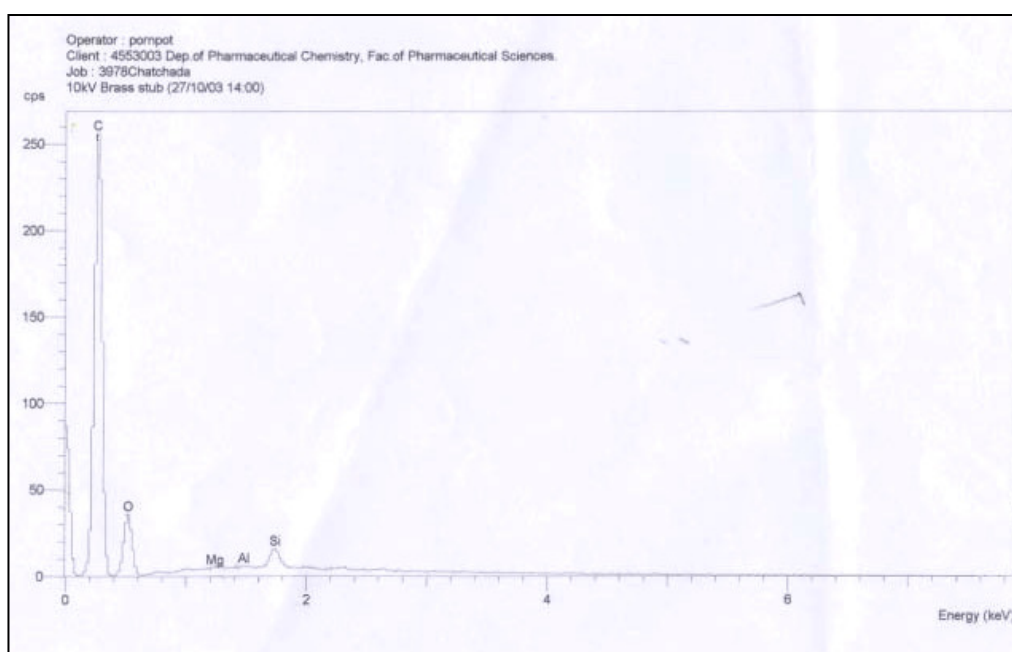
2. The acceptance for animal experiments from local ethics committee.

ที่ ศธ 0521.05/ 054

กองบริการการศึกษา
มหาวิทยาลัยสงขลานครินทร์
อ.หาดใหญ่ จ.สงขลา 90110

หนังสือรับรองโครงการวิจัย

การศึกษาวิจัยที่ทำการทดลองในสัตว์ทดลองเรื่อง : "วิธีการใหม่ของการนำส่งยา propranolol ผ่านทางผิวหนังโดย
ใช้ระบบควบคุมการปลดปล่อยที่เลือกเฉพาะอินแนนทิโอเมอร์"

หัวหน้าโครงการวิจัย : รศ.ดร.รุ่งนภา ศรีชนะ
ภาควิชาเภสัชเคมี คณะเภสัชศาสตร์

ได้ผ่านการพิจารณาและเห็นชอบจาก : คณะกรรมการจรรยาบรรณการใช้สัตว์ทดลอง
มหาวิทยาลัยสงขลานครินทร์

ให้ไว้ ณ วันที่ 23 มกราคม พ.ศ. 2547

(ผู้ช่วยศาสตราจารย์ ดร.กิจจา สว่างเจริญ)
ประธานคณะกรรมการจรรยาบรรณการใช้สัตว์ทดลอง
มหาวิทยาลัยสงขลานครินทร์